



LUND UNIVERSITY

Ongoing research at Lund University, Invited talk given at University of Parma, Italy. Orationem Meam.

Ståhle, P.; Bjerkén, Christina; Tryding, Johan; Kao-Walter, Sharon

2016

Document Version:

Publisher's PDF, also known as Version of record

[Link to publication](#)

Citation for published version (APA):

Ståhle, P., Bjerkén, C., Tryding, J., & Kao-Walter, S. (2016). Ongoing research at Lund University, Invited talk given at University of Parma, Italy. Orationem Meam.

Total number of authors:

4

General rights

Unless other specific re-use rights are stated the following general rights apply:

Copyright and moral rights for the publications made accessible in the public portal are retained by the authors and/or other copyright owners and it is a condition of accessing publications that users recognise and abide by the legal requirements associated with these rights.

- Users may download and print one copy of any publication from the public portal for the purpose of private study or research.
- You may not further distribute the material or use it for any profit-making activity or commercial gain
- You may freely distribute the URL identifying the publication in the public portal

Read more about Creative commons licenses: <https://creativecommons.org/licenses/>

Take down policy

If you believe that this document breaches copyright please contact us providing details, and we will remove access to the work immediately and investigate your claim.

LUND UNIVERSITY

PO Box 117
221 00 Lund
+46 46-222 00 00

UNIVERSITÀ DEGLI STUDI DI PARMA

DIPARTIMENTO DI INGEGNERIA CIVILE, DELL'AMBIENTE, DEL TERRITORIO E ARCHITETTURA



AVVISO SEMINARIO

Mercoledì 21 dicembre 2016, ore 10:30-12:30

(aula 8, Plesso Ingegneria Didattica)

Ongoing research at Lund University (Per Ståhle, Lund University, Sweden)

The presentation will give an overview of ongoing research at Lund University. Four projects will be reviewed. 1) The necking type of fracture that occur in elastic plastic materials with a sub-critical thickness that reduces the fracture process to pure necking is described. Laminate applications will be discussed. 2) Stress corrosion crack growth with a moving mesh is described. A single chemical criterion for removal of matter replaces the crack growth, crack path and crack branching criteria. 3) A phase field model of delayed hydride cracking. The mechanics of surface blister hydrides forming at cold spots on zirconium surfaces and hydrides at crack tips will be presented. 4) Bone growth controlled by stress driven diffusion will be demonstrated. Both a switch of state and an alternative, a set of coupled PDEs derived for a phase field model are used to trace the growth of a bone exposed to mechanical load.

Biosketch

Per Ståhle addresses problems in the theoretical and applied mechanics of solids. His research involves stress corrosion, hydrogen embrittlement and materials testing. He has a focus on the mechanical conditions leading to dissolution of materials, instabilities at material surfaces, growth of precipitates and initiation and growth of cracks. He became honorary doctor and professor at Uppsala University 1986, Professor of Mechanics of Materials at Malmö University and is since 2009 Professor of Solid Mechanics at Lund University.

Per was visiting Professor at Brown university 1989/90, University of California Santa Barbara 1992, Tokyo Institute of Technology and Academy of Science Beijing 1997. From 2004 to 2009 he was the chairman of the National Committee for Theoretical and Applied Mechanics at the Swedish Royal Academy of Science, correspondent of EuroMech, expert for the Swedish Research Council, the NATO Collaborative Research Council and the Royal Society of London. He is presently Swedish representative in The International Union of Theoretical and Applied Mechanics since 2012, the official blogger for the Elsevier publication Engineering Fracture Mechanics and a member of the executive committee of the European Society of Structural Integrity.

Mercoledì 21 dicembre 2016, ore 10:30-11:30 (aula 8, Plesso Ingegneria Didattica)

Ongoing Solid Mechanics Research at Lund University

Per Ståhle, Lund University, Sweden

- 1) Necking Type of Fracture of Laminates**
- 2) Stress Corrosion Crack Growth - a Moving Boundary Mod.**
- 3) Modelling of delayed hydride cracking**
- 4) Bone Growth Controlled by Stress Driven Diffusion**



A Strong Toughening Mechanism in an Elastic Plastic Laminate

P. Ståhle¹, C. Bjerkén², J. Tryding³ and S. Kao-Walter⁴

¹Lund University, Lund

²Malmö University, Malmö

³TetraPak AB, Lund

⁴Blekinge Technical University, Karlskrona

Necking vs fracture

Fracture toughness of aluminium is $\approx 24 \text{ MPa m}^{1/2}$.

Measured toughness of an $9\mu\text{m}$ aluminium foil is $3.5 \text{ MPa m}^{1/2}$ due to necking.

The stress intensity factor is

$$K \sim \text{sheet thickness}^{1/2}$$

A sheet thickness $> 400\mu\text{m}$ is needed to restore K_{Ic} fracture control.

The largest load per unit of length

$$P \sim \text{sheet thickness}^{3/2}$$

A sheet thickness $> 32\mu\text{m}$ is needed to provide the strength of a non necking $9\mu\text{m}$ aluminium foil.

Layers and laminate properties

Metal foil (fully annealed AA1200 aluminium) **Stiff and Brittle**

$$t_A = 9\mu\text{m}, E_A = 71\text{GPa}, \sigma_{bA} = 73\text{MPa}, \nu_L = 0.33, F_A = 12.5\text{N}$$

Polymer (PolyEthene LDPE, LD270) **Weak and Soft**

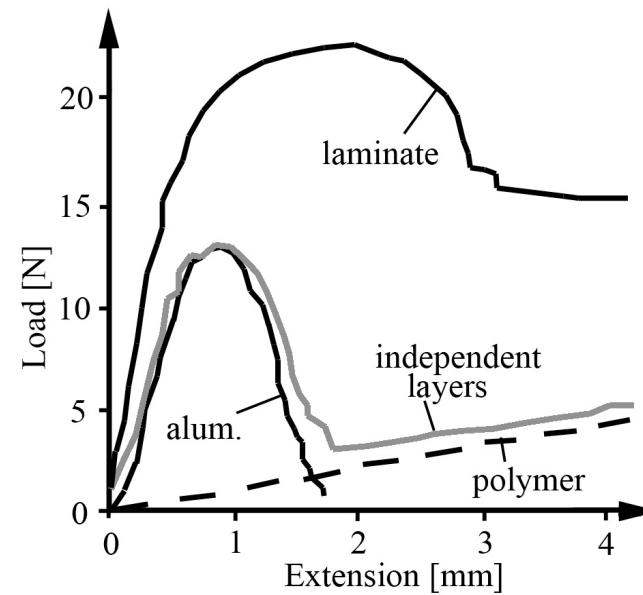
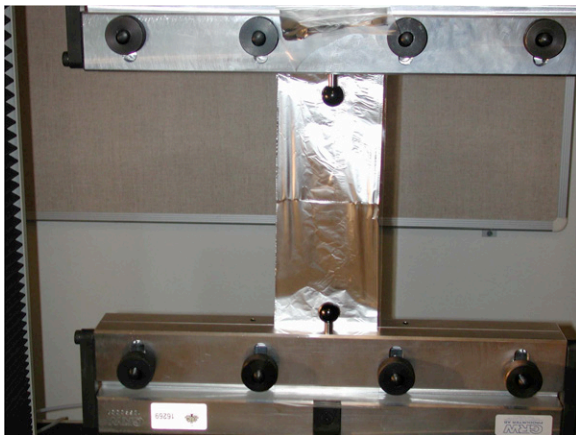
$$t_L = 27\mu\text{m}, E_L = 126\text{MPa}, \sigma_{bL} = 8\text{MPa}, \nu_L = 0.45, F_L = 2\text{N}$$

The laminate (homogenized, plane stress) **Stiff and Ductile**

$$t_{lam} = 36\mu\text{m}, E_{lam} = 18\text{GPa}, \sigma_{blam} = 27\text{MPa}, \nu_{lam} = 0.3, F_{lam} = 22.5\text{N}$$

Test results

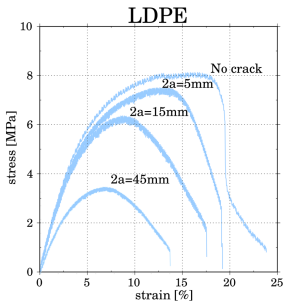
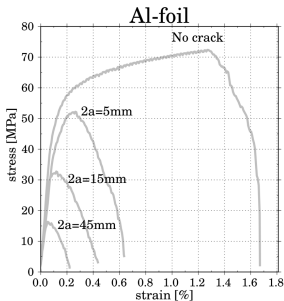
(Kao-Walter *et al.*, 02, Macionczyk and Bruckner, 99)



Fracture mechanical test

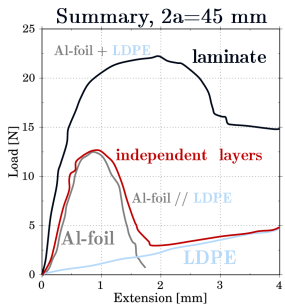
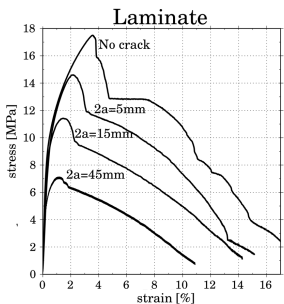
Load displacement curves

Test results



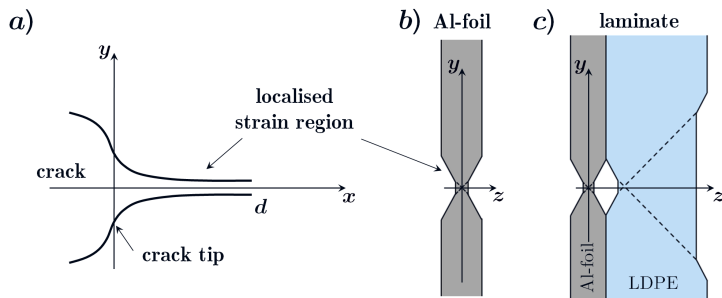
Stress vs. strain for tensile tests

a) Al-foil, b) Polymer



a) Stress vs. strain for the laminate. b) Load vs. extension. Summary of the aluminium, polymer and laminate results. Crack length 45mm (Kao-Walter et al., 2002), (Hutchinson, 2013)

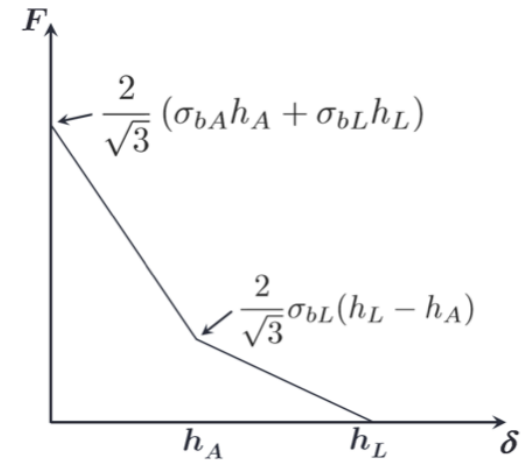
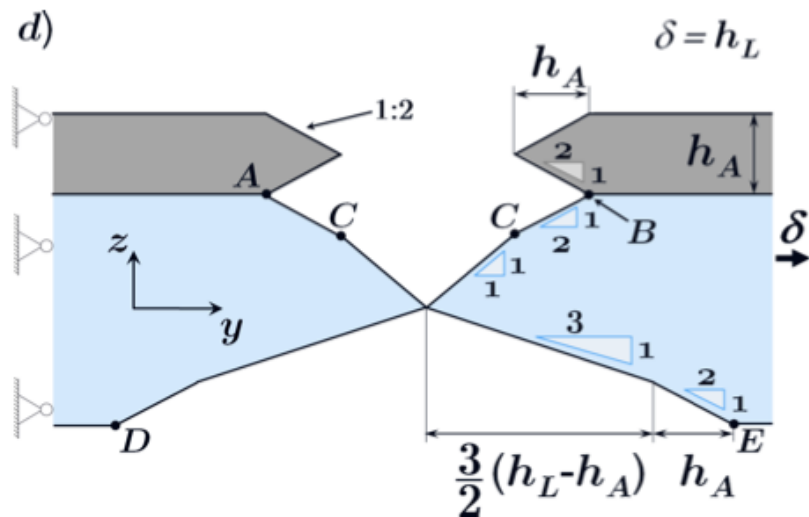
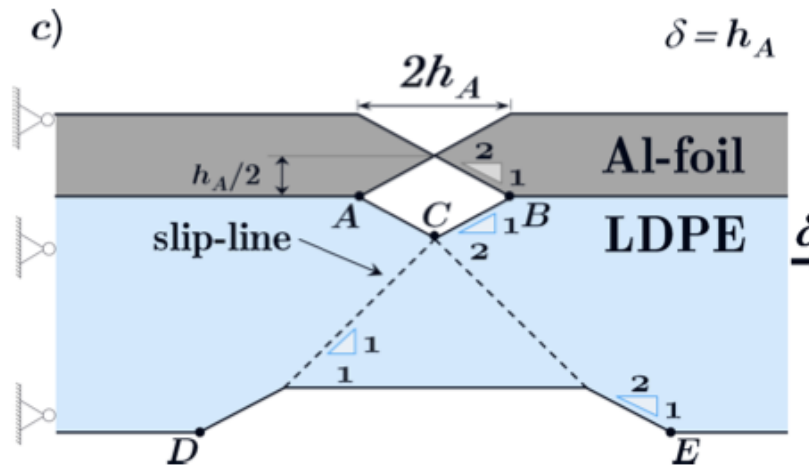
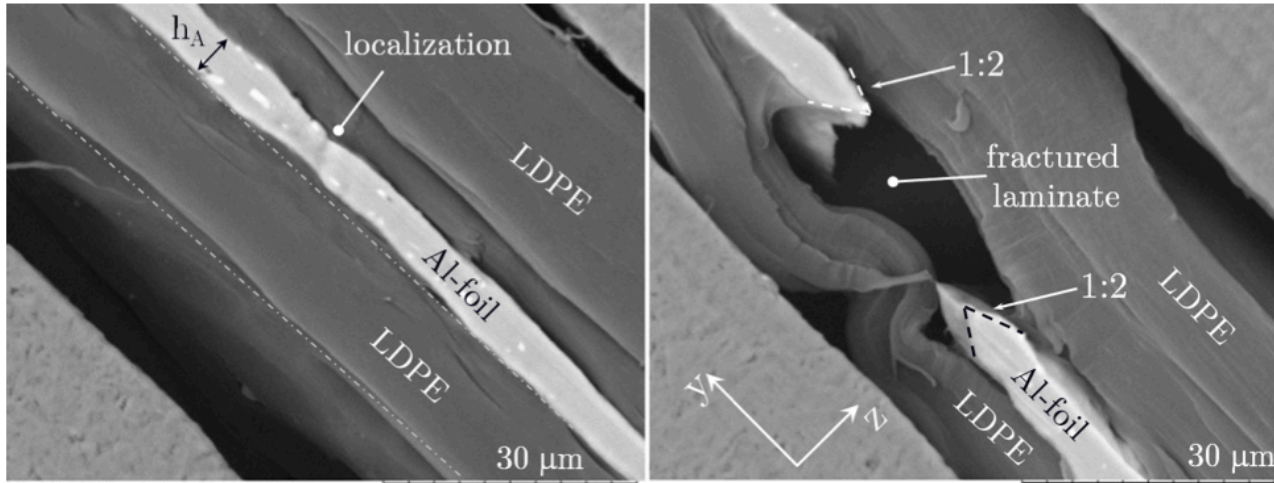
Work of failure



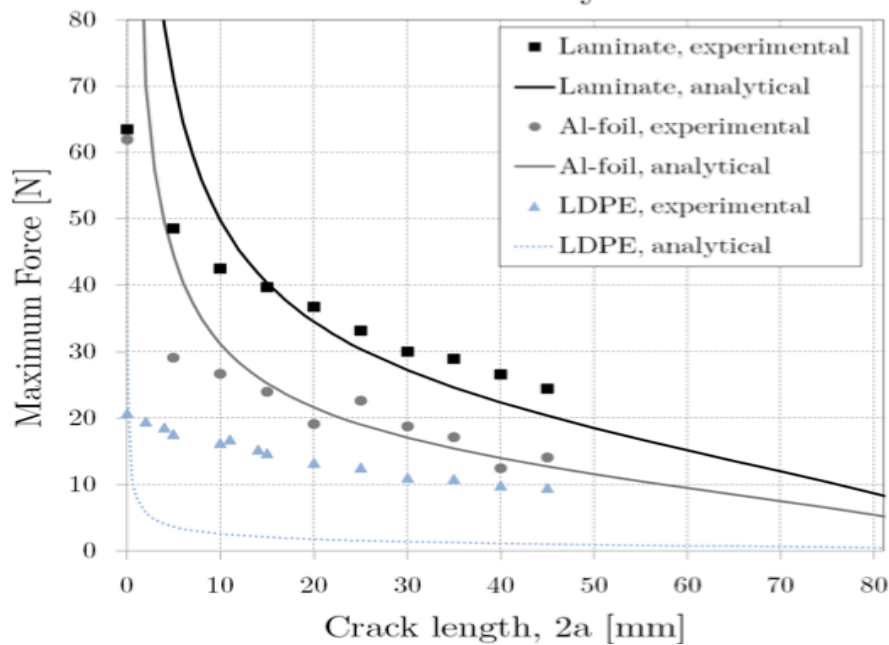
Strip yield zone ahead a crack tip. a) the crack geometry in the plane $z = 0$. b and c) the slip region as seen in a plane $x = \text{const}$.

Super-tough Thin Film Laminates

Sharon Kao-Walter, Rickard Hägglund, Eskil Andreasson



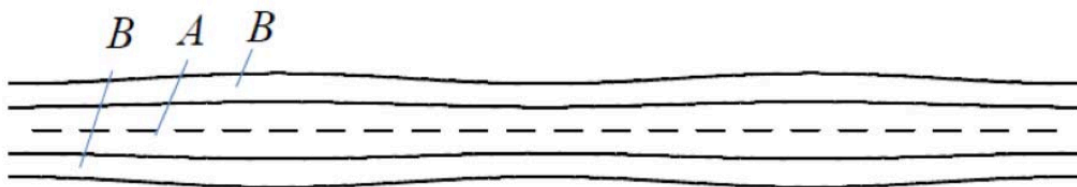
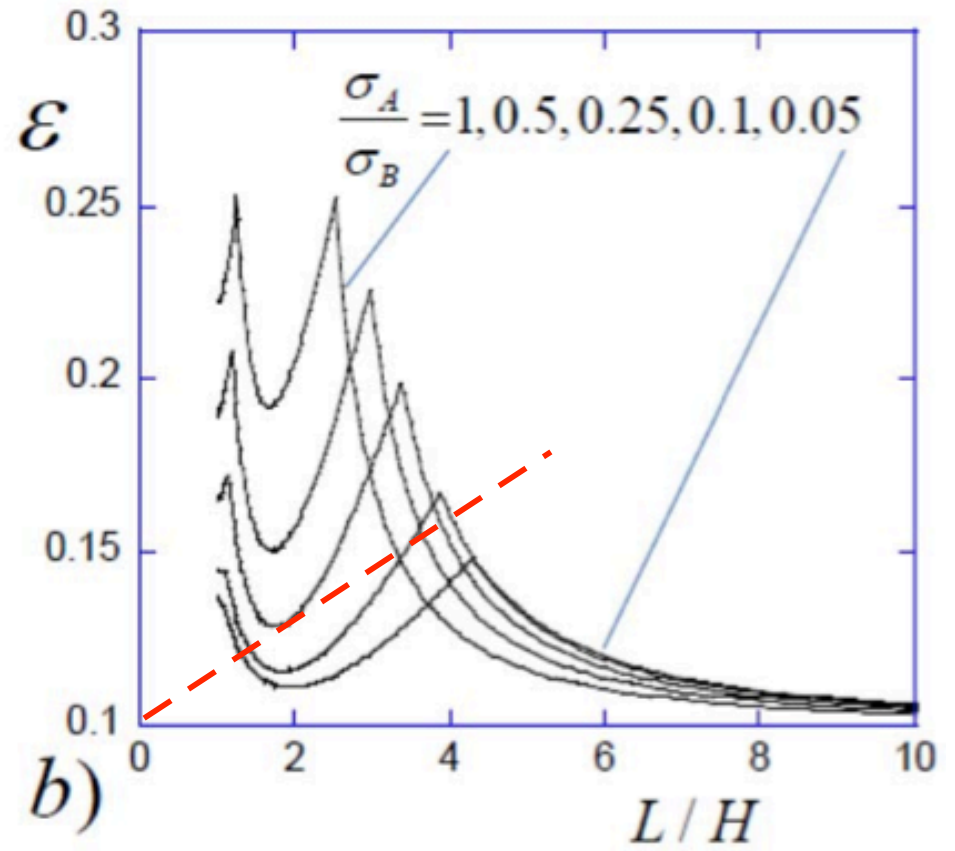
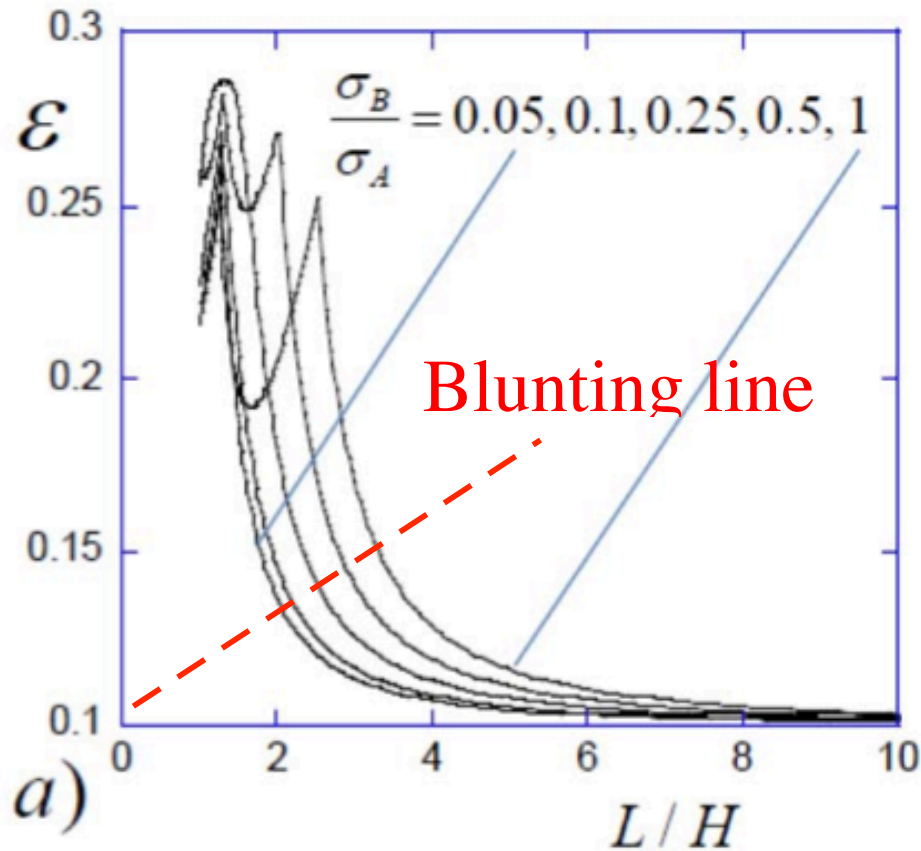
Summary



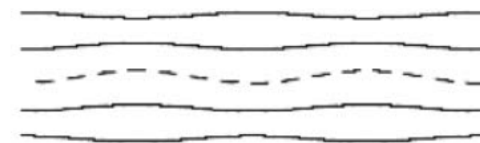
$$N_A = N_B = 0.1 \text{ and } h_A/h_B = 2$$

(Hutchinson, 2013)

$$\sigma_B/\sigma_A = 0.002 \text{ or } \sigma_A/\sigma_B = 0.002$$



$L/H = 10$, symmetric mode



$L/H = 2$, anti-symmetric mode

Material parameters

Comparison of structural and material parameters for the different test specimens.

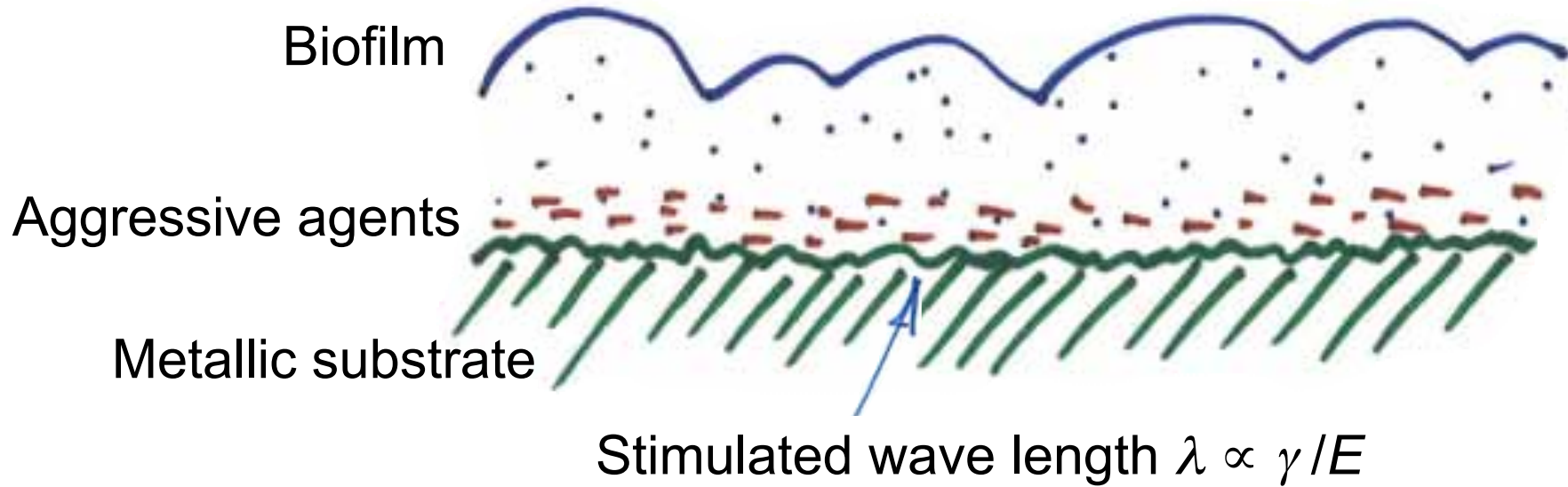
	Al-foil	LDPE	laminate
$h[\mu m]$	9,0	27	36
$E [GPa]$	71,0	0.126	17.9
$\nu[-]$	0.33	0.45	0.30
$\sigma_b [MPa]$	73.0	8.0	26.6
$J_c [N/m]$	188	82.6	109
$F_{max} [N] \{2a=45mm\}$	14,0	9,4	24,4

$$\sigma_c = \sqrt{J_c \frac{E}{\pi a \phi \left(\frac{a}{W}\right)}} = \sqrt{\frac{1}{\sqrt{3}} \left(\frac{\sigma_{bA} h_A^2 + \sigma_{bL} h_L^2}{h_A + h_L} \right) \frac{E}{\pi a \phi \left(\frac{a}{W}\right)}}. \quad (13)$$

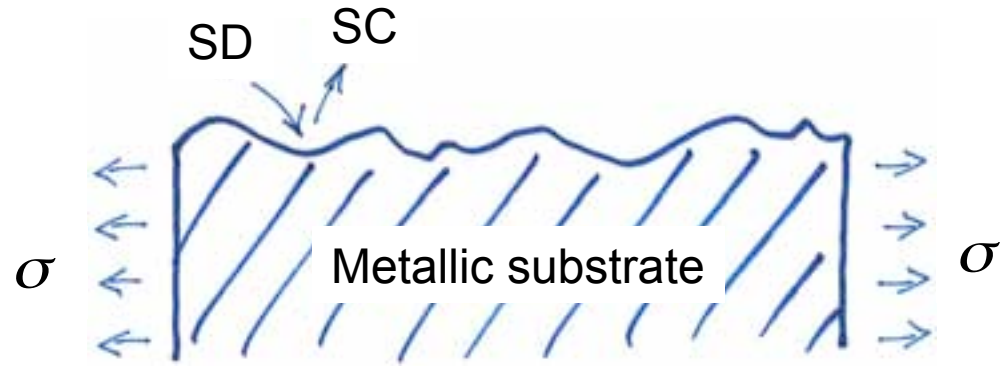
Stress Corrosion Crack Growth

Per Ståhle, Andrey Jivkov and Christina Bjerken
Malmö University, Sweden

Biocorrosion



Competing mechanisms
SD - surface diffusion
SC - stress corrosion

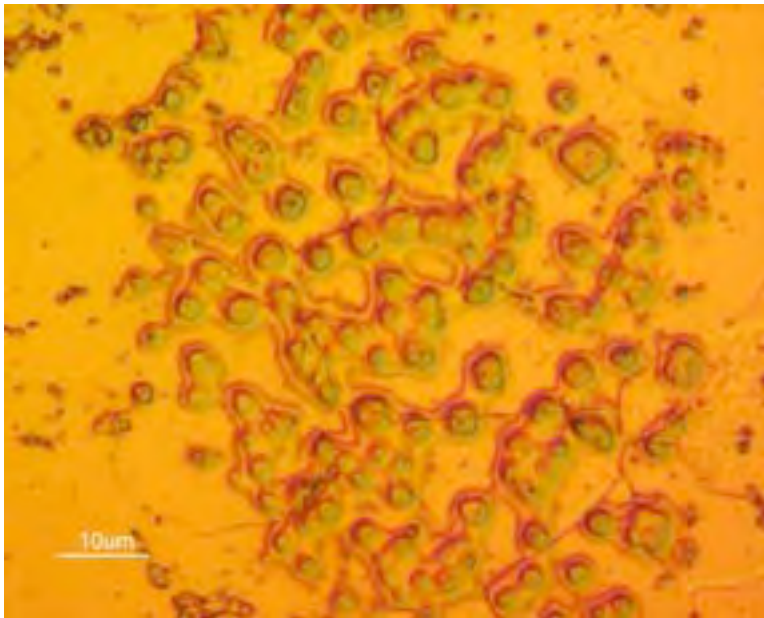


Organisms believed to cause SC

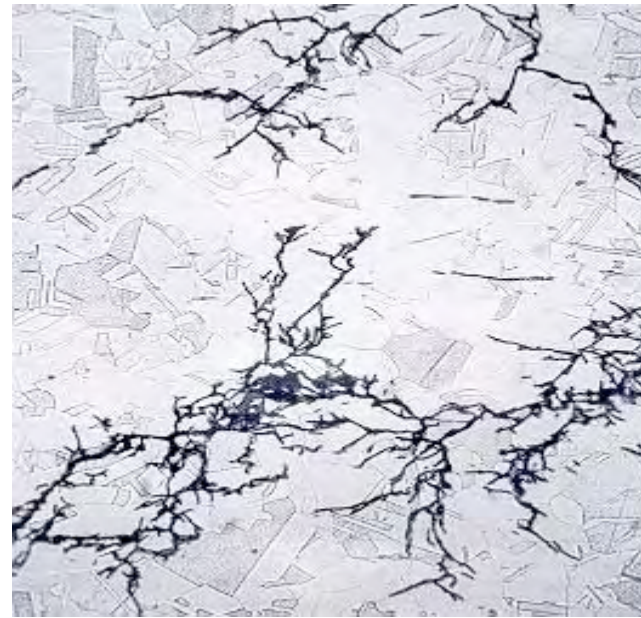
Anaerobic Bacteria: *Desulfovibrio*, *-maculum*, *-monas*

Aerobic Bacteria: *Thiobacillus*

Fungi, Algae, Protozoans



Surface with different levels of pitting



Corrosion in stainless steel in the presence of *Gallionella Bacillus*

Corroding environment leads to:

1. Continuous loss of mass

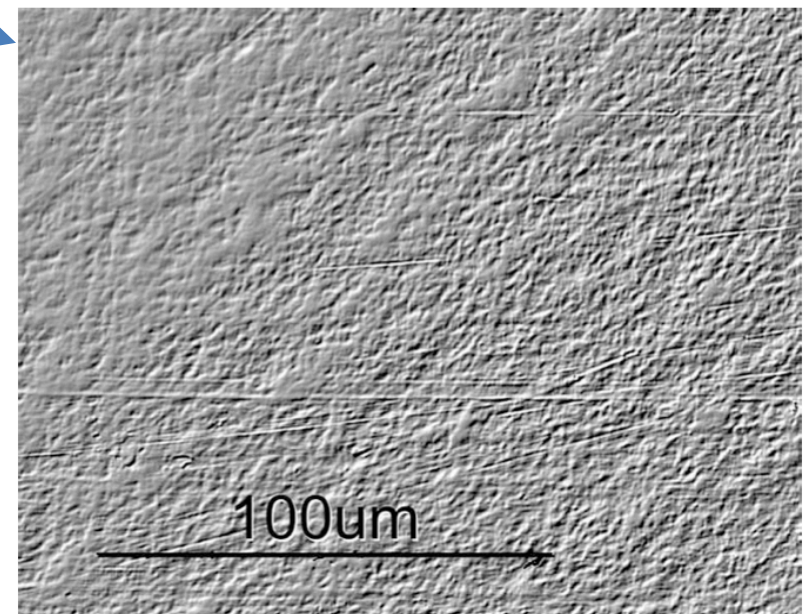
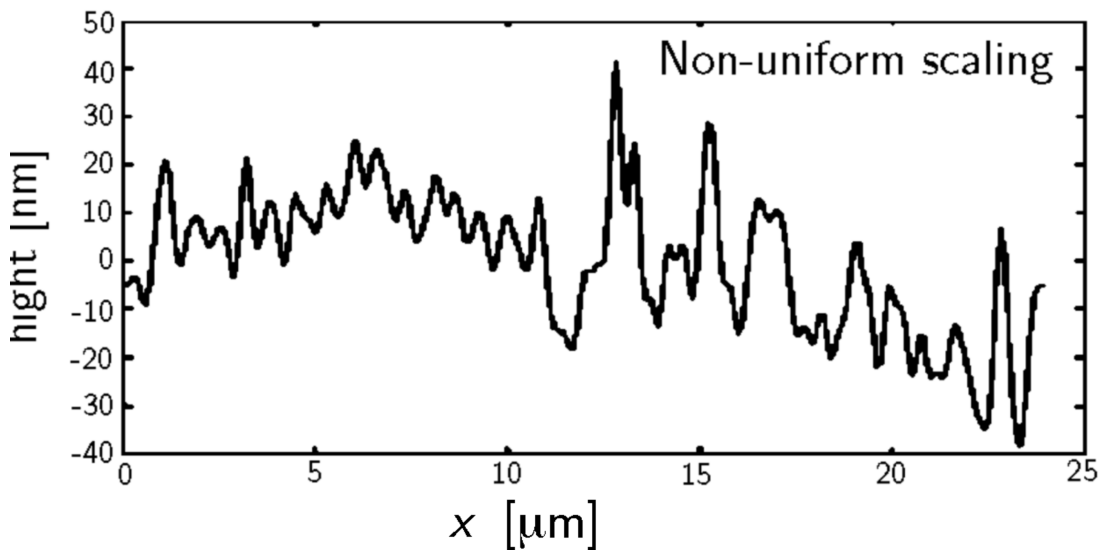
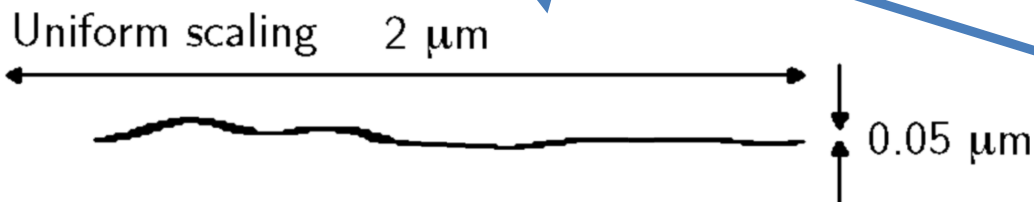
2. Pitting

... and with mechanical stress present

3. Surface roughening



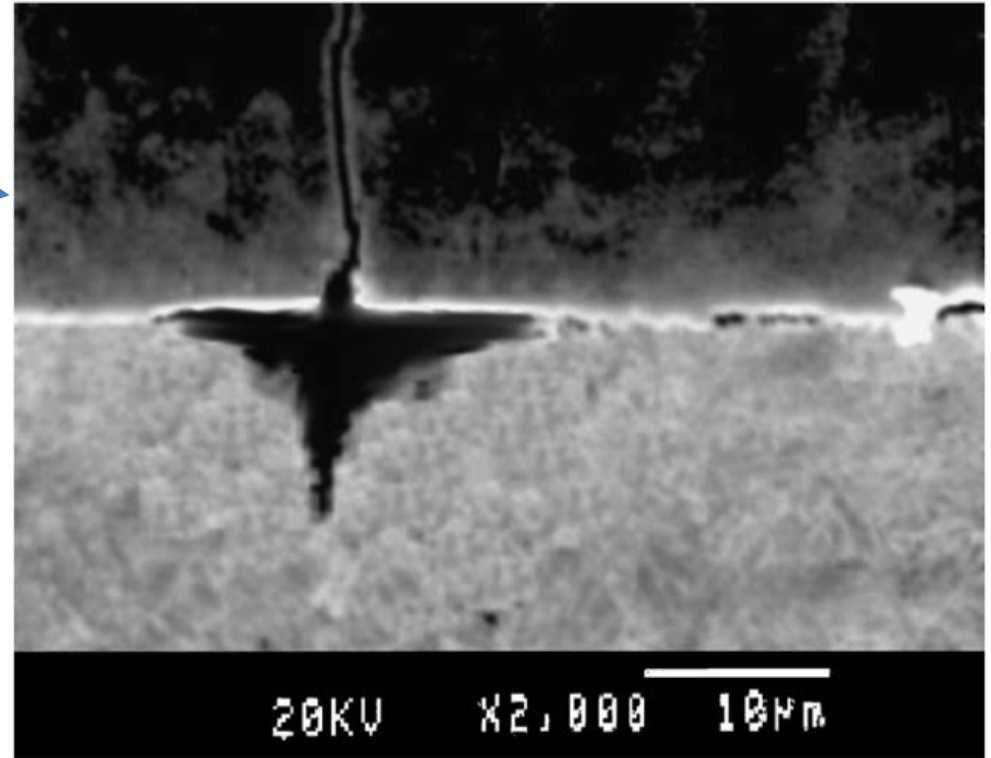
(from Kim *et al.* 2000)



4. Evolving pits
5. Formation of cracks
6. Crack growth
7. Crack branching

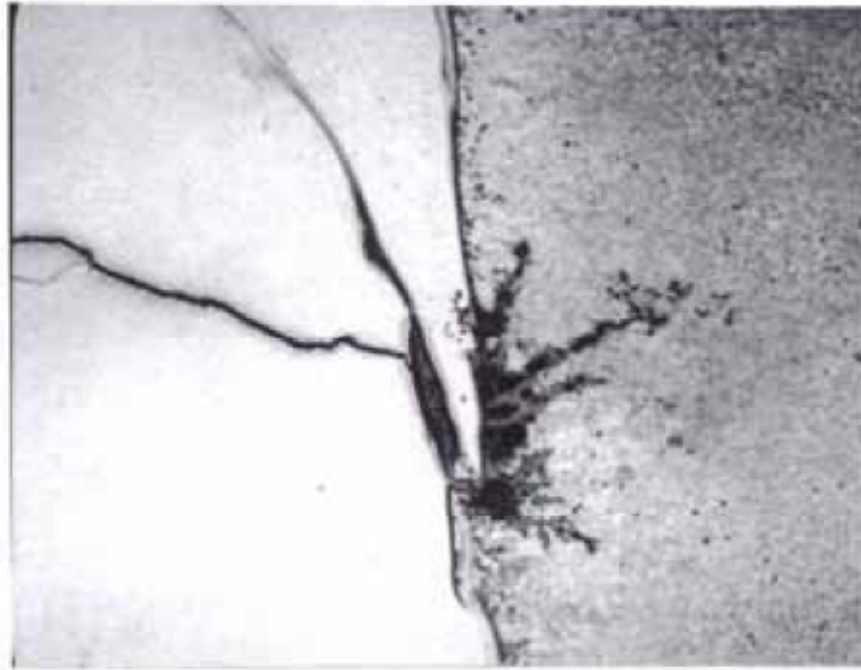


Growing crack in a polycarbonate exposed to acetone (Hejman 2011)

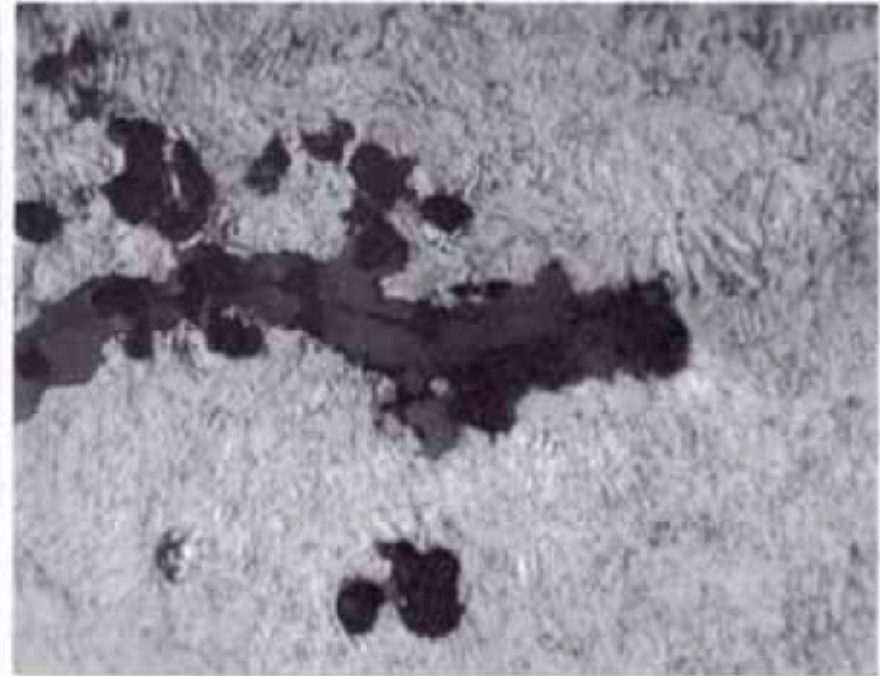


Cr/zone six charge related of land and groove substrate erosion through a micro-crack at the 12:00 bore origin. (Sopok *et al.* 2005)

Corrosion Crack crossing a bi-material interface



Corrosion crack penetrating a bimaterial interface between austenitic and pressure vessel steel of type SA533C11.



The tip of one of the crack branches. Crack length 7 mm, notch width 10 μm . *Reproduced with permission from Vattenfall AB.*

Surface Morphology:
Surface Wave Spectrum

Crack Initiation:
Pit, Cusp and Crack

Crack Growth:
Crack Growth, Blunting and Branching

Evolving Surface Morphology

Asaro-Tiller (1972), Grinfeld (1986, 1993),
Srolovitz (1989), Freund (1995), Kung-Suk (2000)

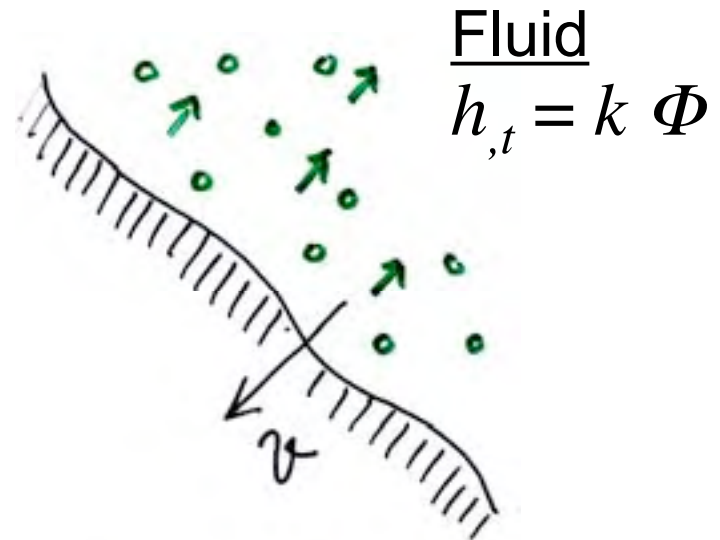
Chemical potential,

$$\Phi = U_c + U$$

U_c surface energy, U elastic strain energy

Surface diffusion

$$h_{,t} = D \nabla^2 \Phi$$



Governing equations:

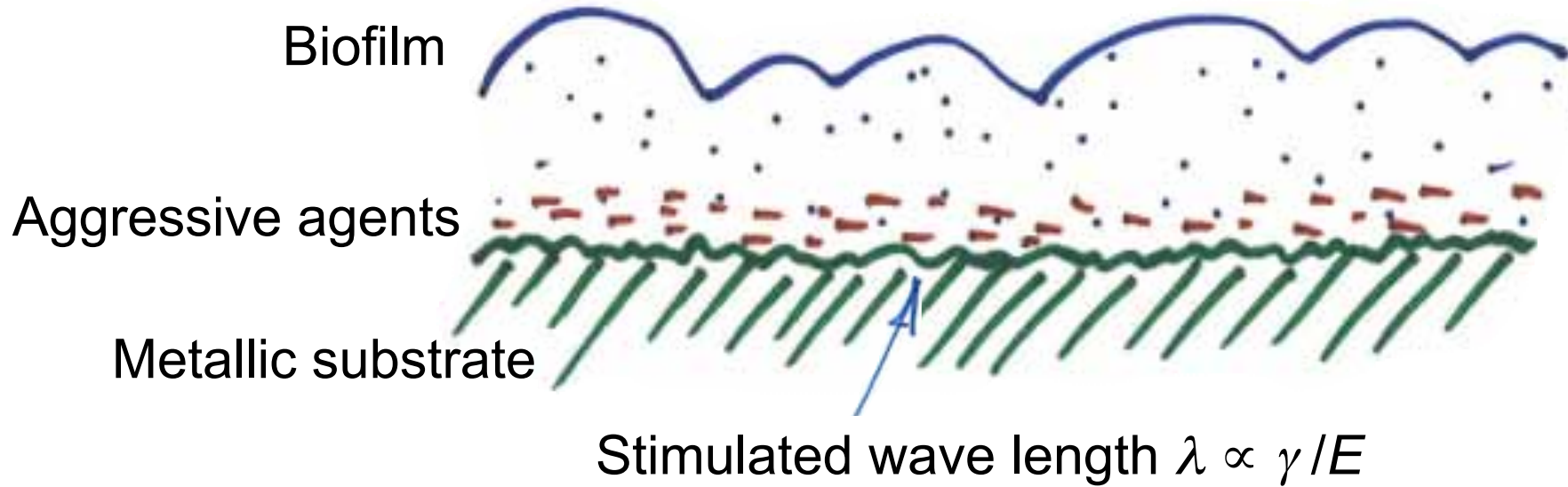
Evaporation-condensation

$$\frac{\partial h}{\partial t} = L_1 \left(\gamma \frac{\partial^2 h}{\partial x^2} - \frac{k}{2^\mu} \frac{\partial h}{\partial x} \right)$$

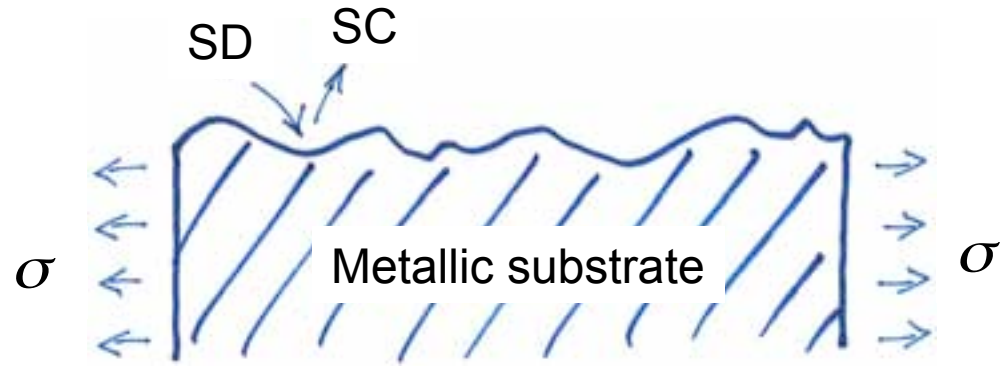
or surface diffusion

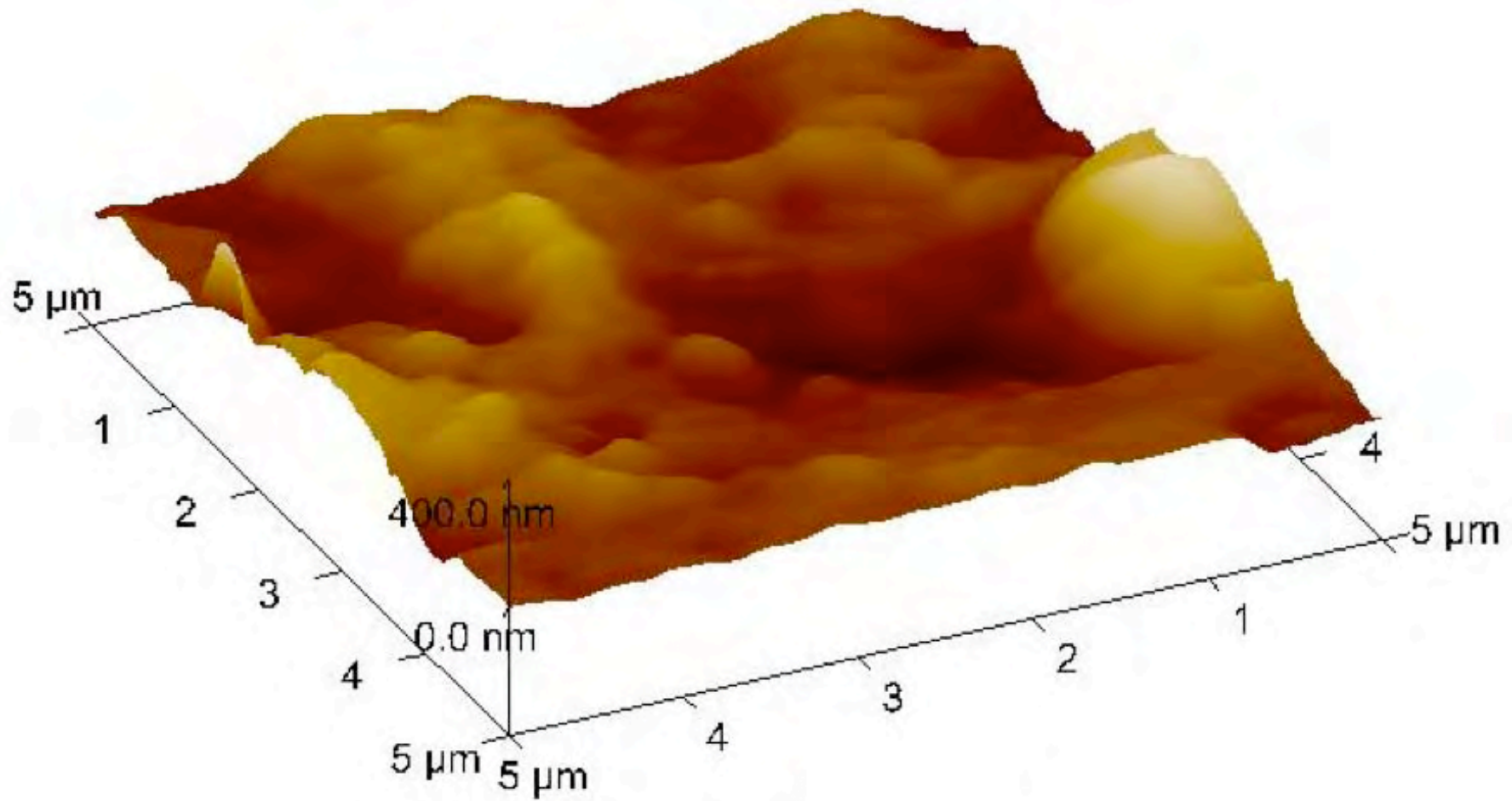
$$\frac{\partial h}{\partial t} = L_2 \frac{\partial^2}{\partial x^2} \left(-\gamma \frac{\partial^2 h}{\partial x^2} + \frac{k}{2^\mu} \frac{\partial h}{\partial x} \right)$$

Biocorrosion

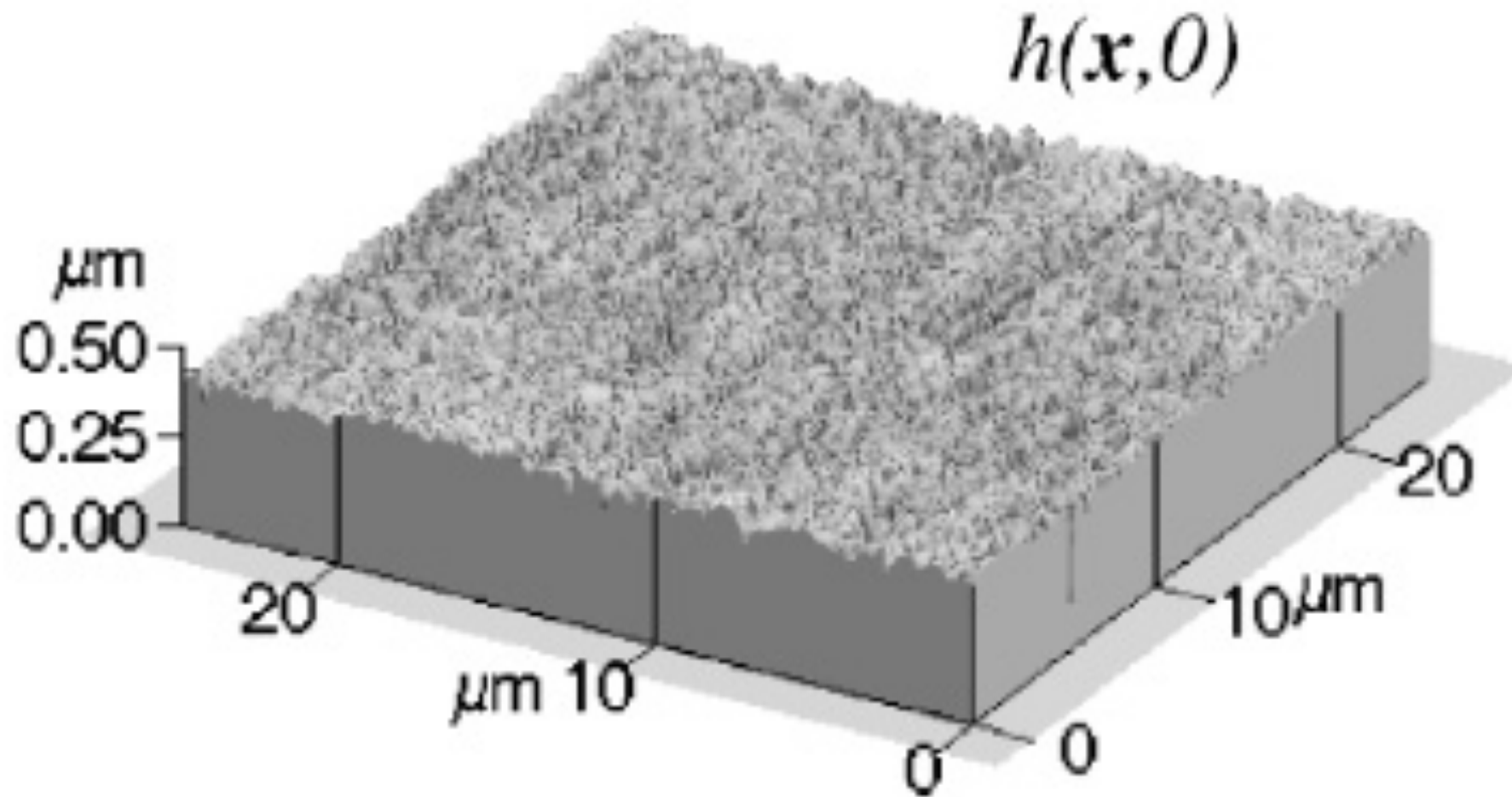


Competing mechanisms
SD - surface diffusion
SC - stress corrosion





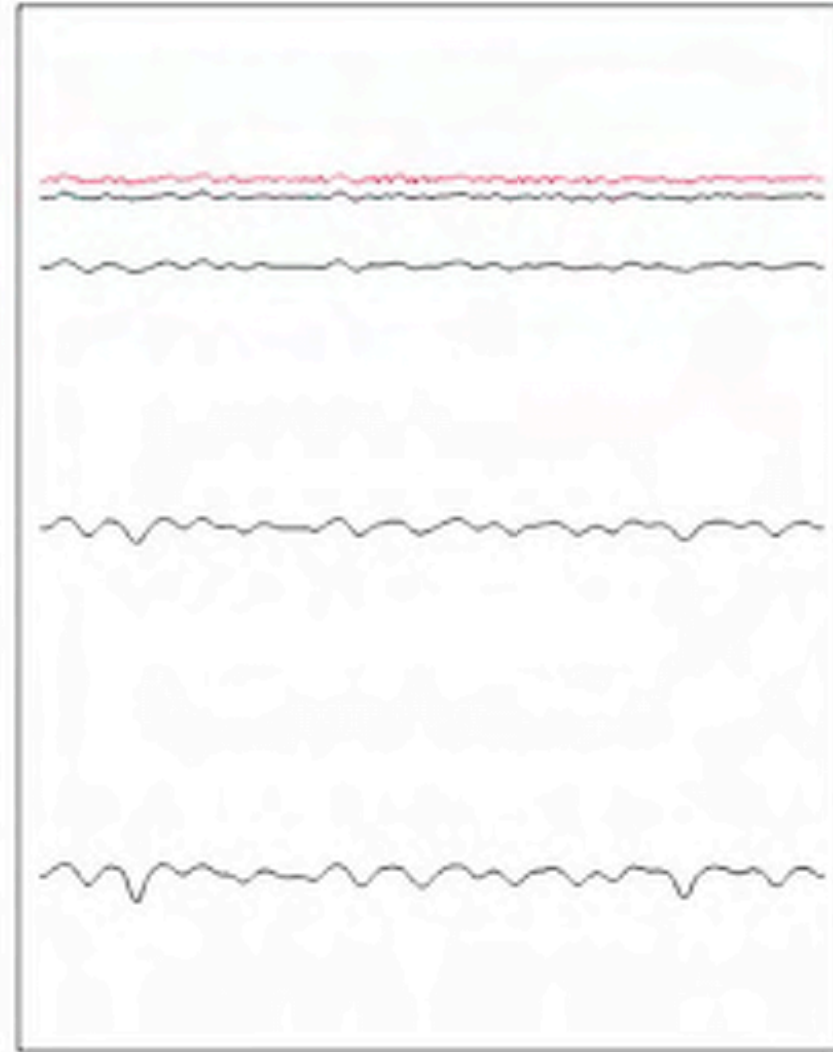
AFM image of corroded EBM surface (Hejman 06)



AFM image of shallow etched aluminium (Kim *et al.* 2000)

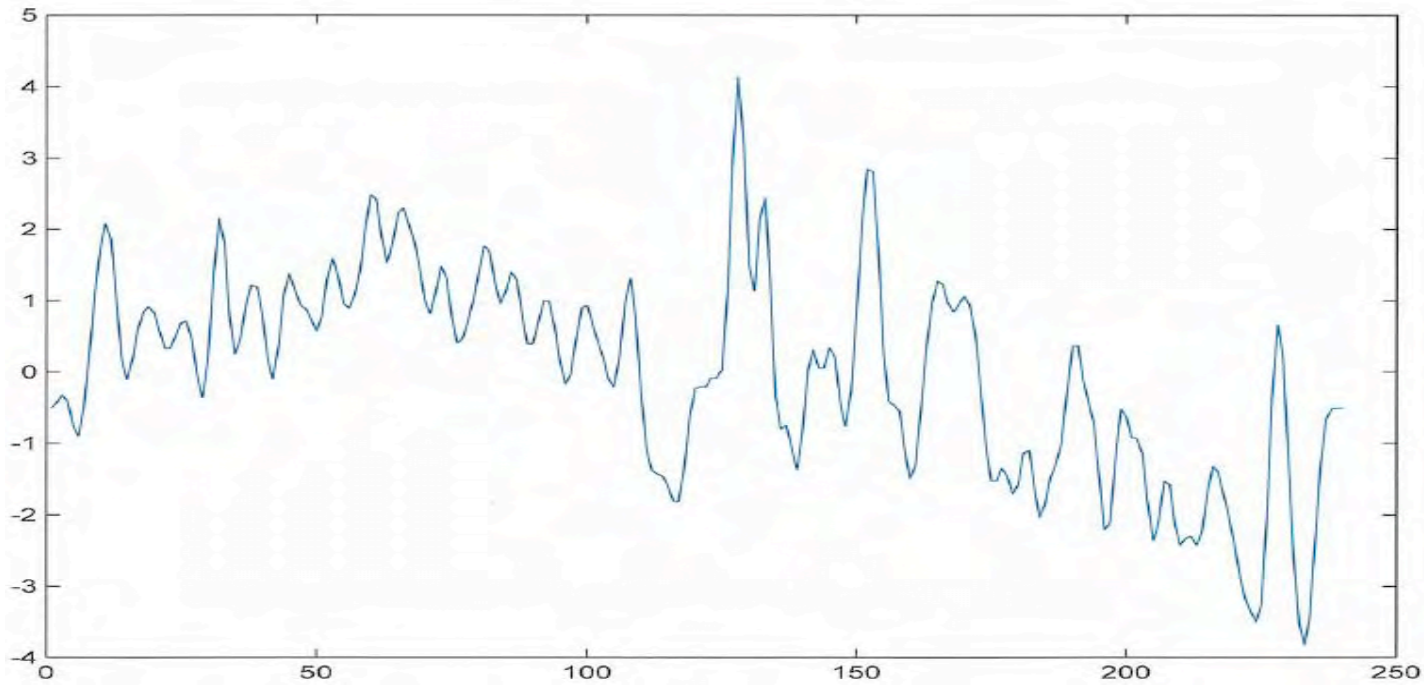
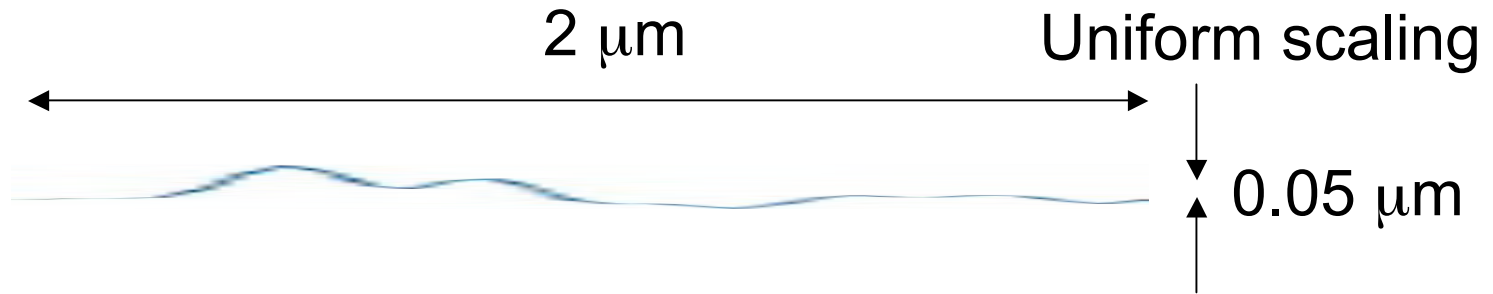
FEM calculation of an evolving surface

Increasing time
and depth



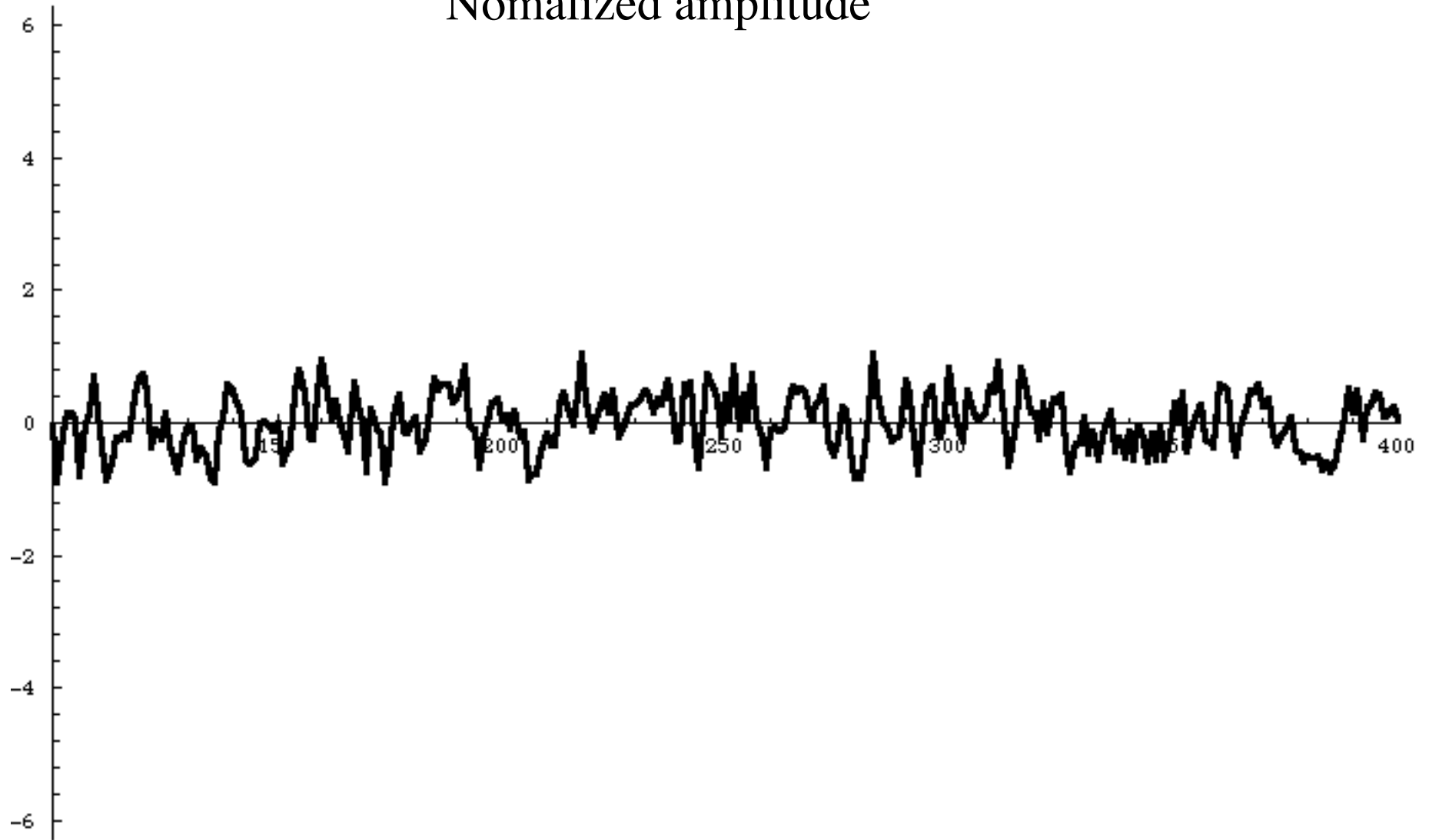
Original surface

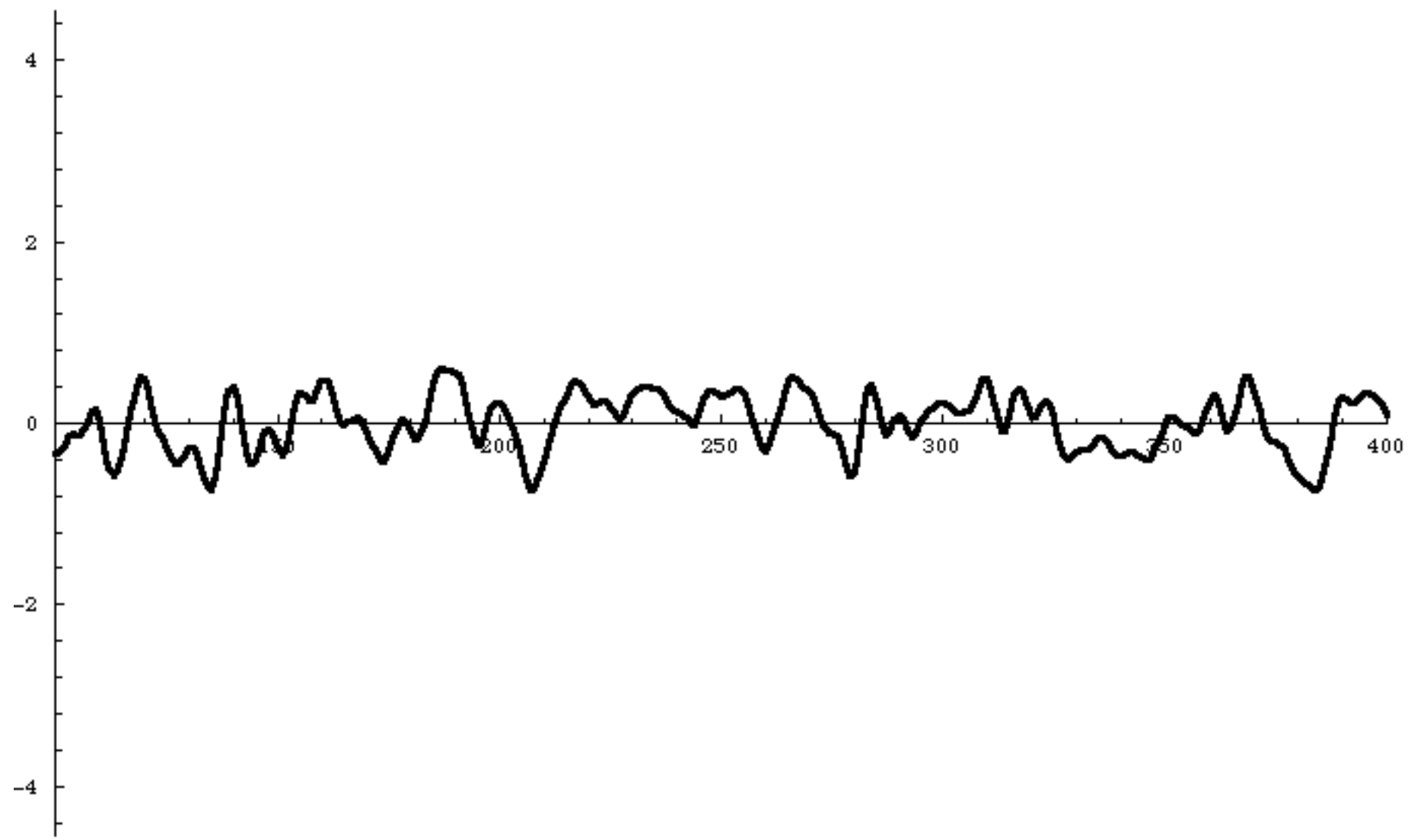
Surface Roughness

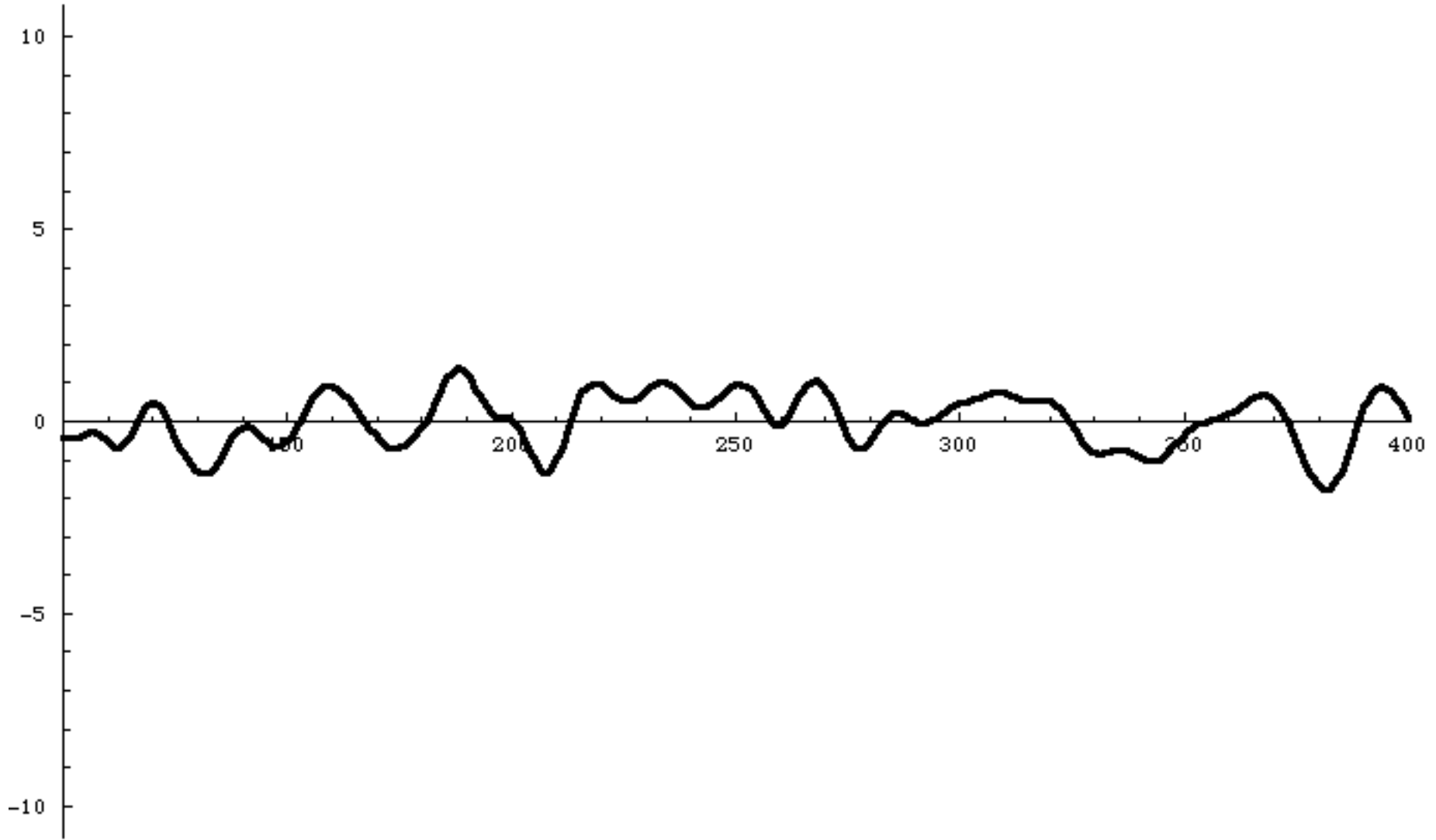


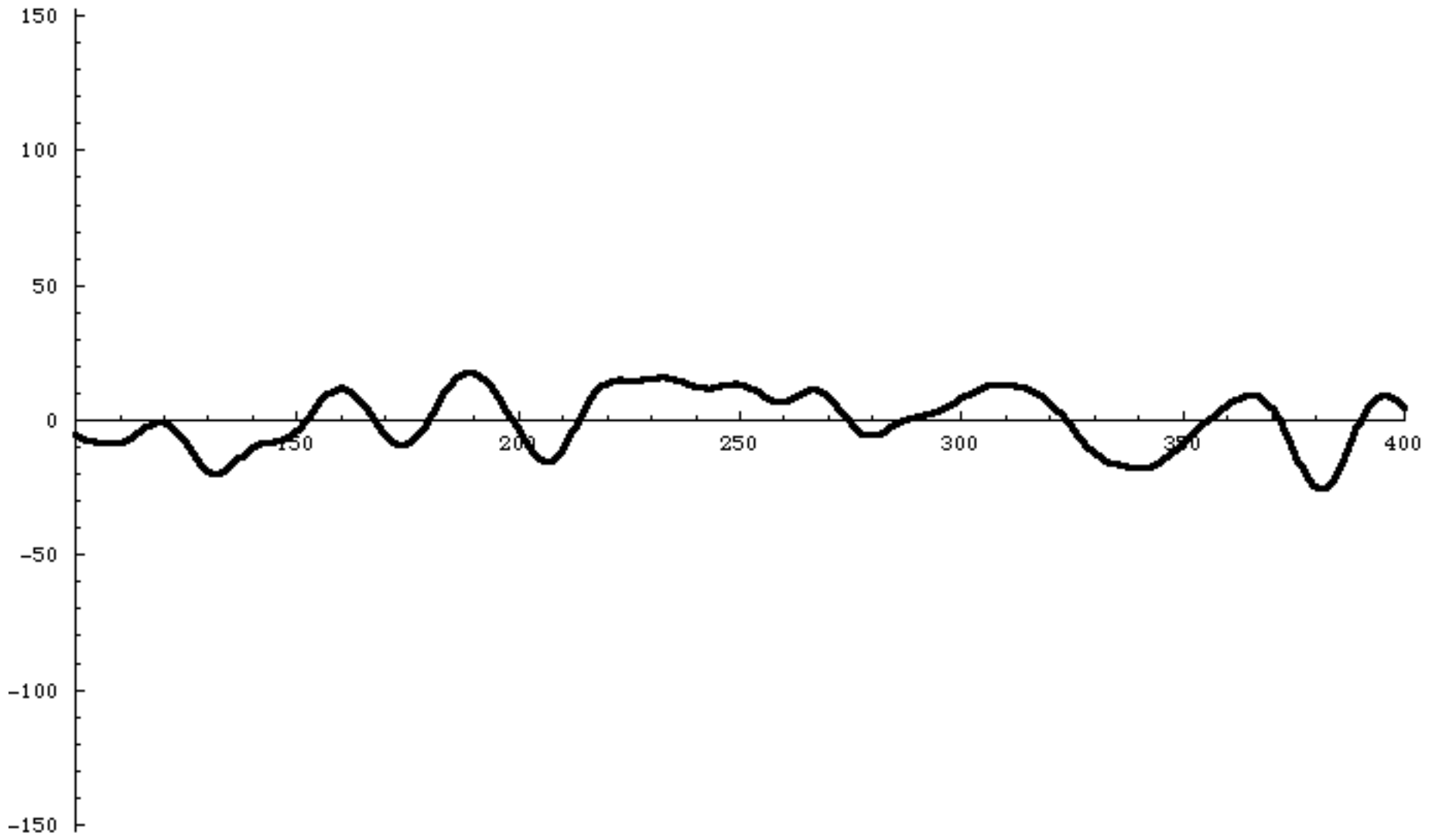
From Kim Kung Suk

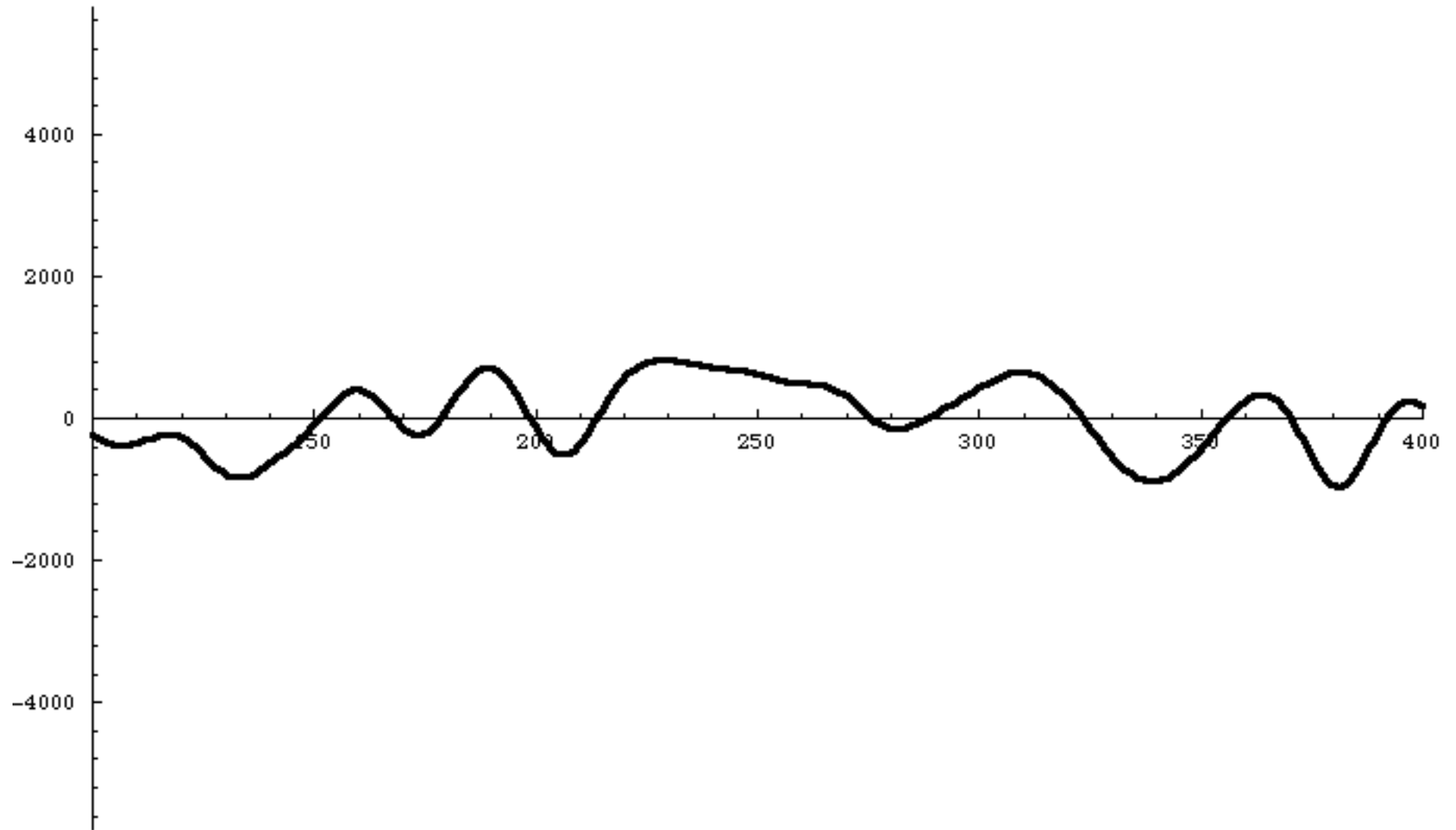
Normalized amplitude

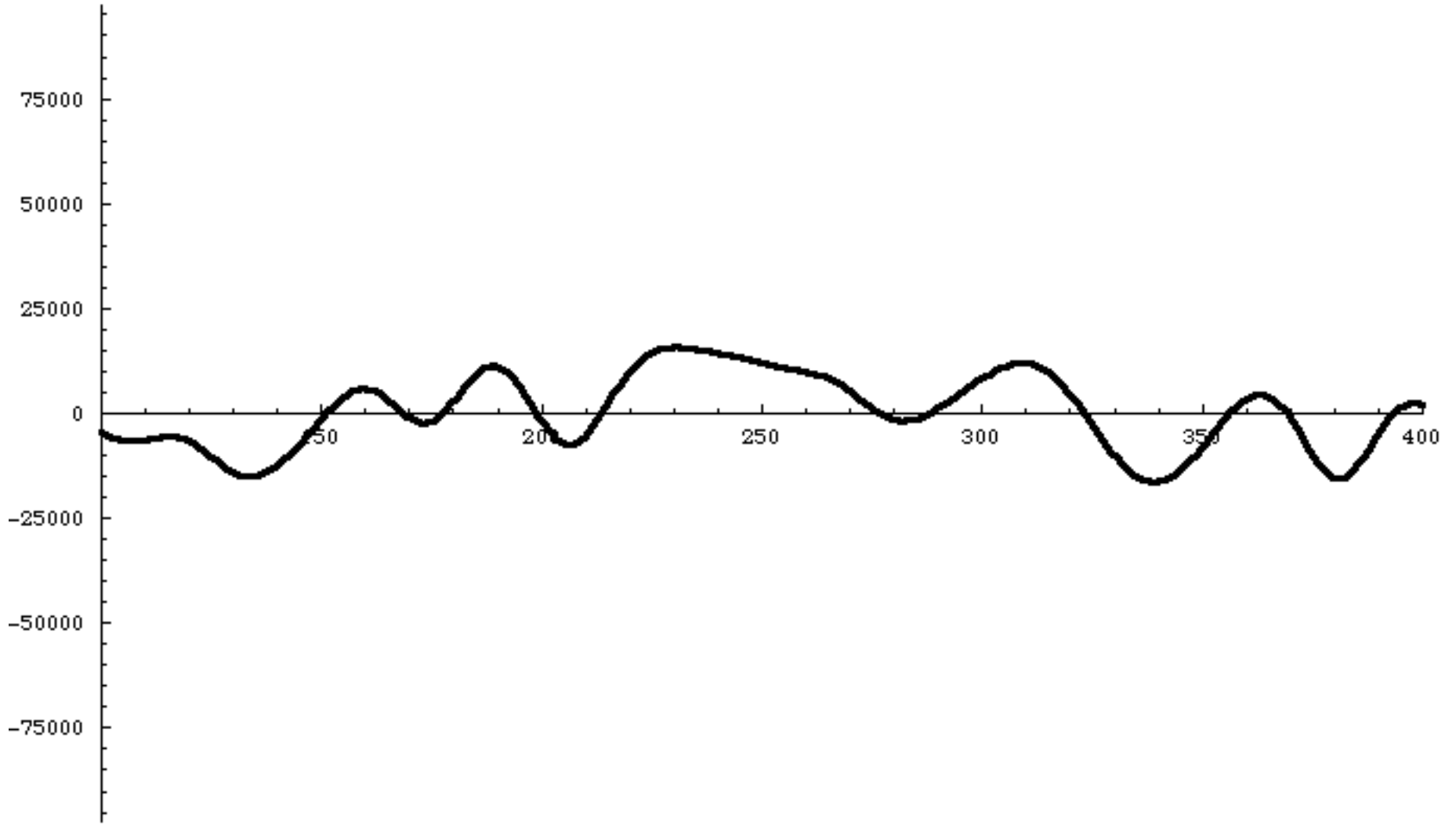




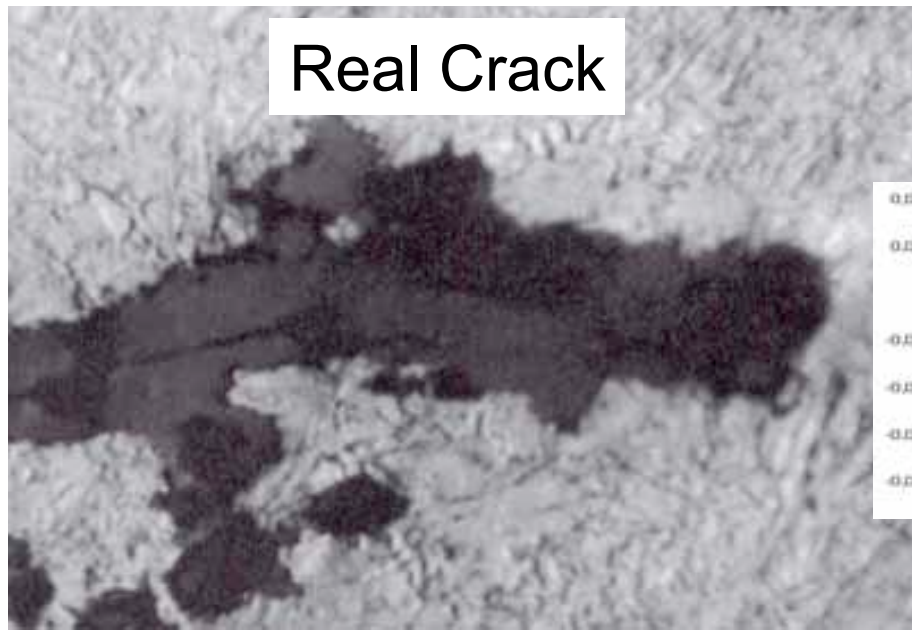




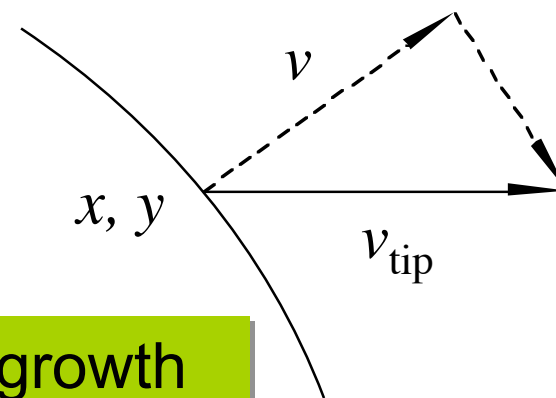
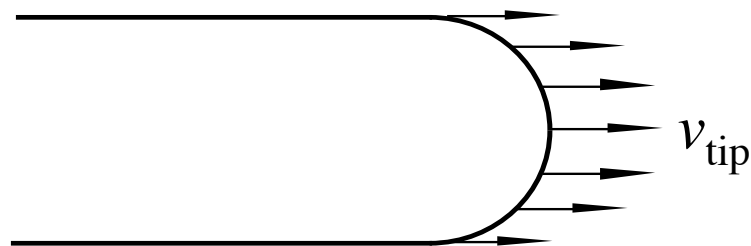
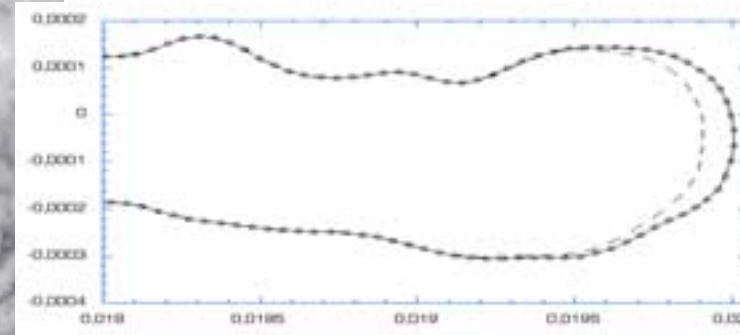




Steady State Crack-tip Shape

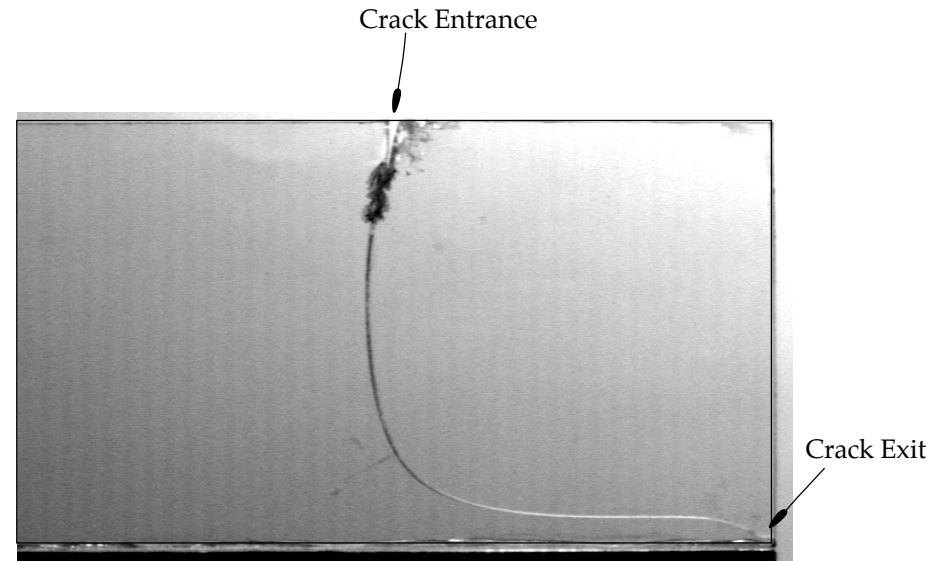
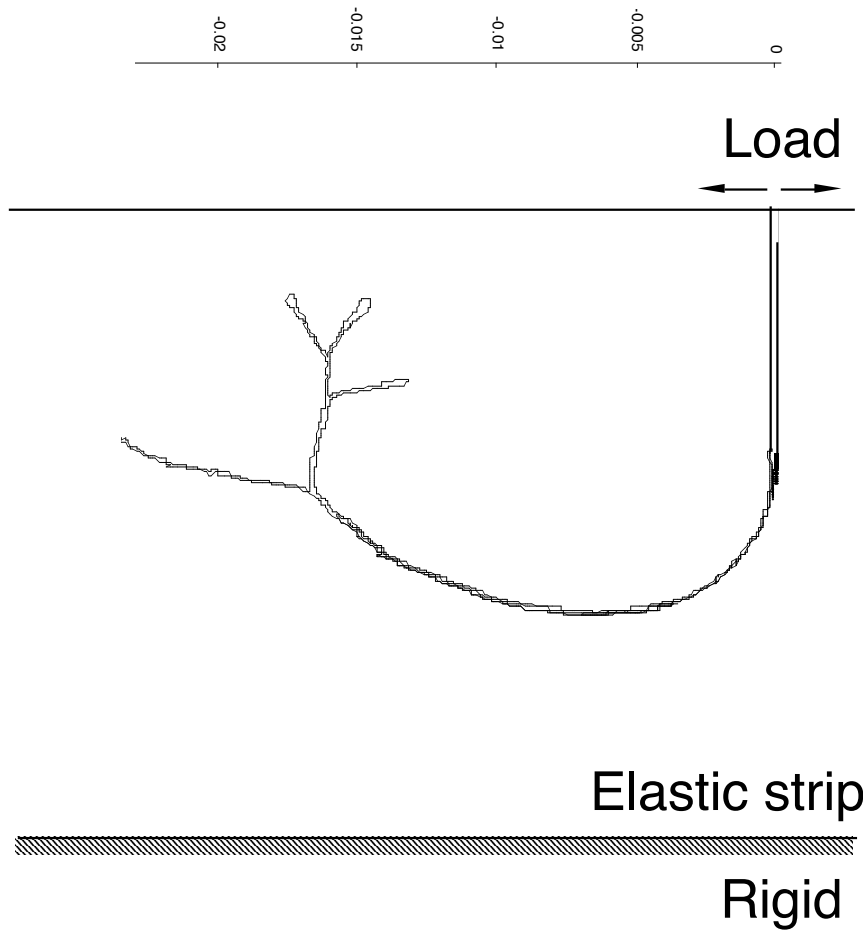


FEM result

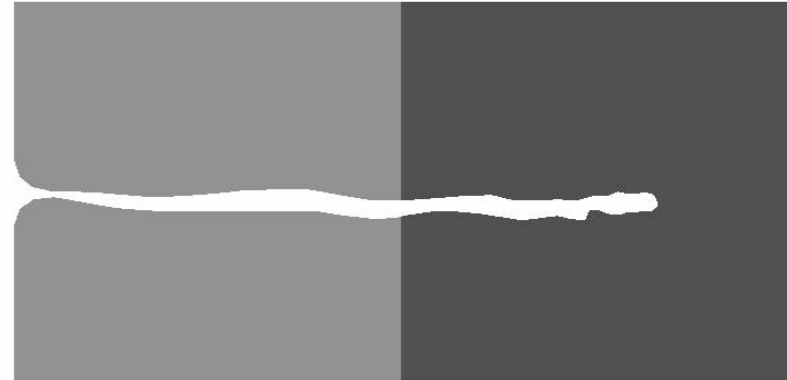
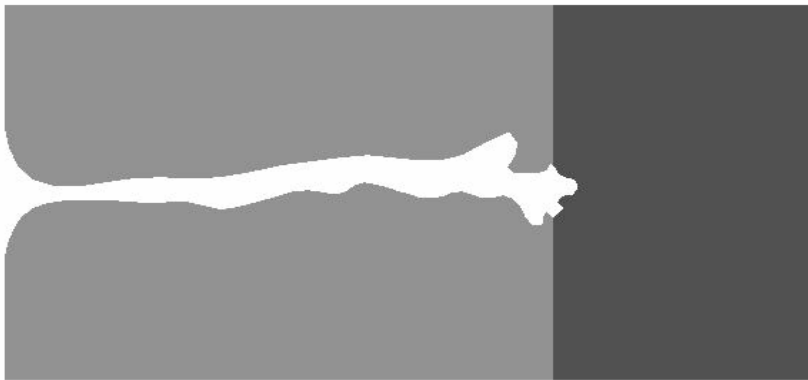
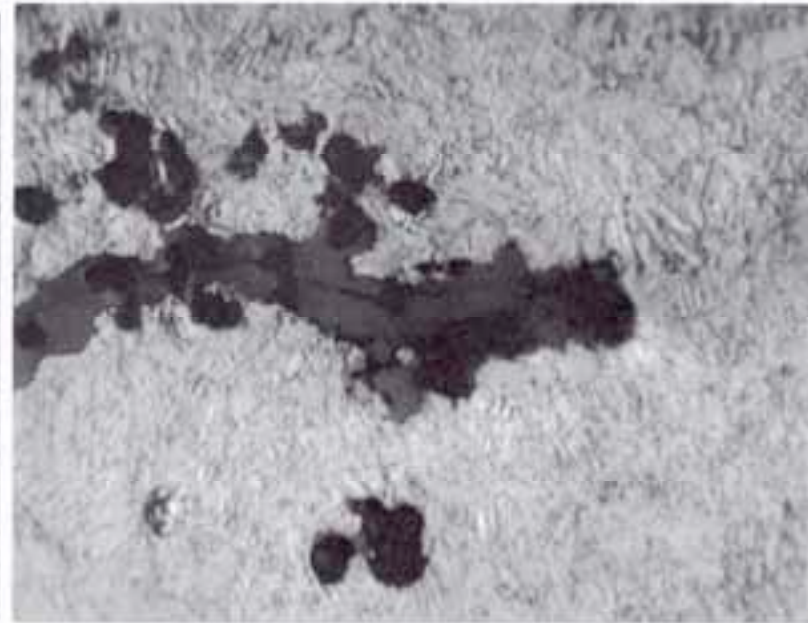
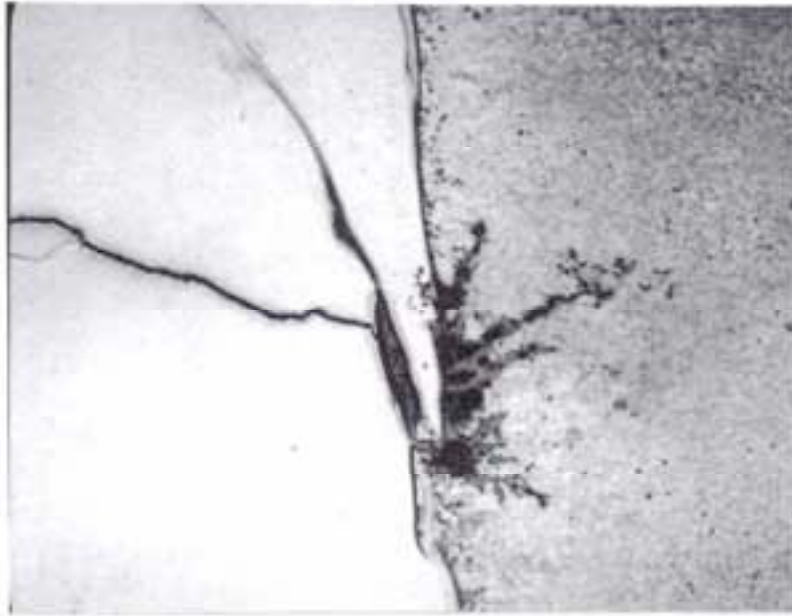


Constant Component in the growth
direction: $v = (x/\rho) v_{\text{tip}}$

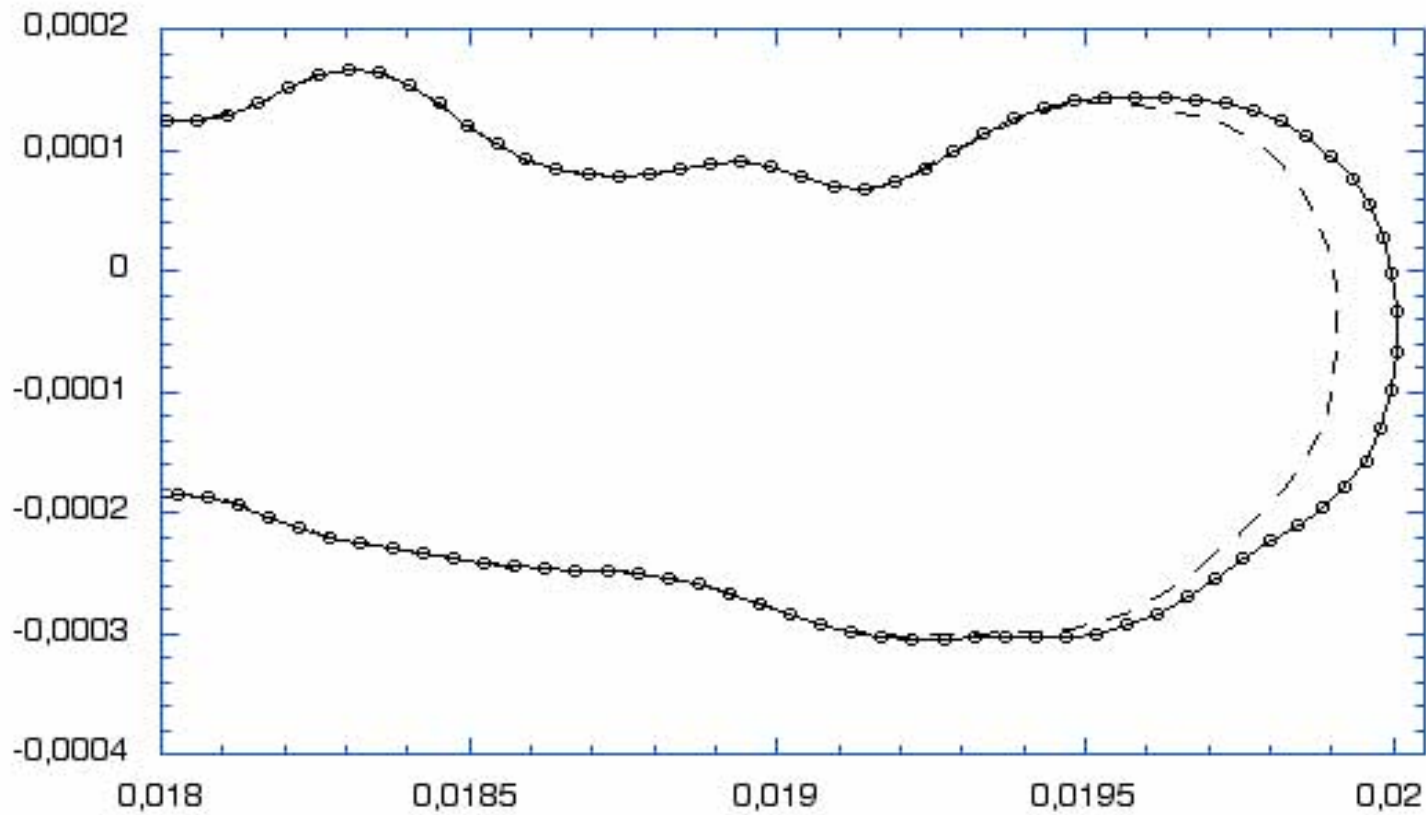
Crack seem to follow a mode I path



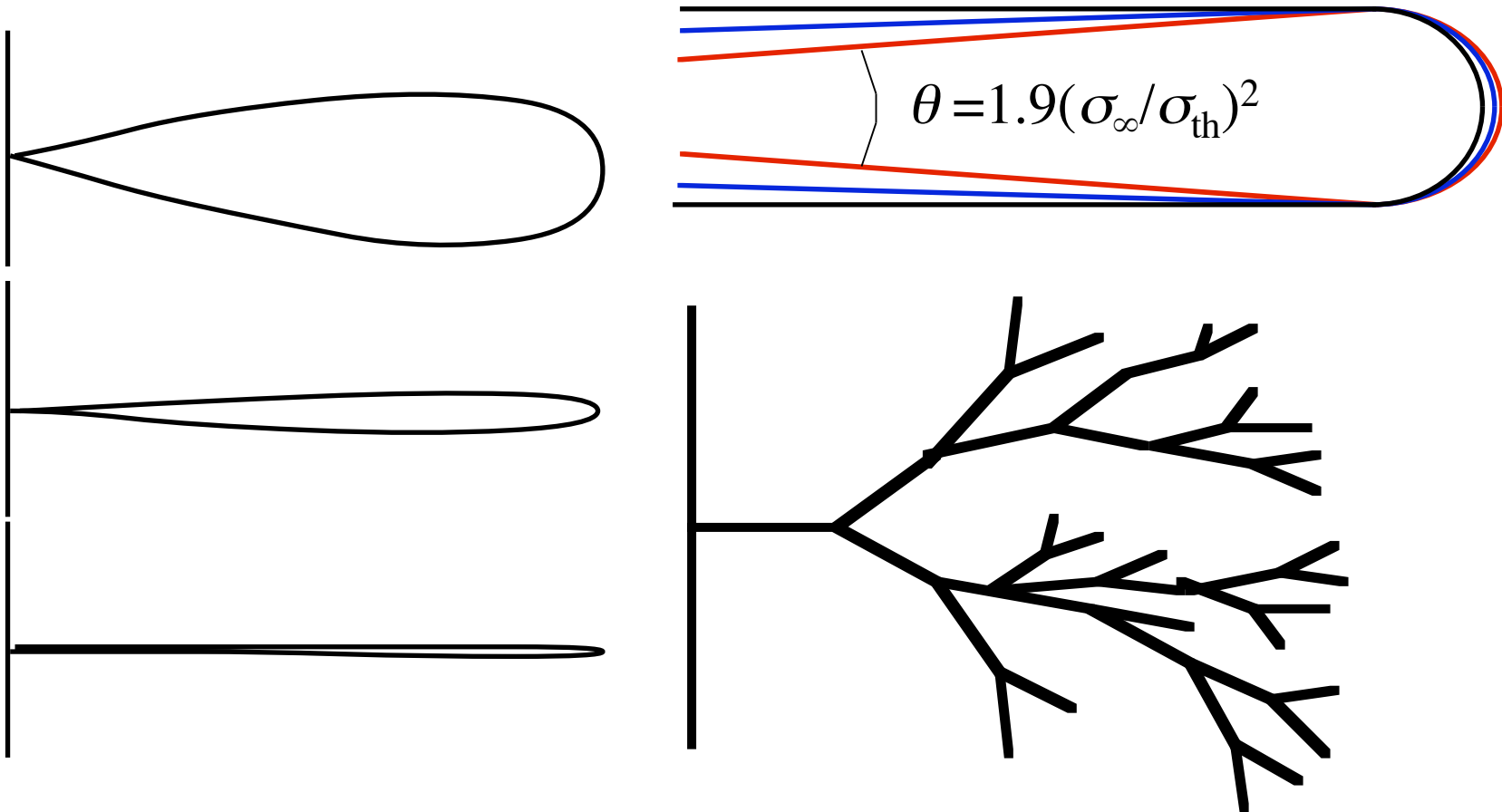
From Cladding to Grey Material



Steady-state Advancing Crack Tip



Missing lengthparameter => Selfsimilar growth



2. Cusp solutions

Spencer and Meiron(94), Chiu and Gao (95),
Yang Xiang and Weinan (02)

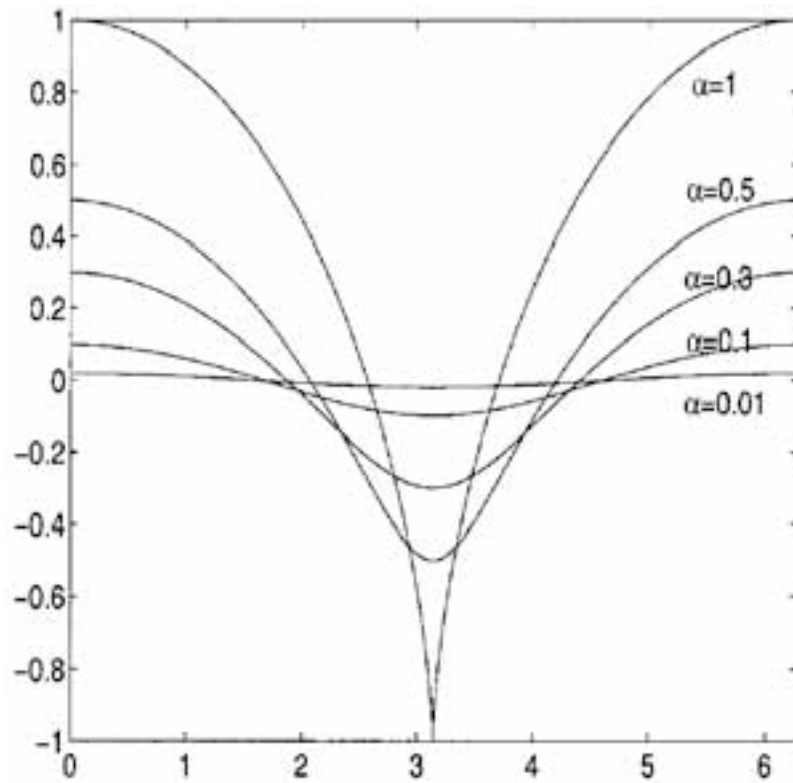


FIG. 1. Cycloid surfaces.

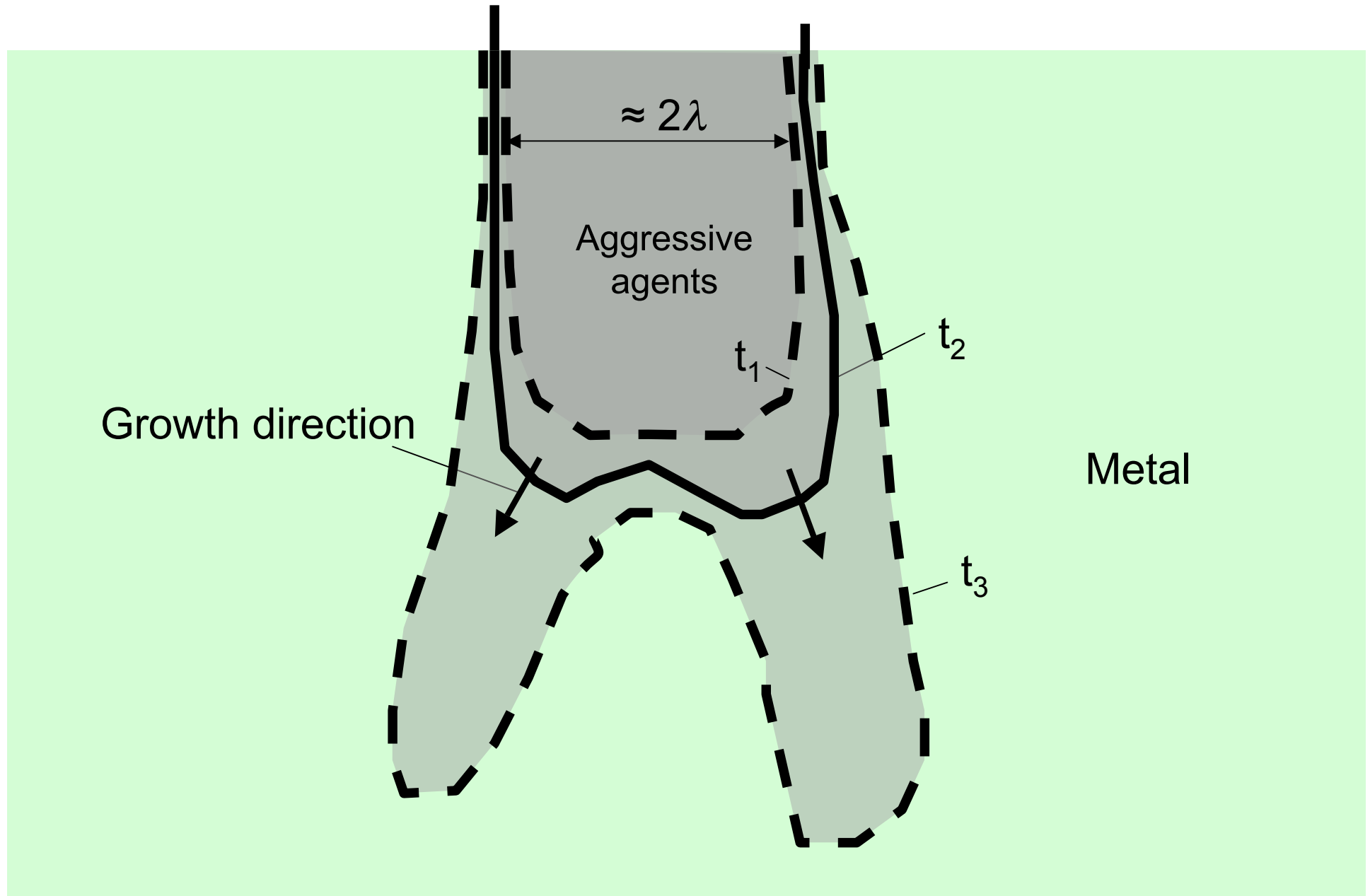


FEM stress corrosion

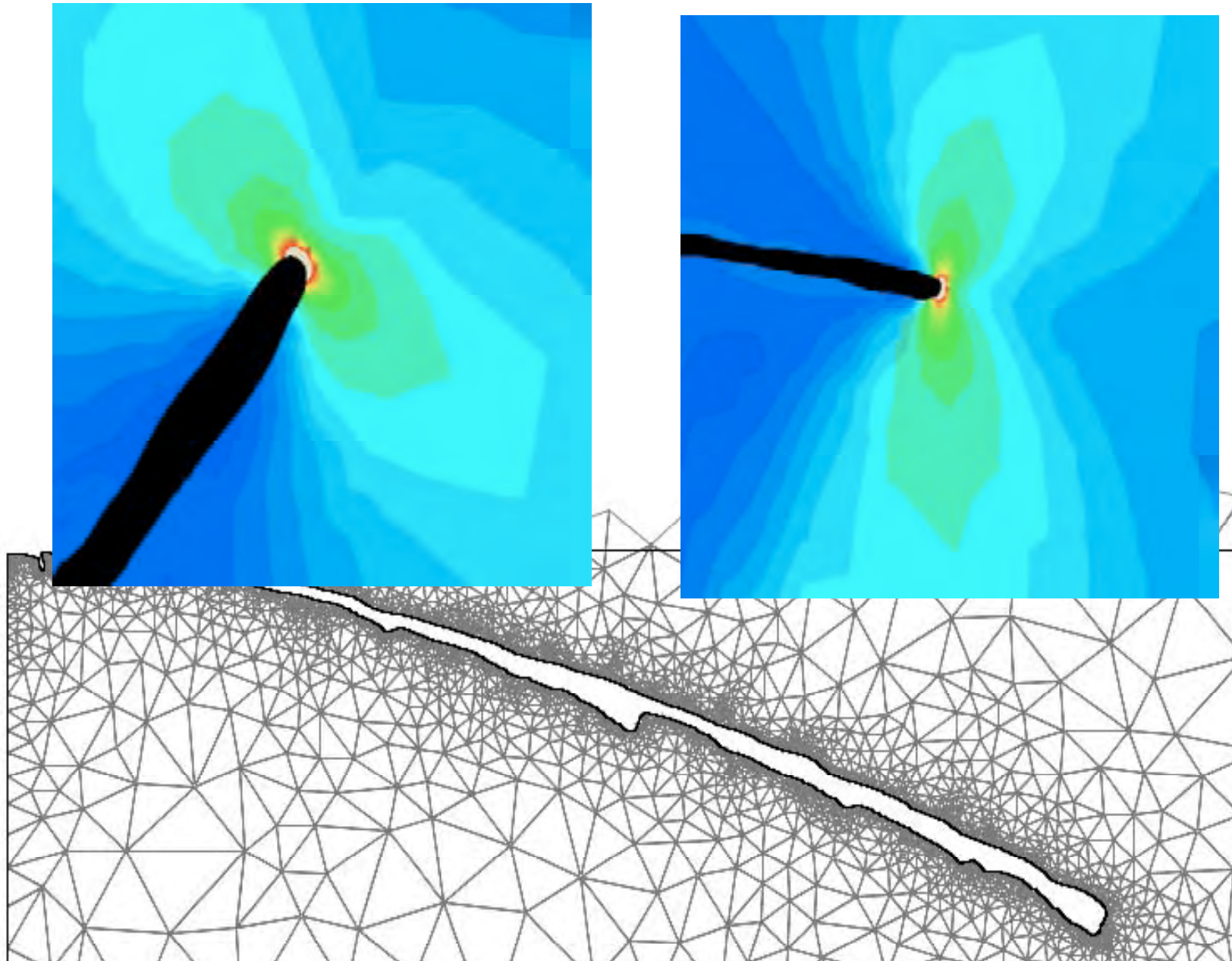
	$\varepsilon_f/\varepsilon_\infty = 0$	0.3	0.5	0.75	1	1.2
$\sigma_x/\sigma_y = 0$						
0.5						
0.7						
0.9						



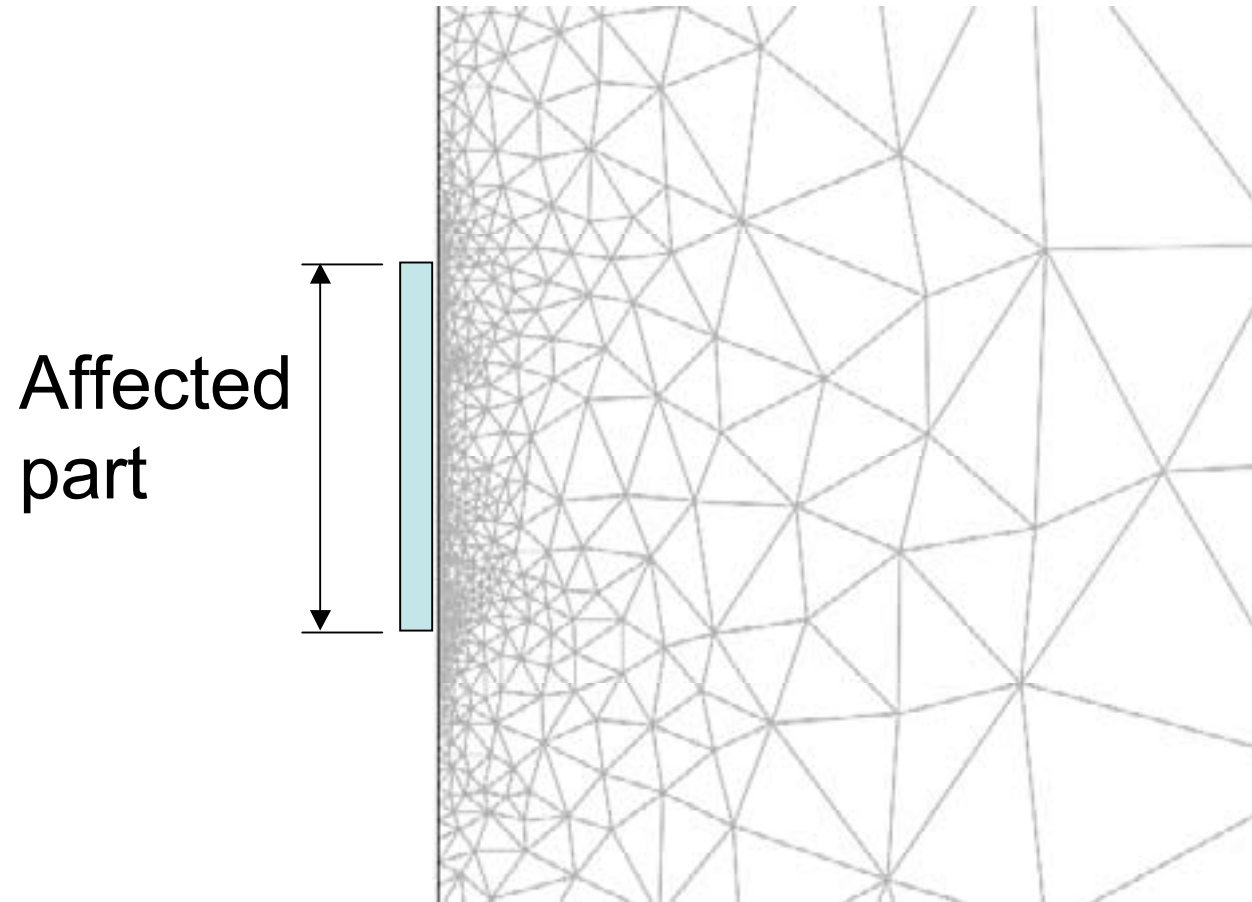
Branching



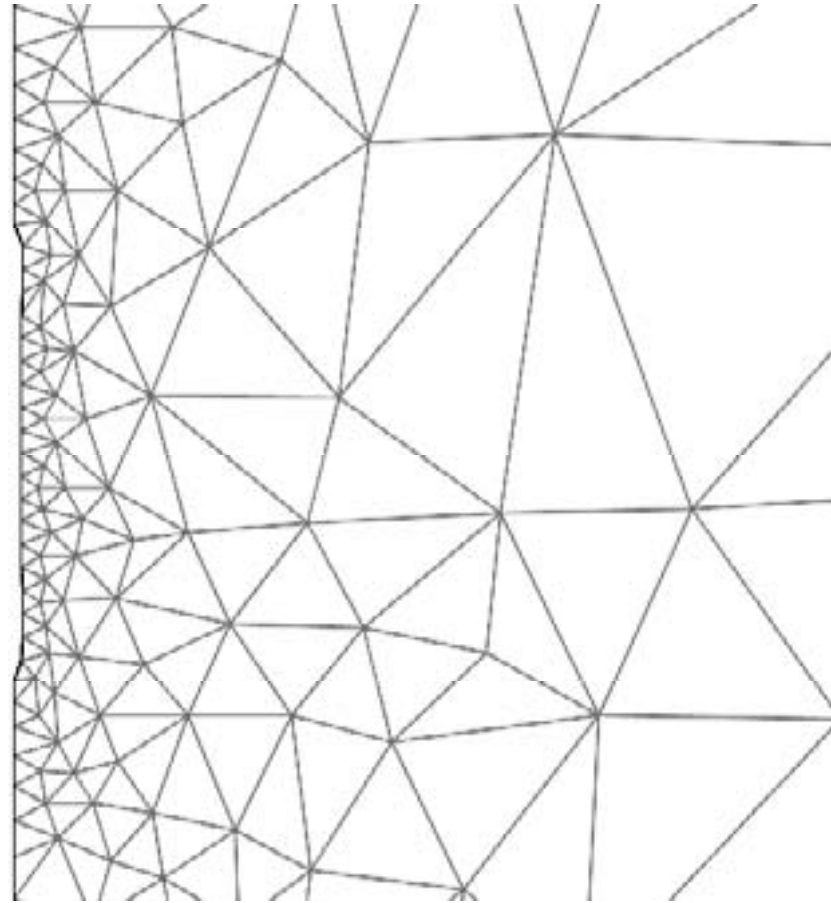
Crack-tip Load



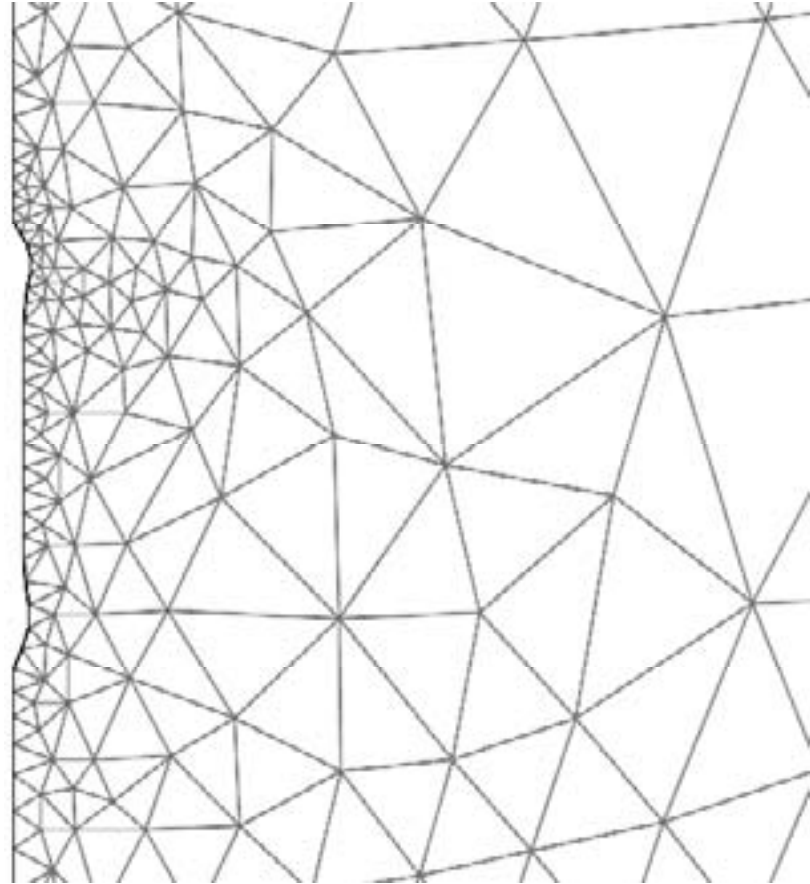
Corroding Surface



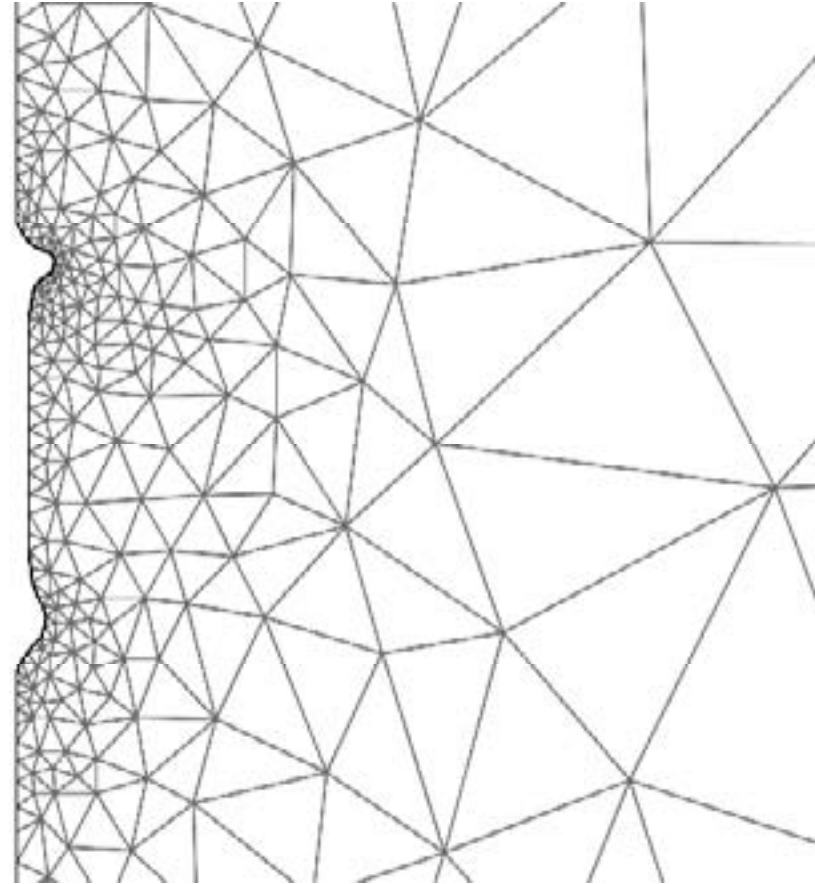
Corroding Surface



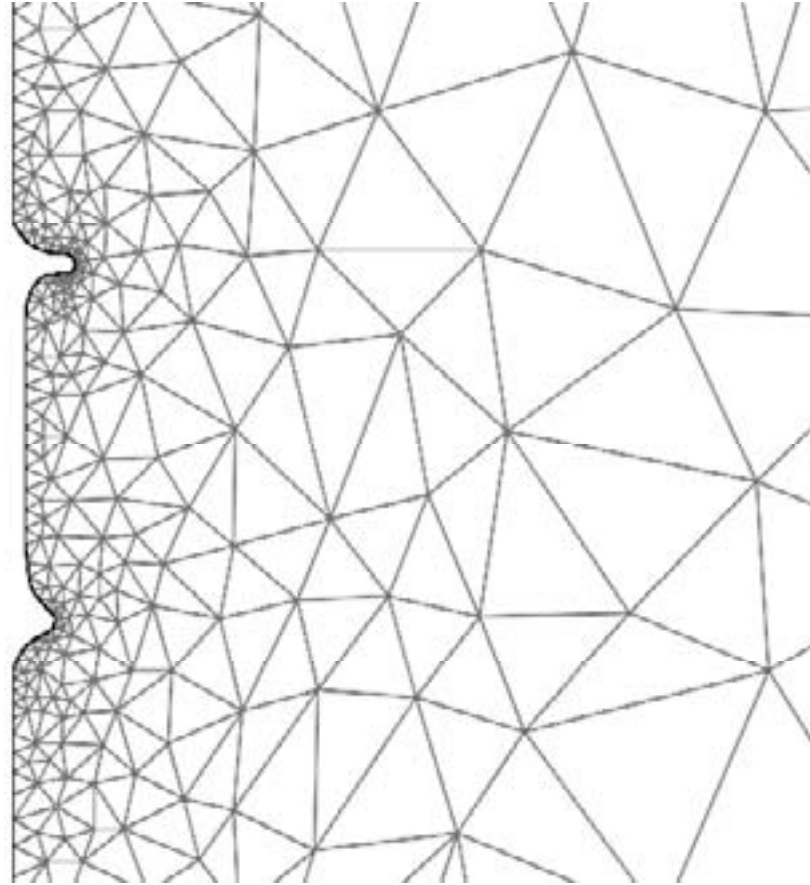
Corroding Surface



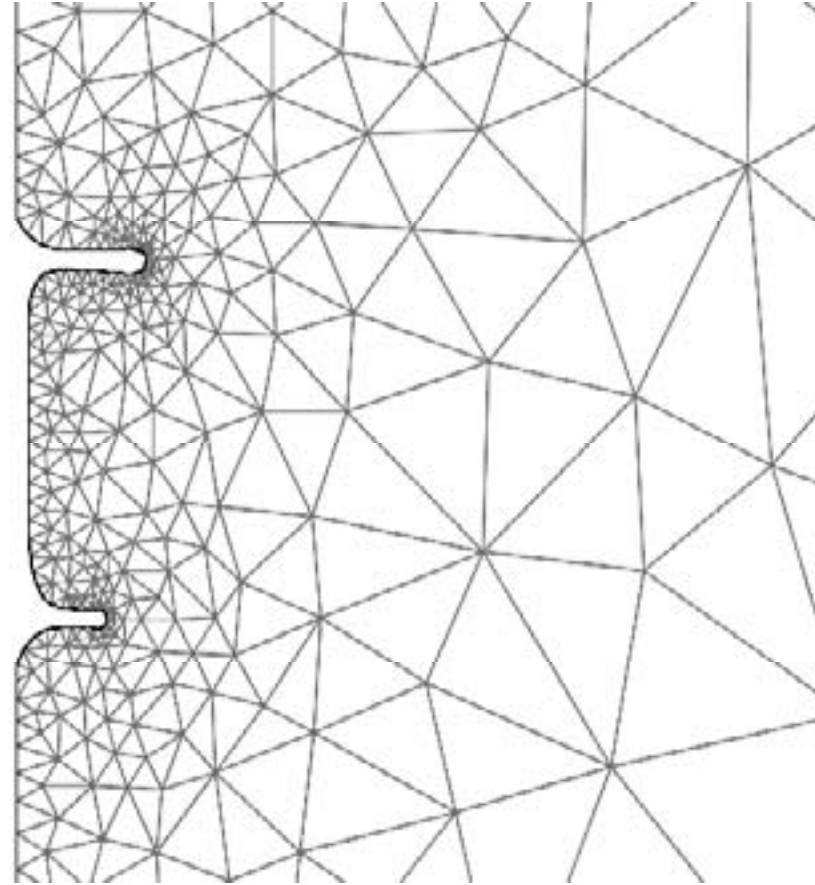
Corroding Surface



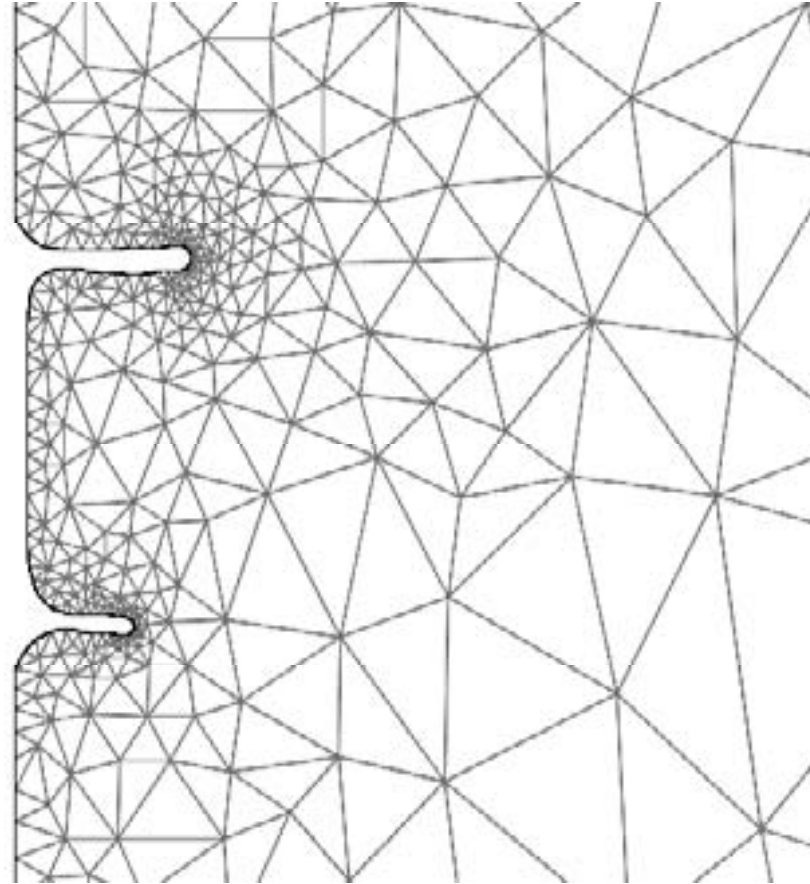
Corroding Surface



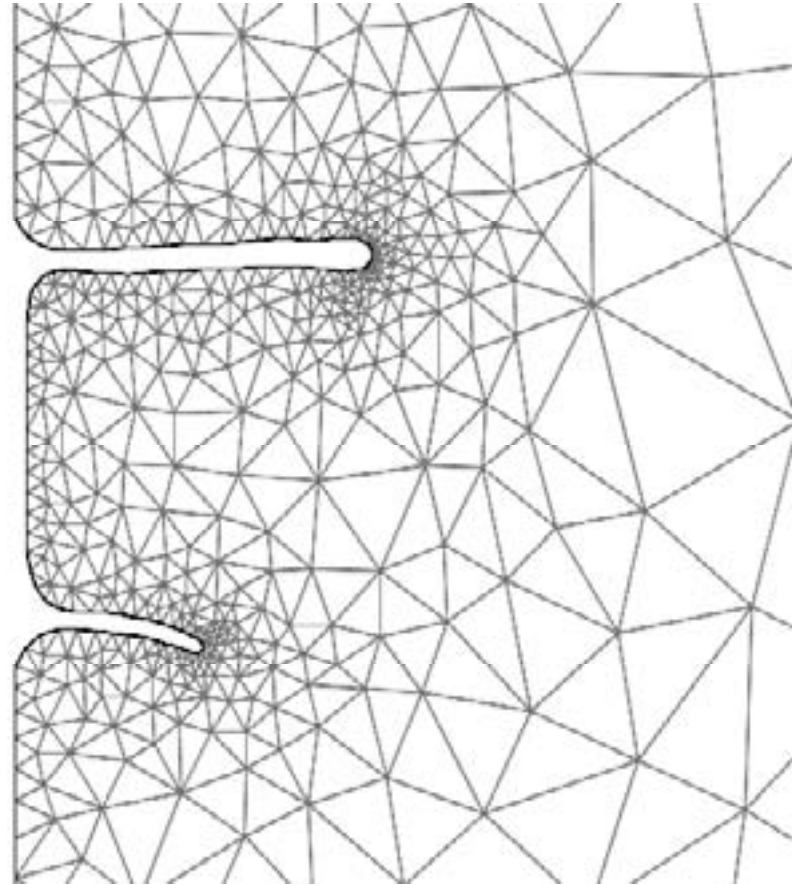
Corroding Surface



Corroding Surface



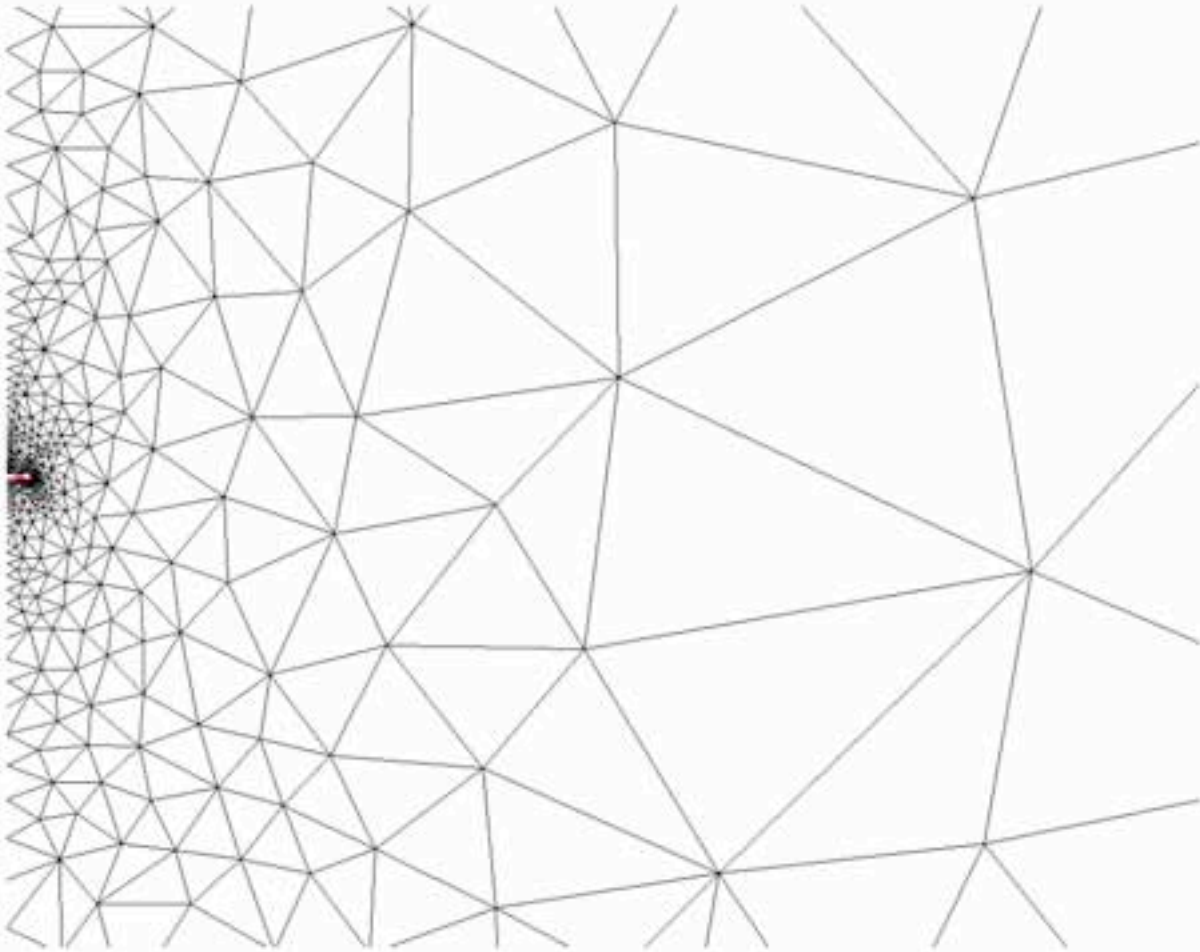
Corroding Surface



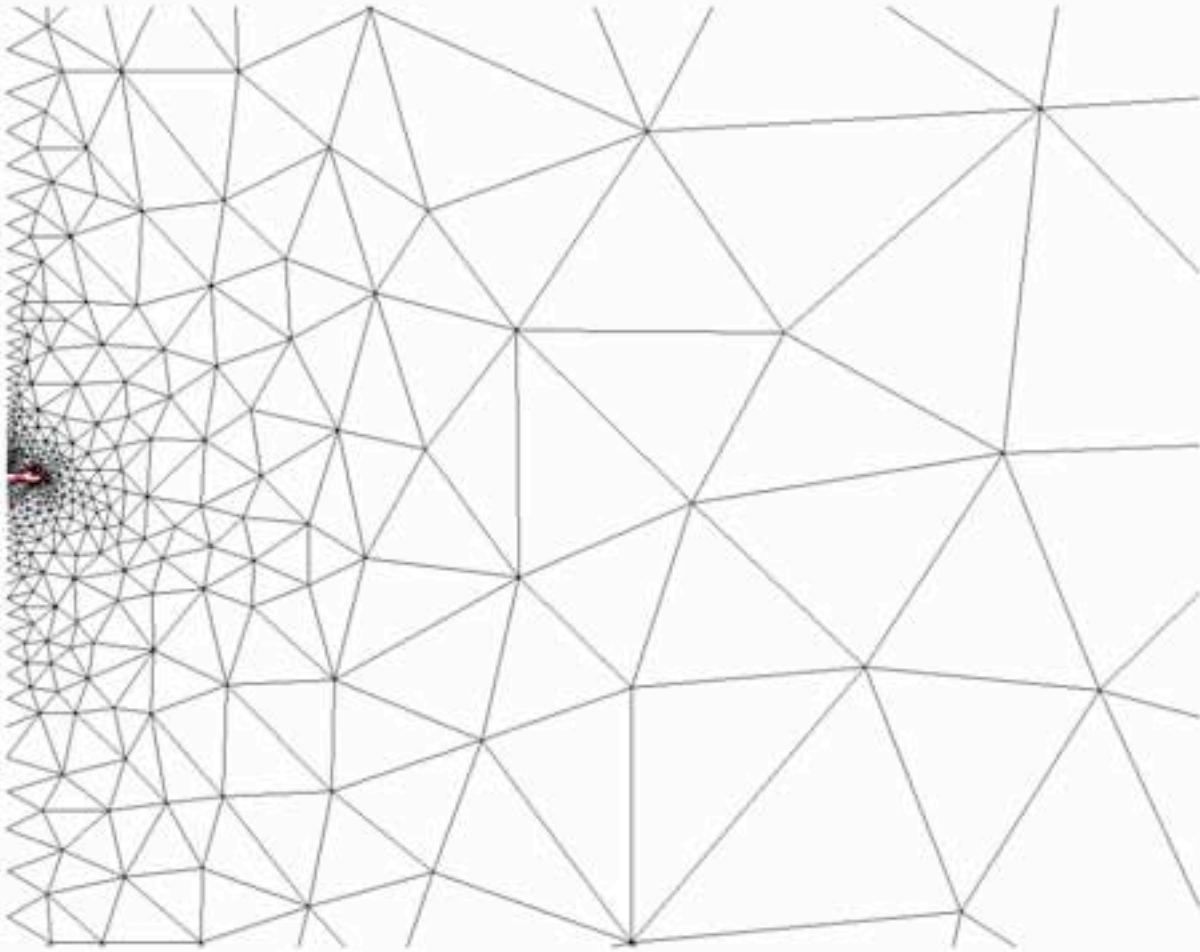
Branching



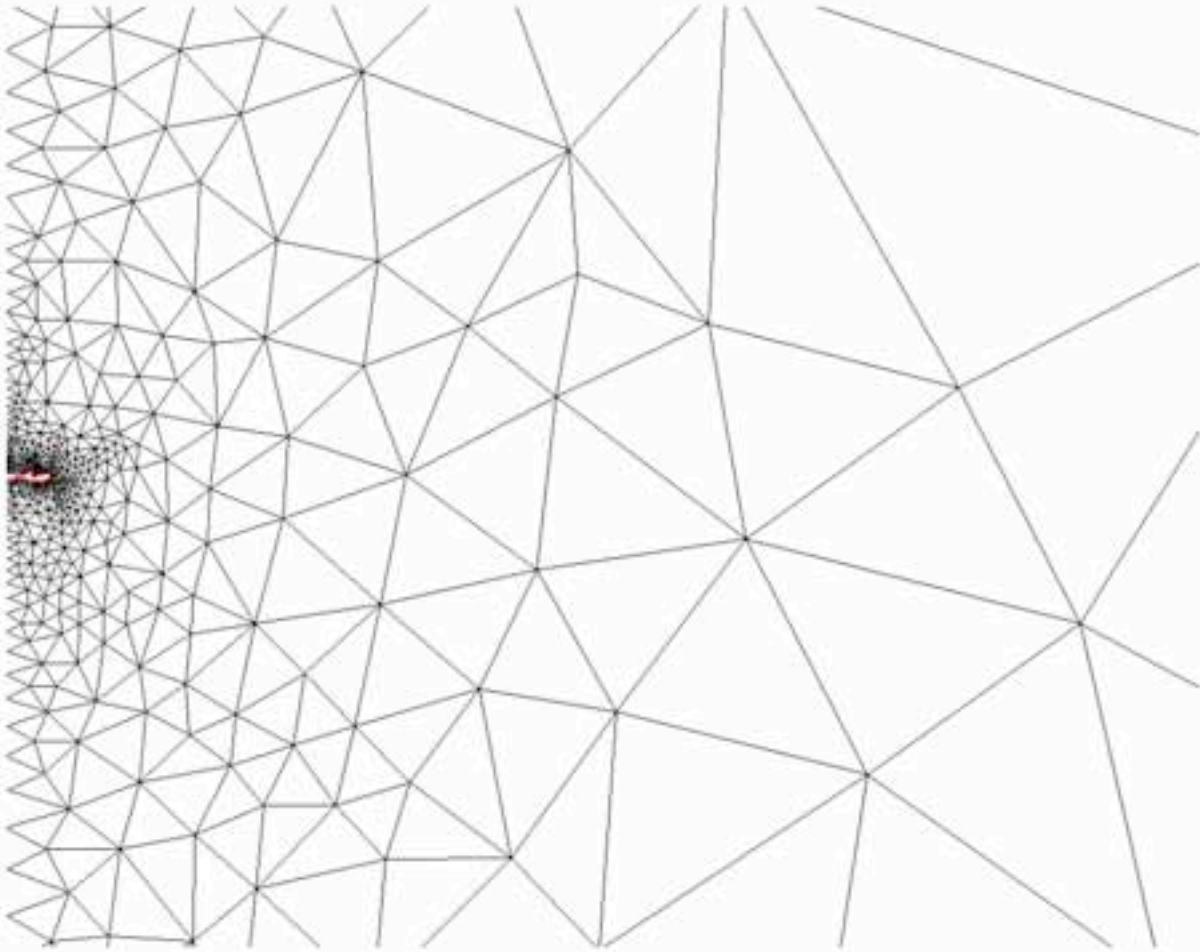
Branching



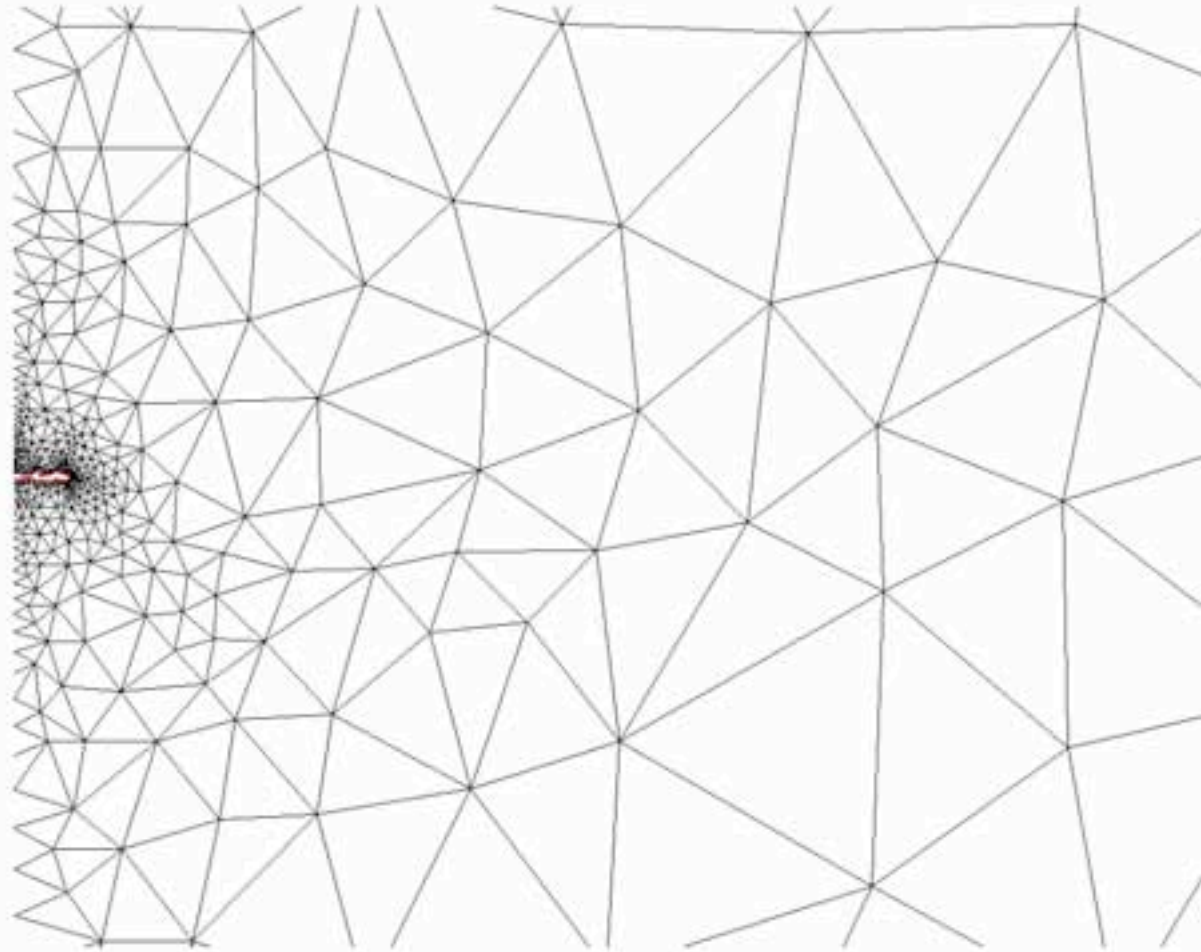
Branching



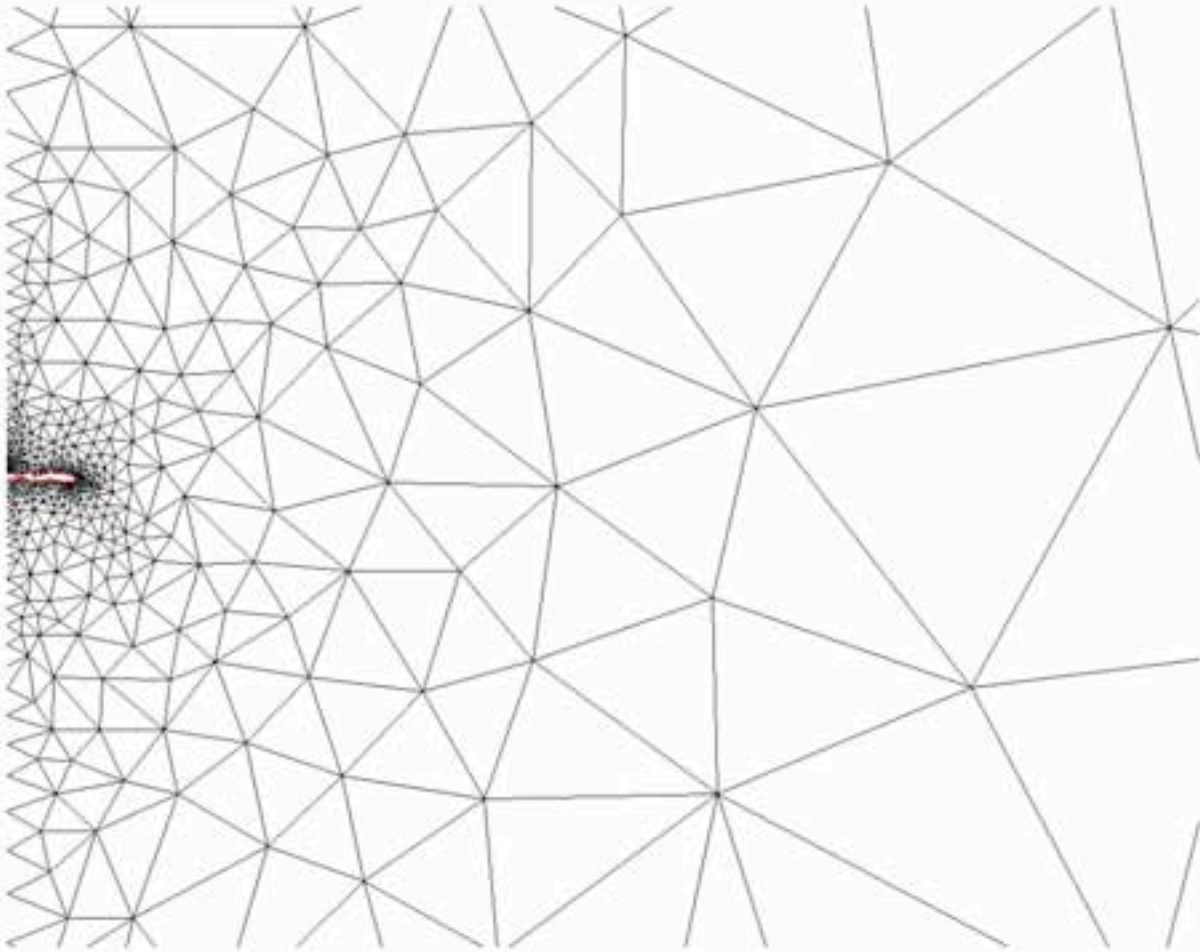
Branching



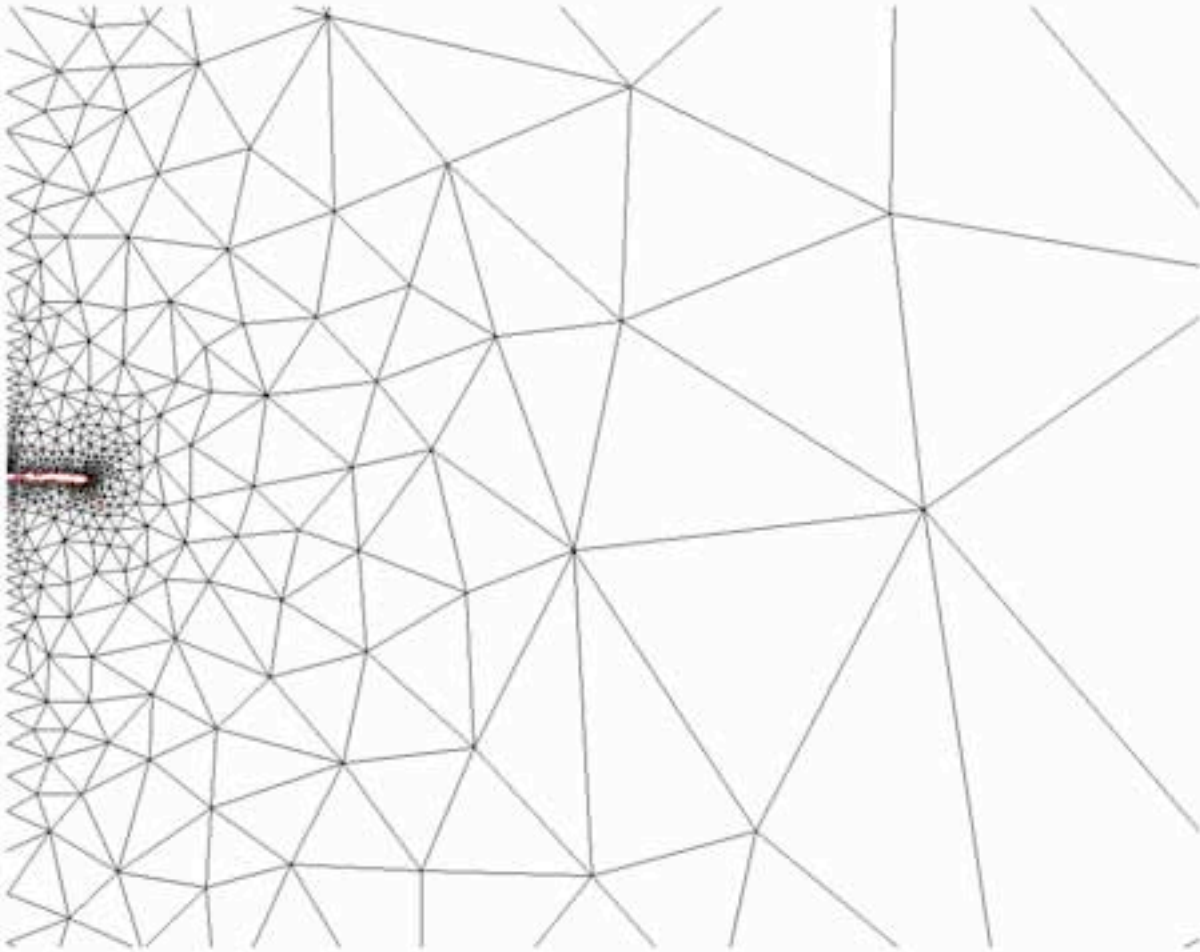
Branching



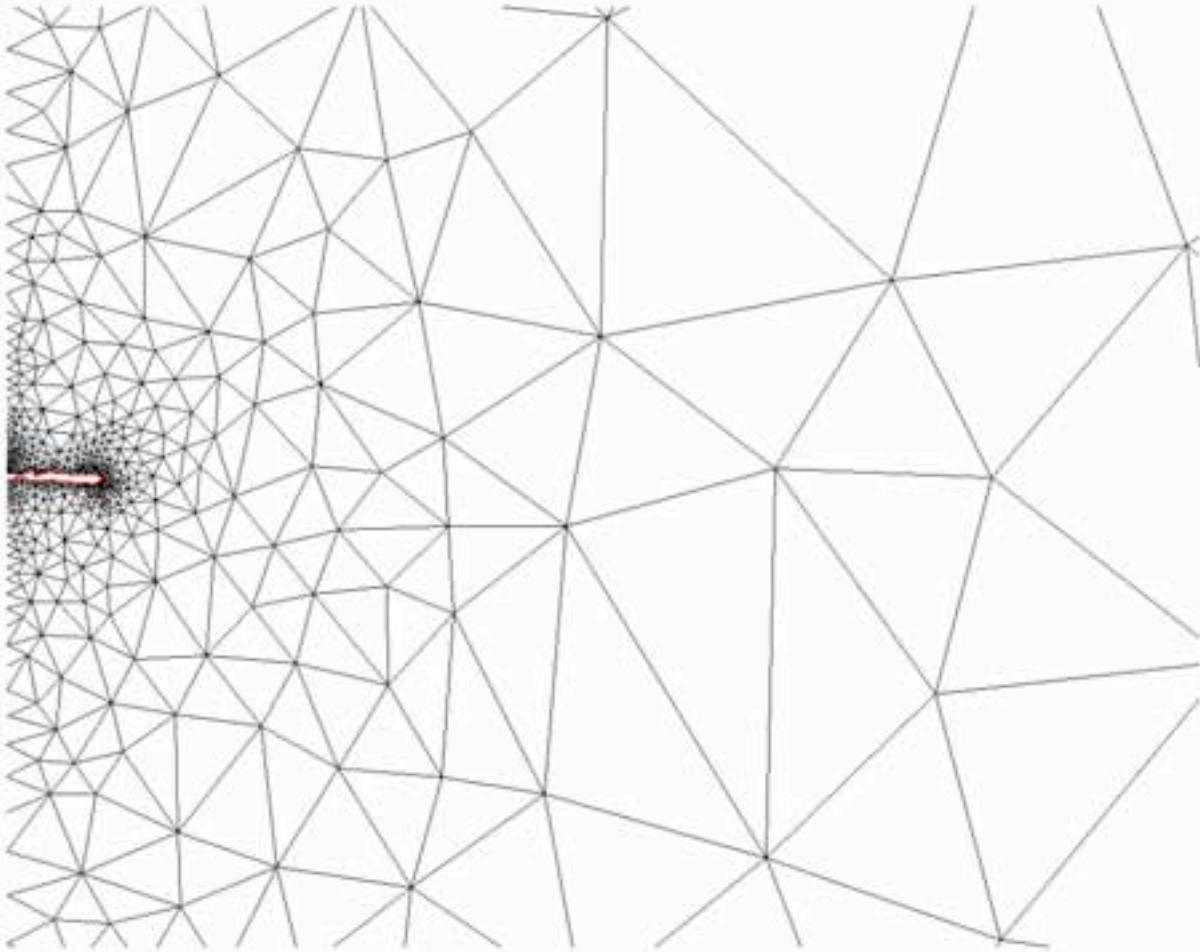
Branching



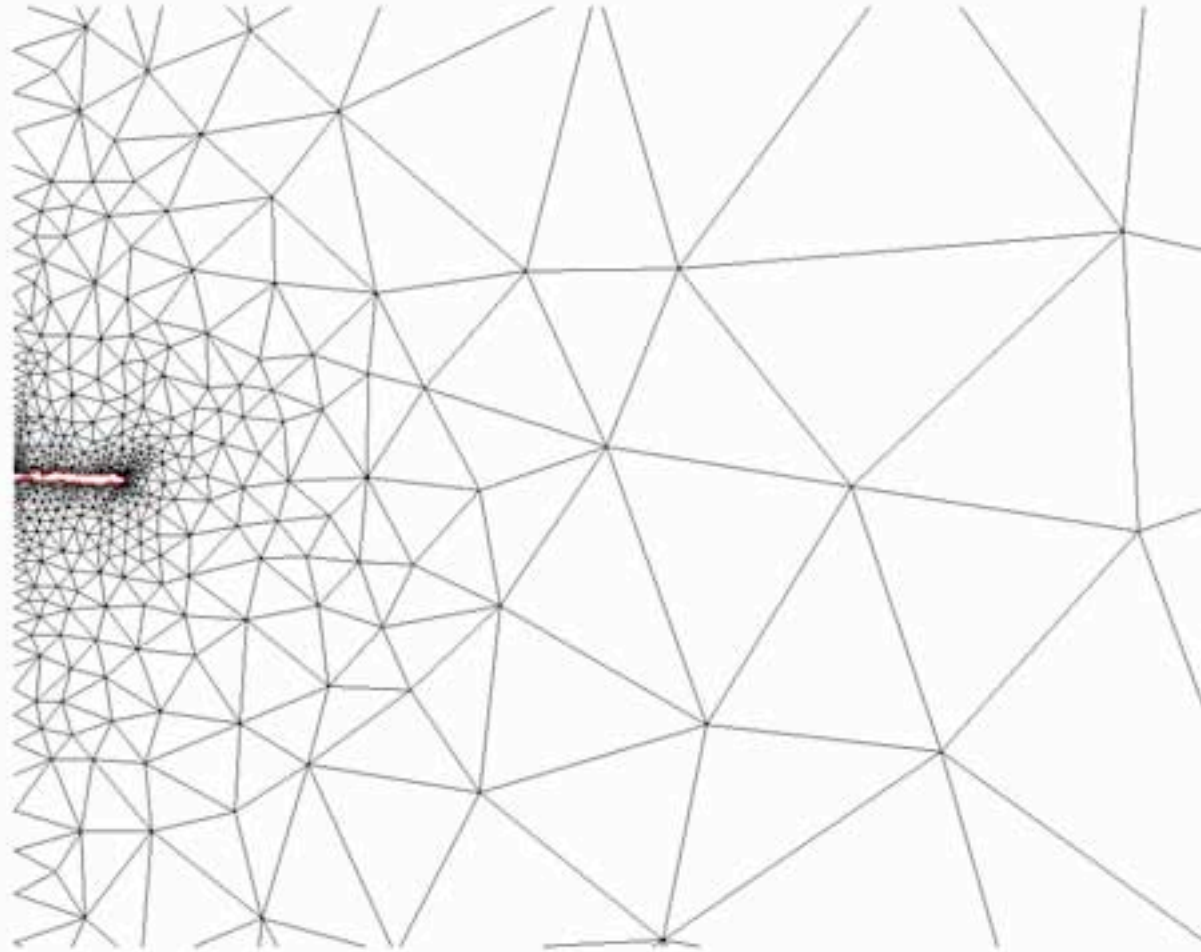
Branching



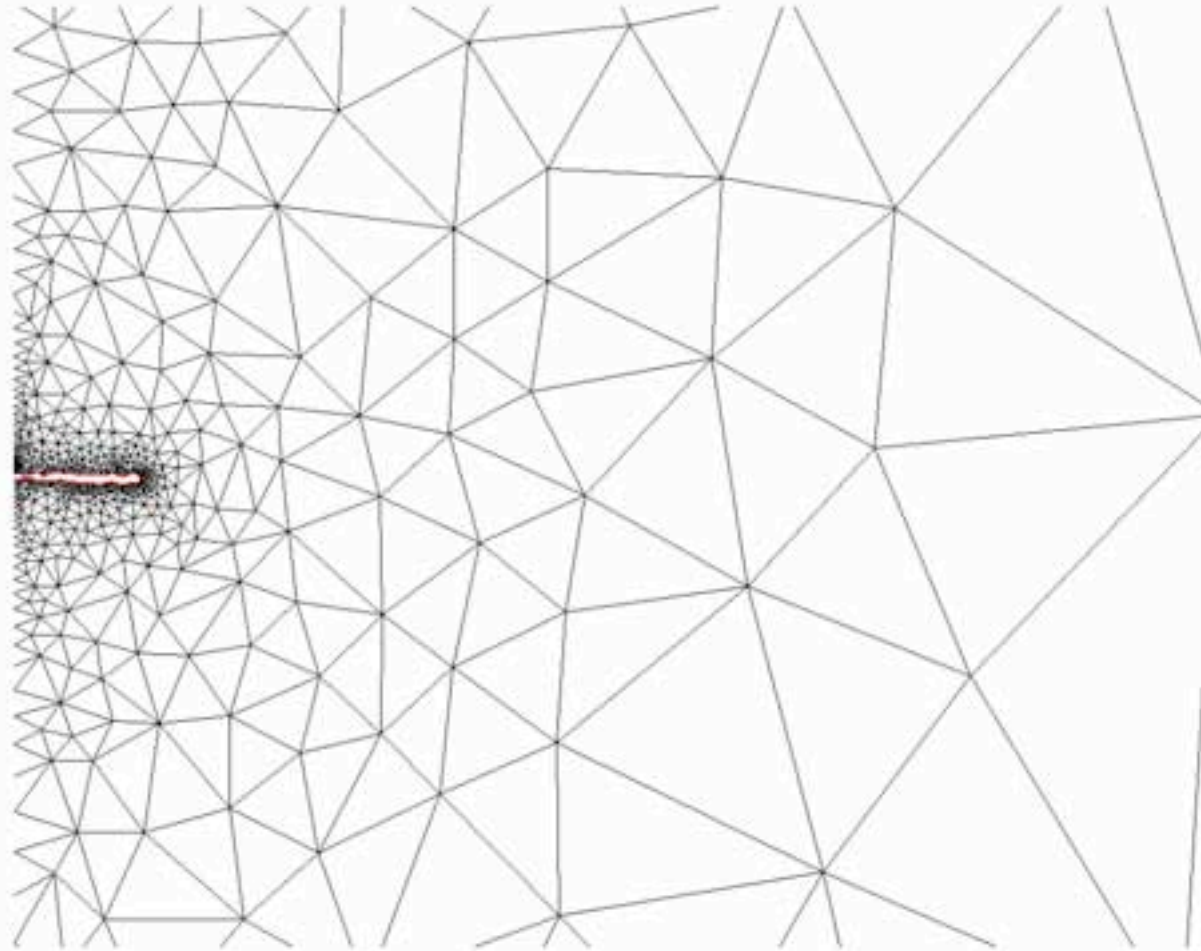
Branching



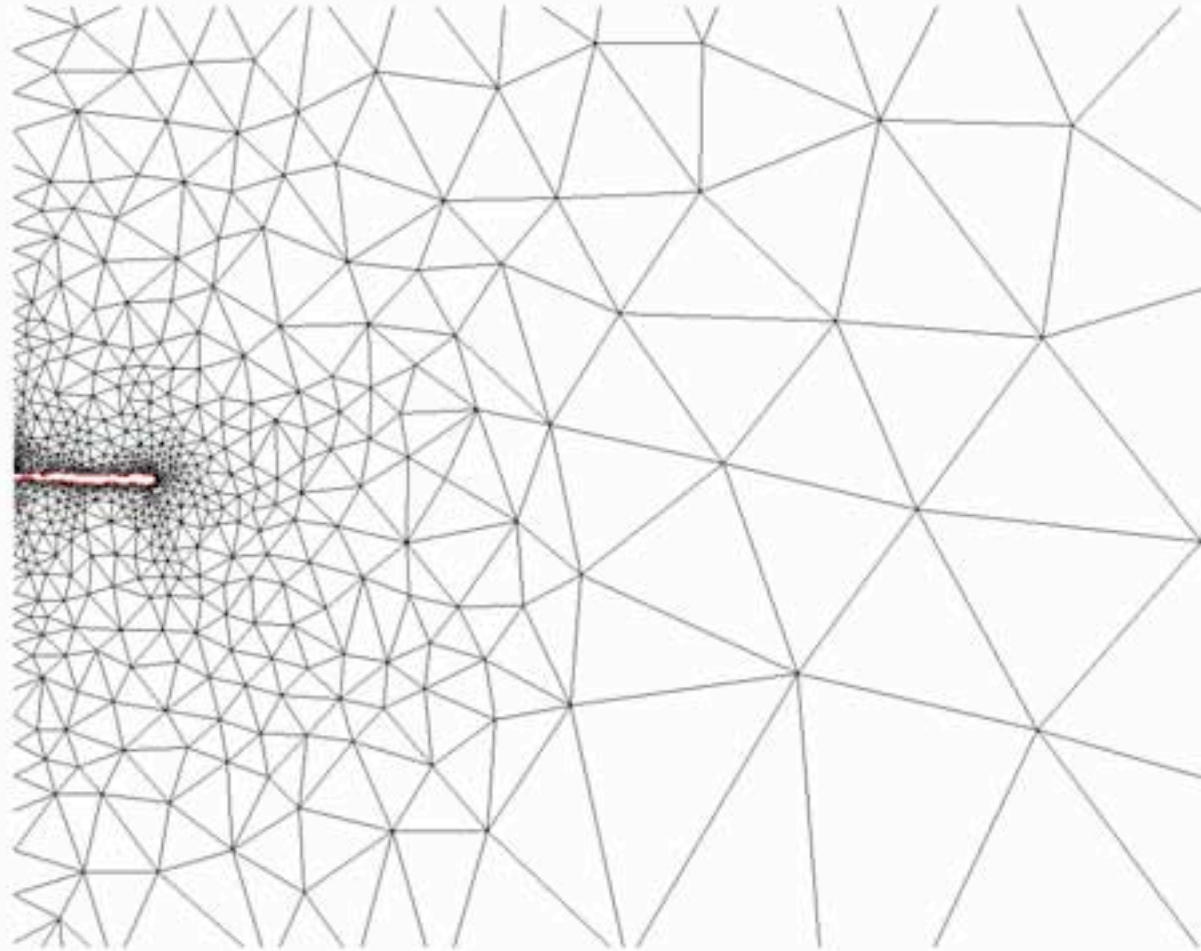
Branching



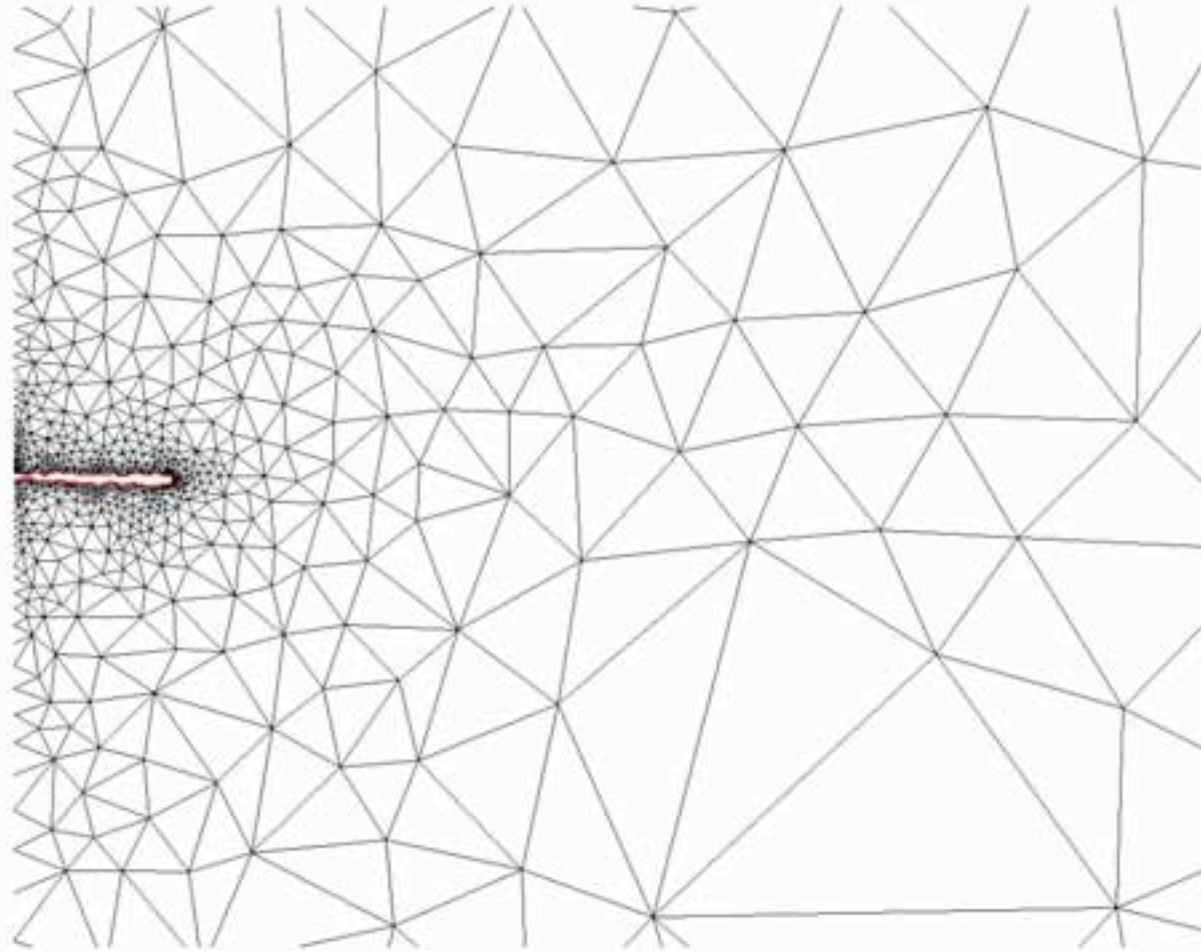
Branching



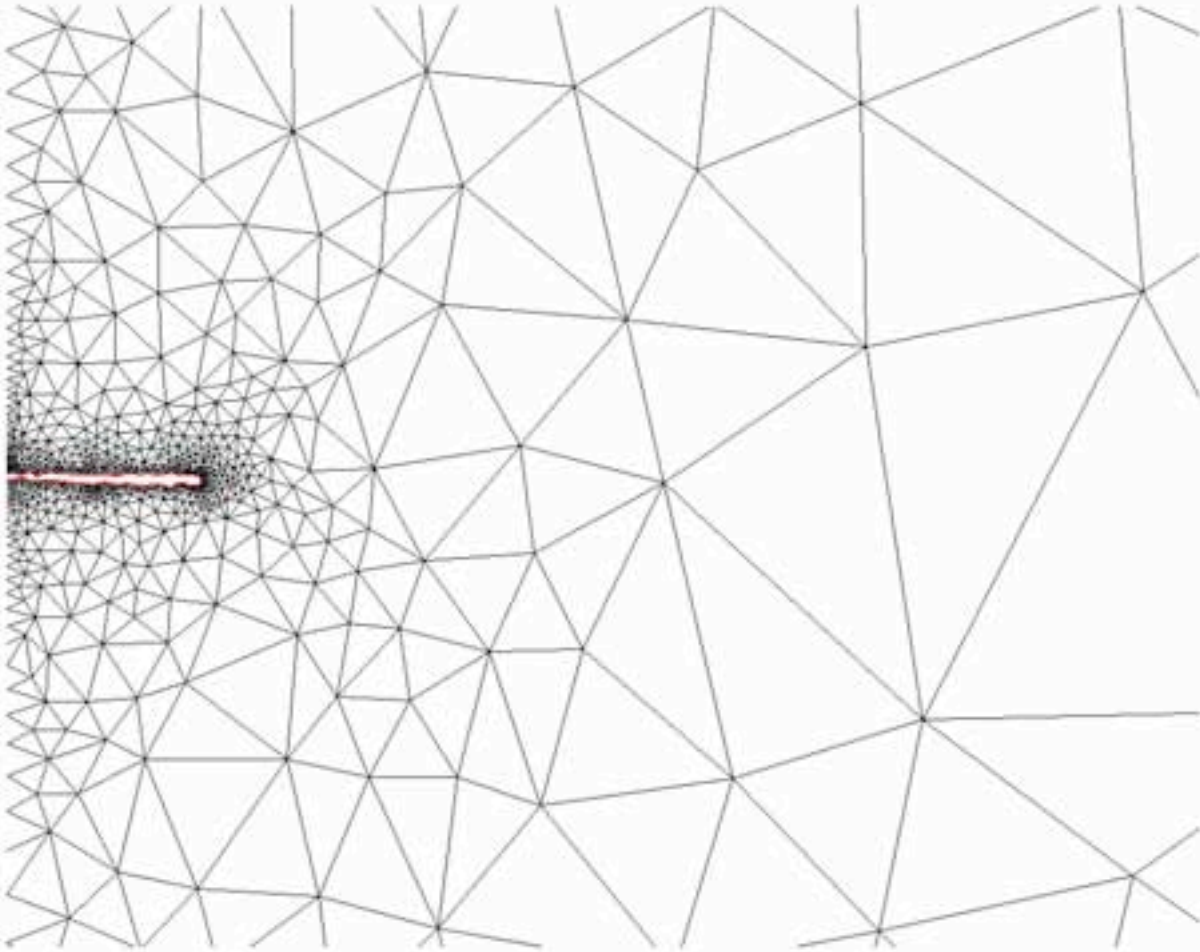
Branching



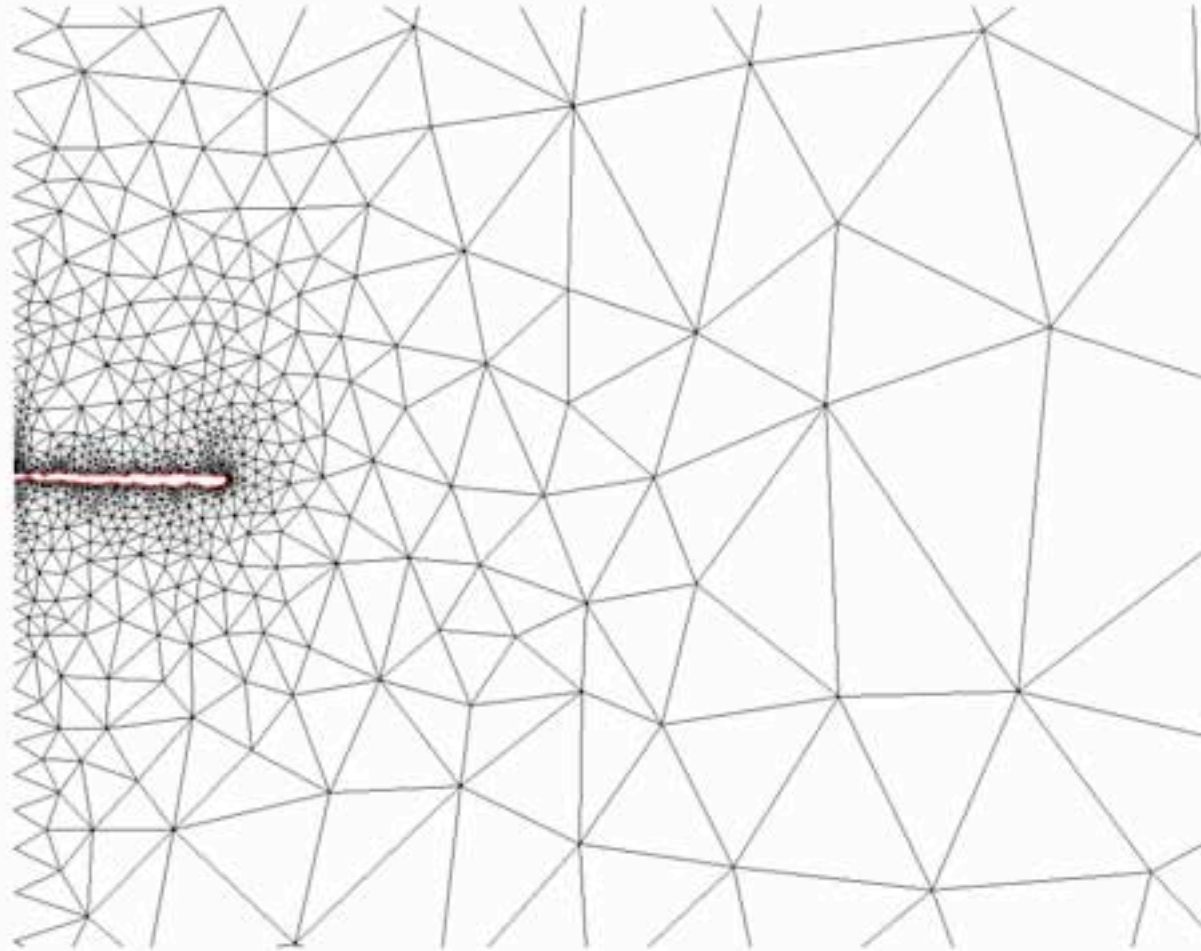
Branching



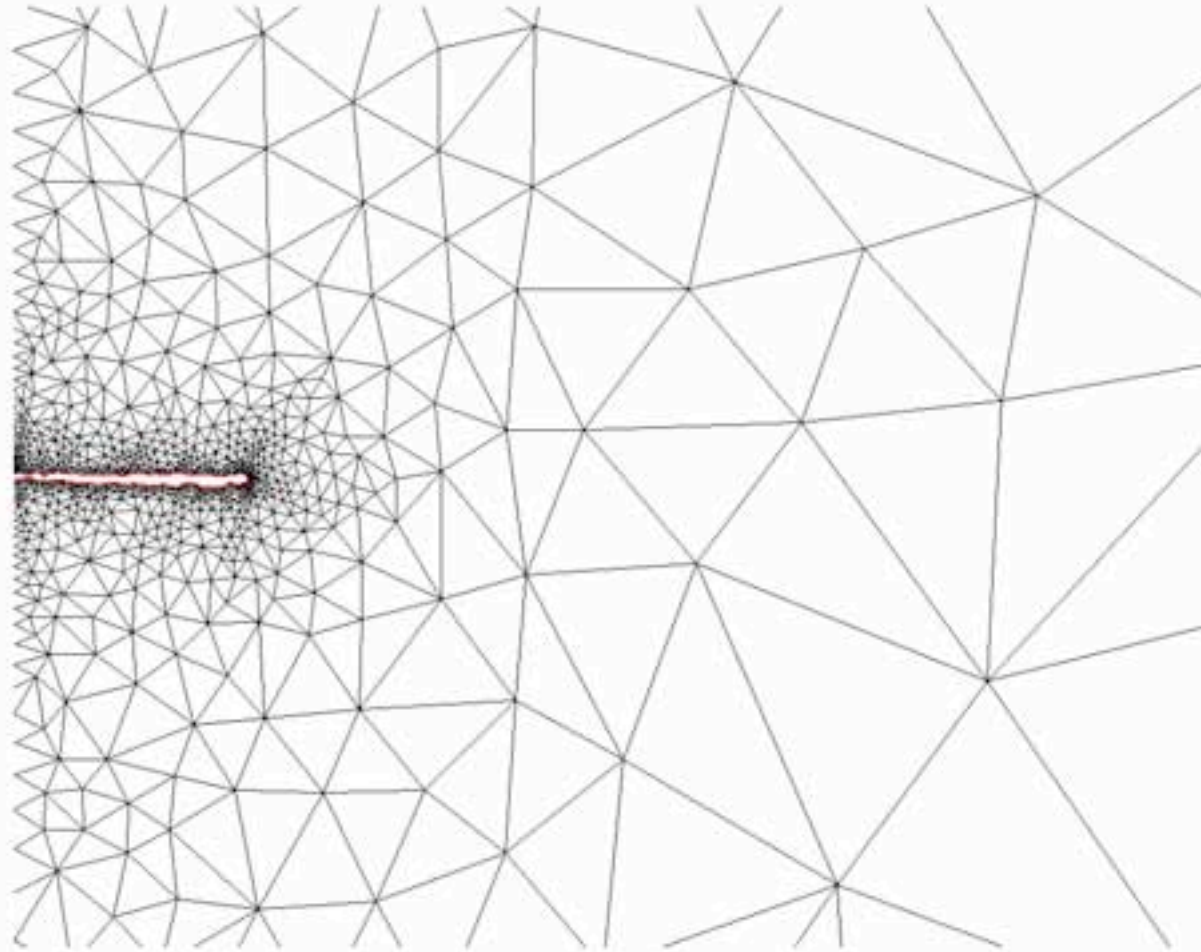
Branching



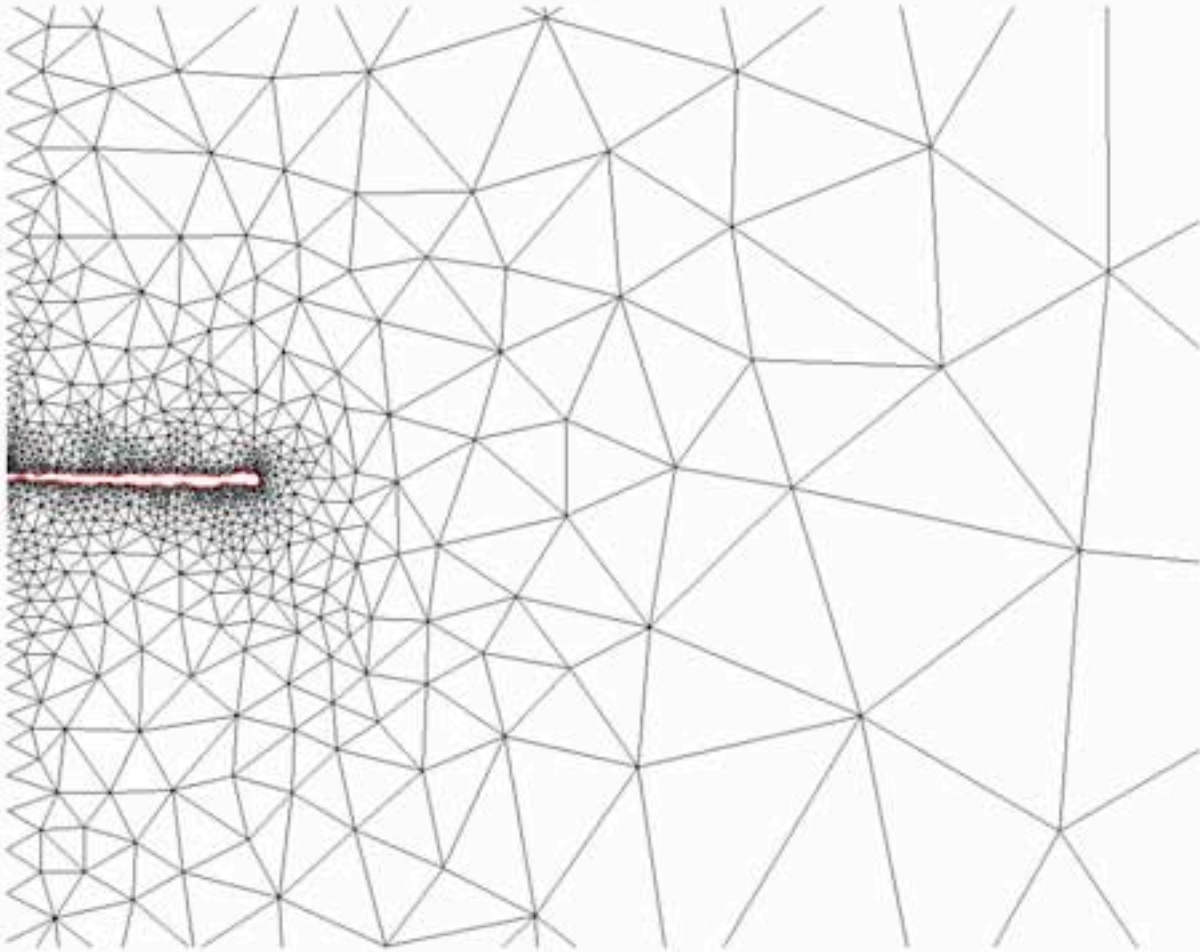
Branching



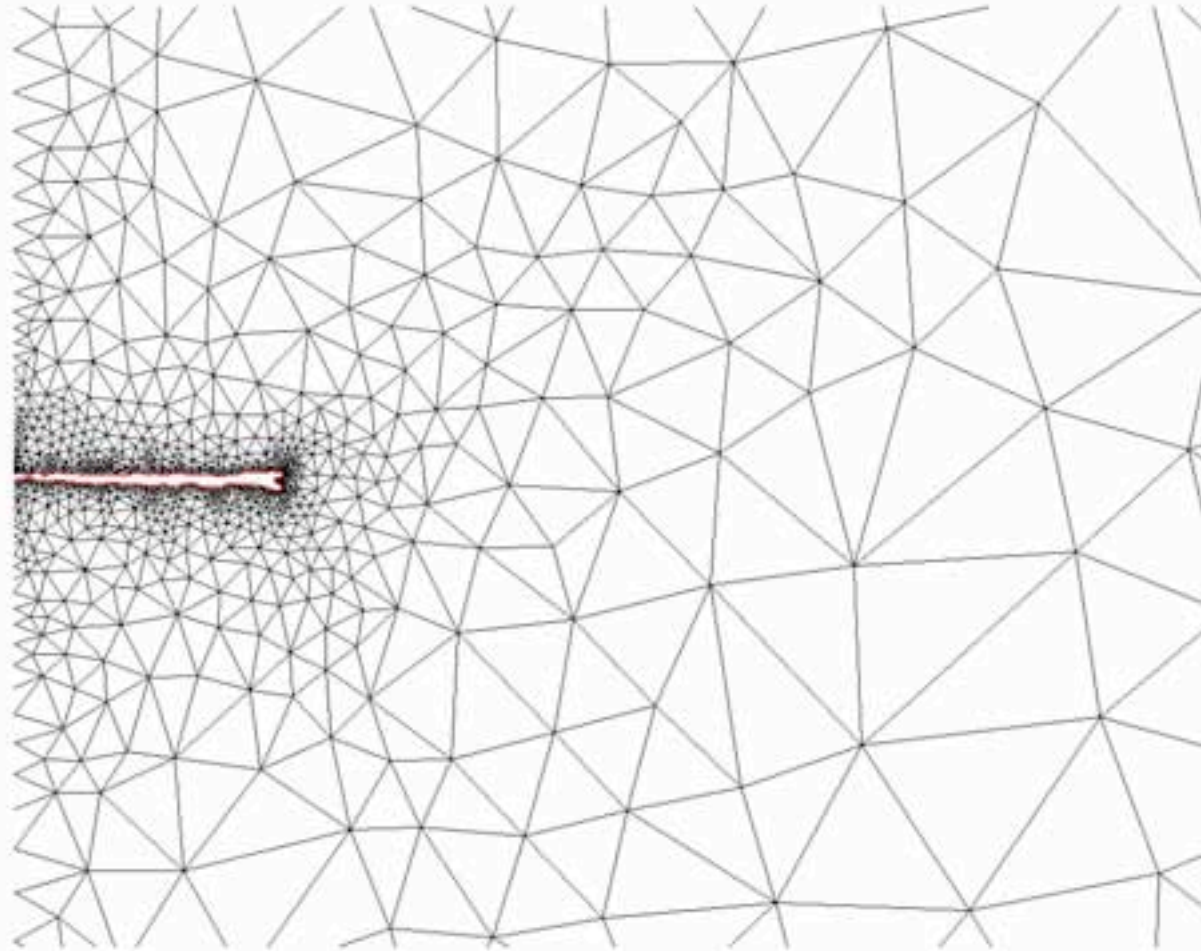
Branching



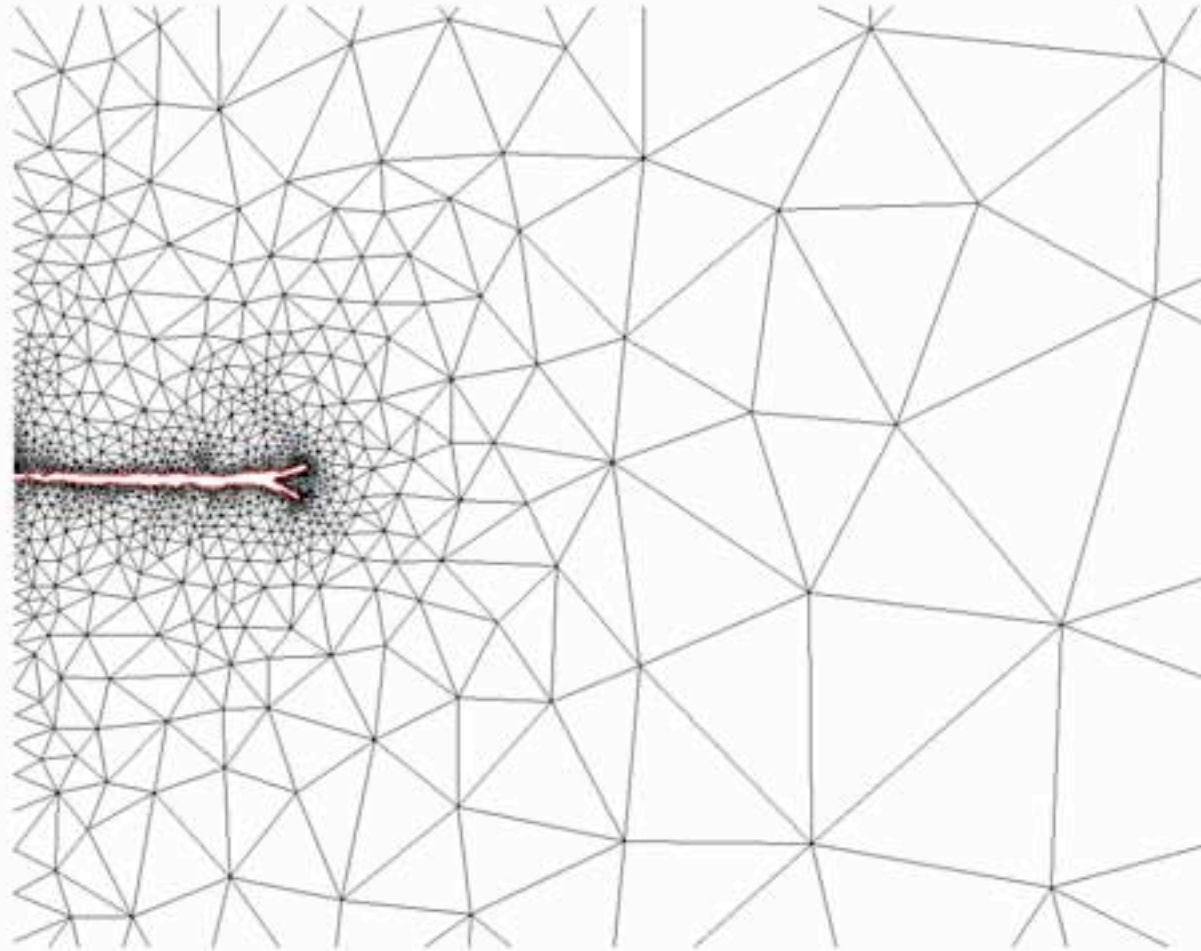
Branching



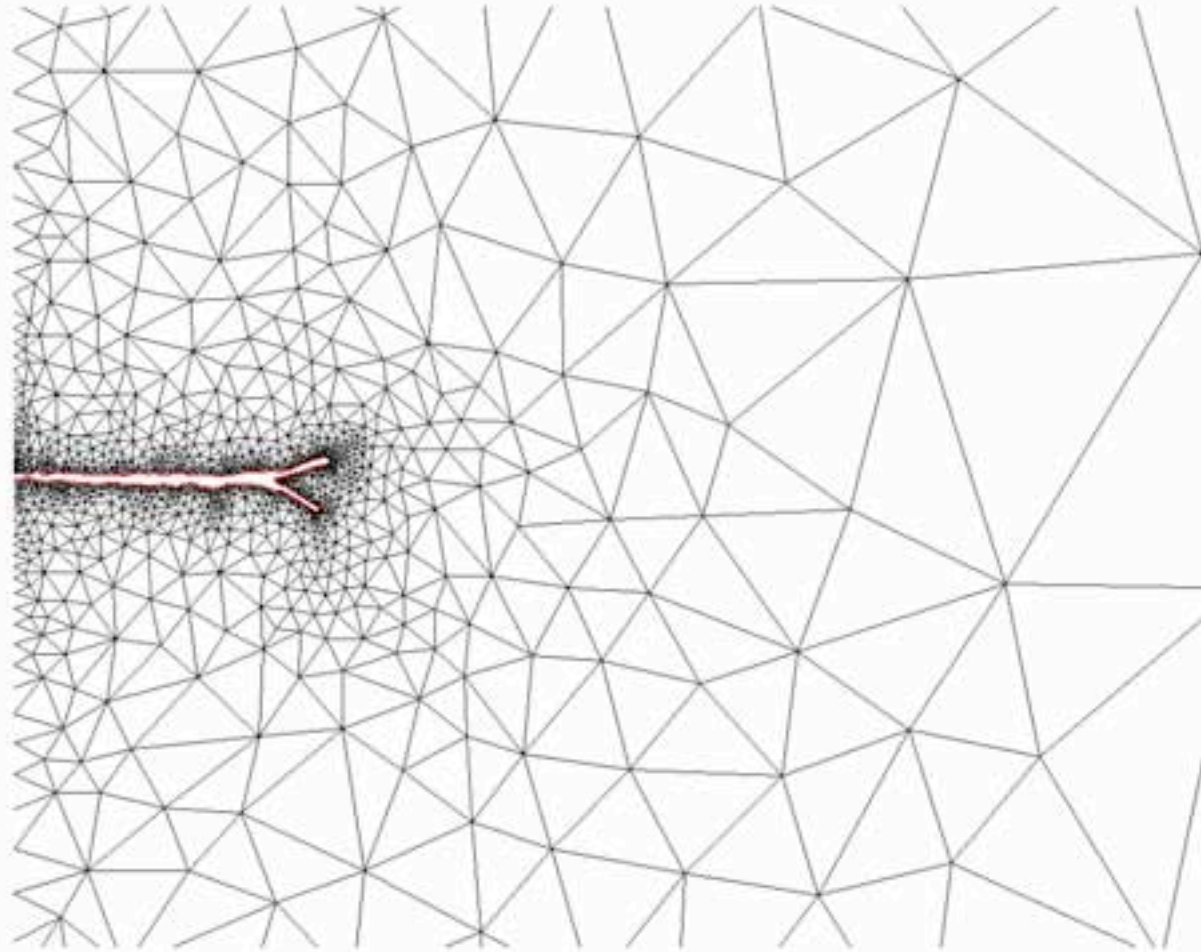
Branching



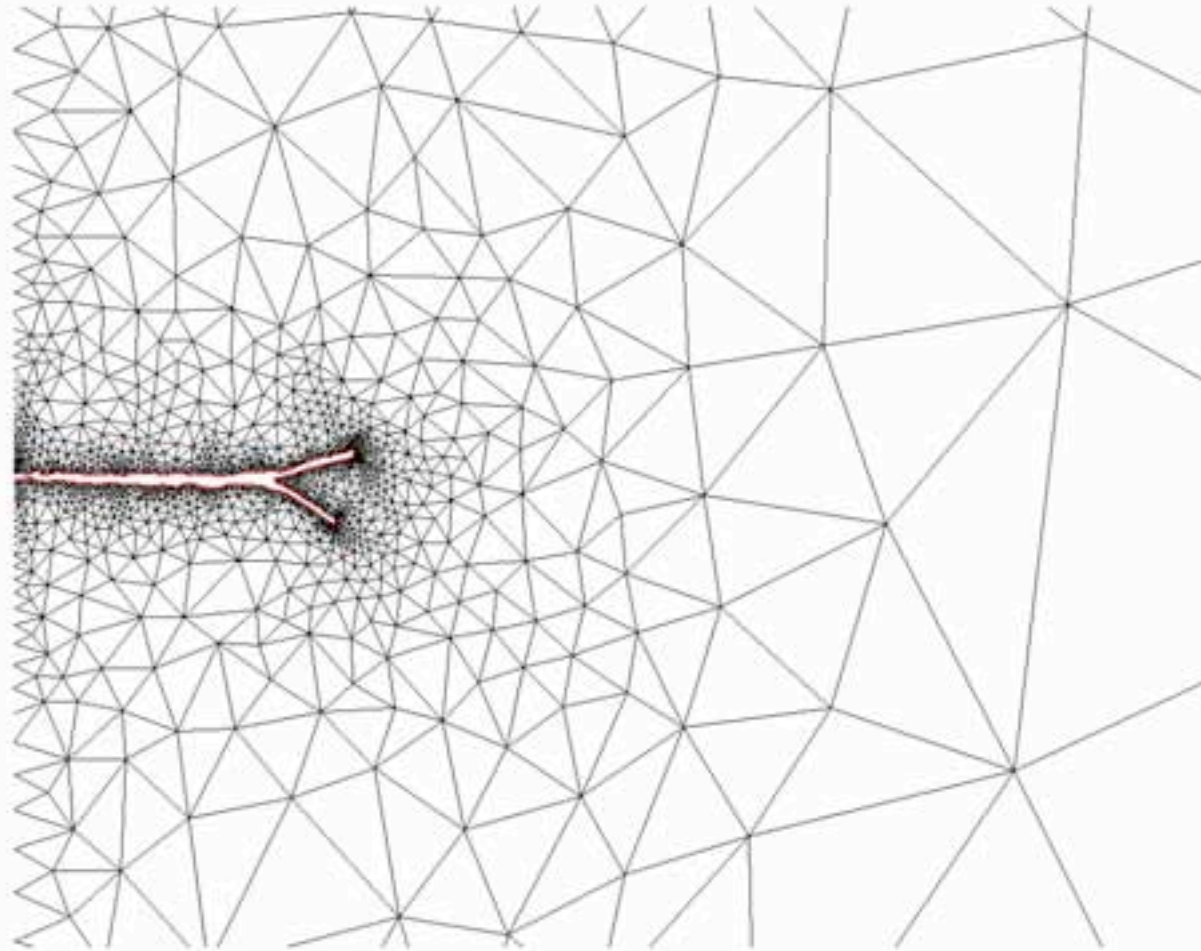
Branching



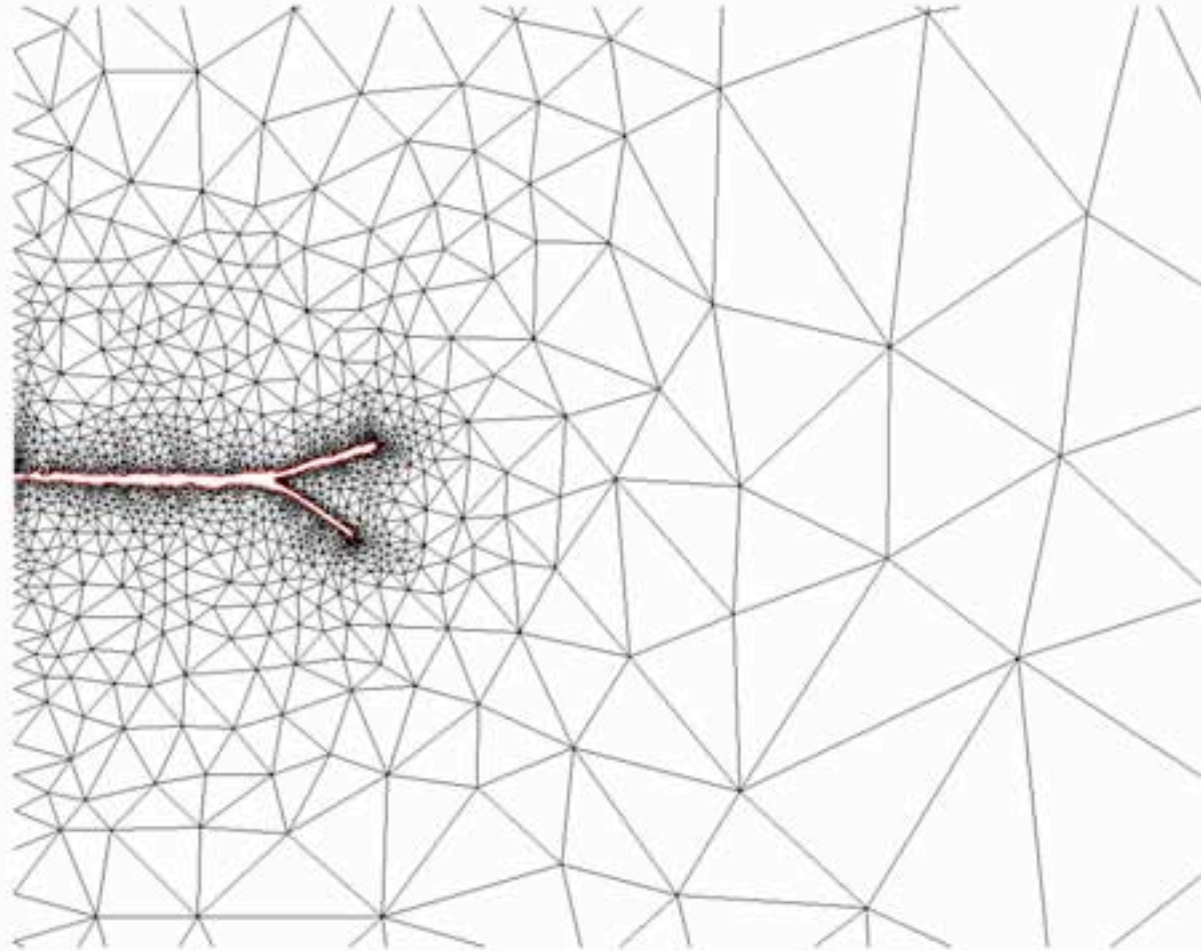
Branching



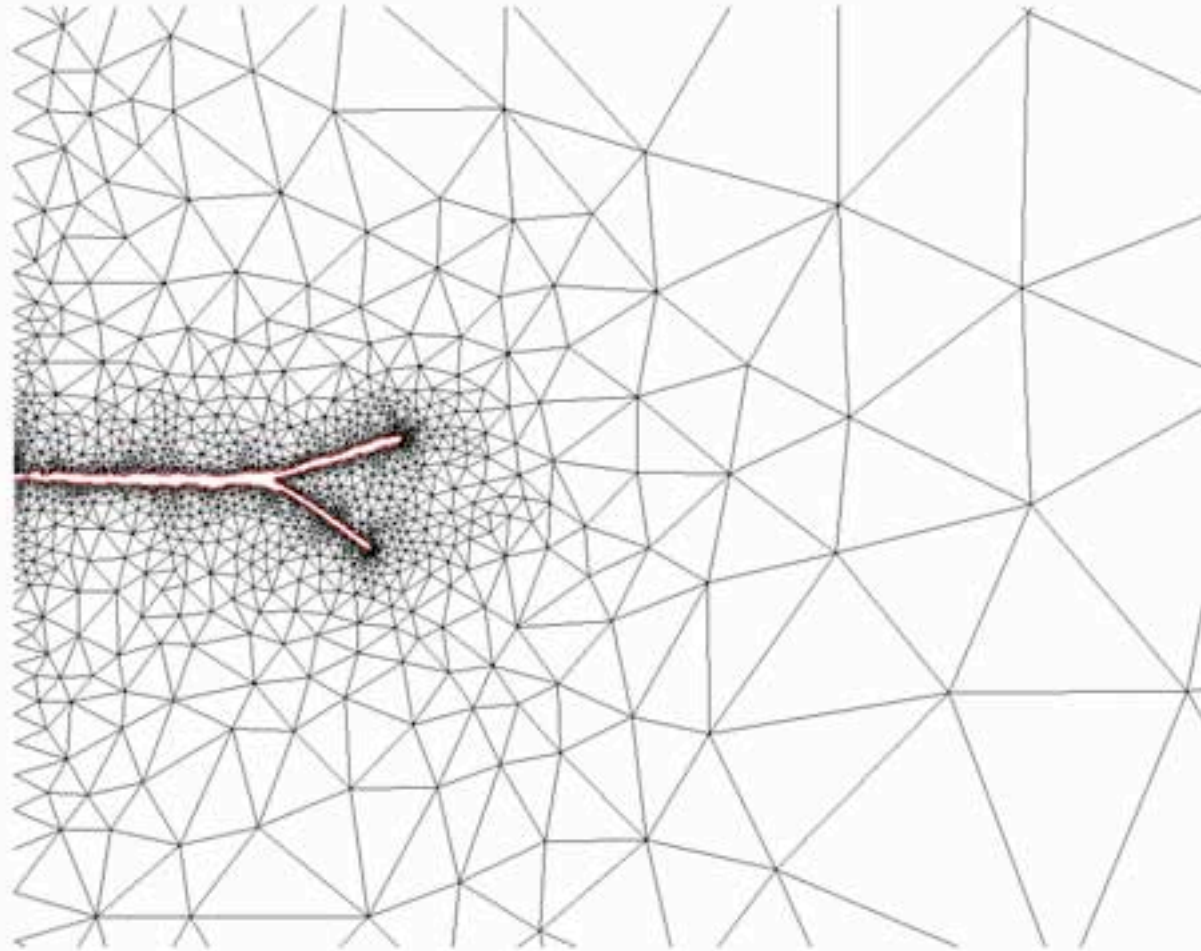
Branching



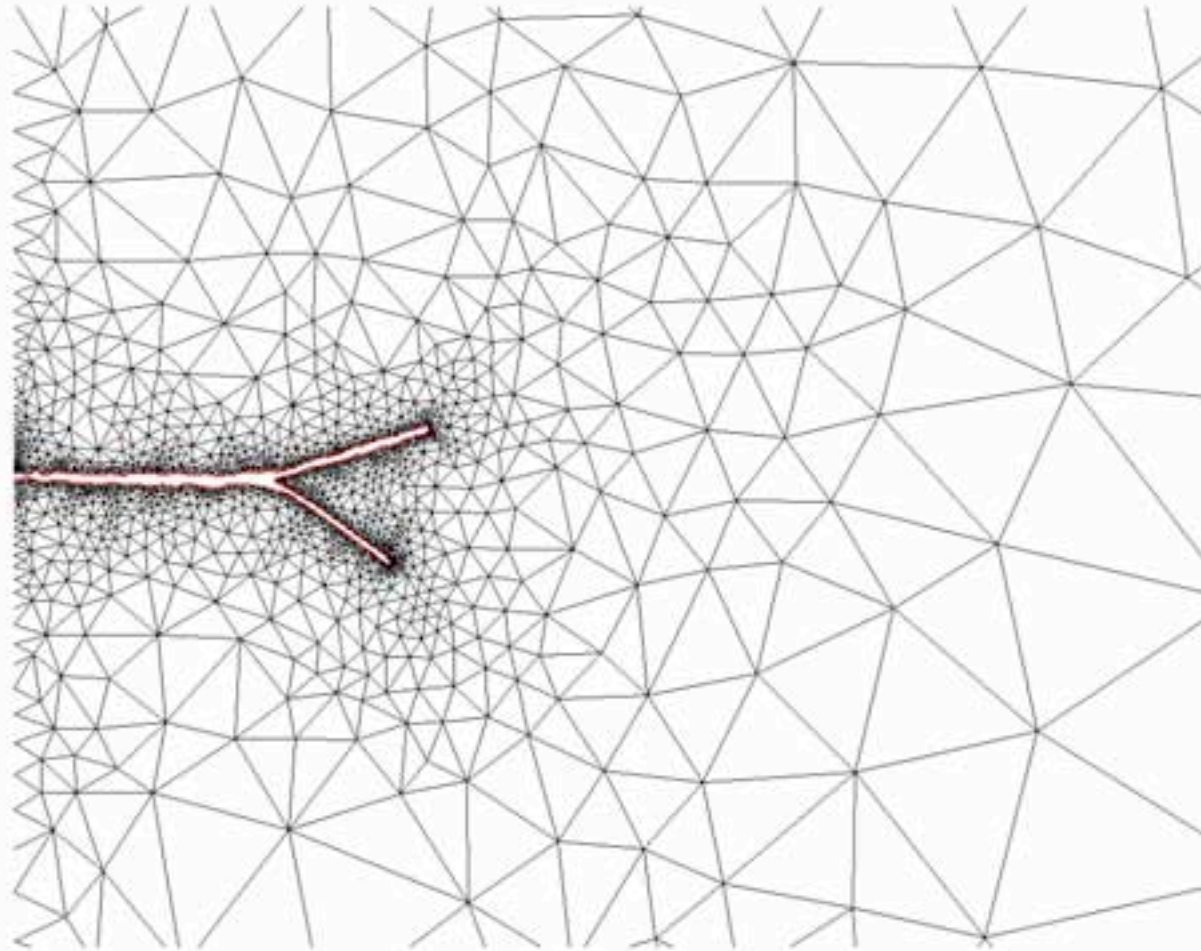
Branching



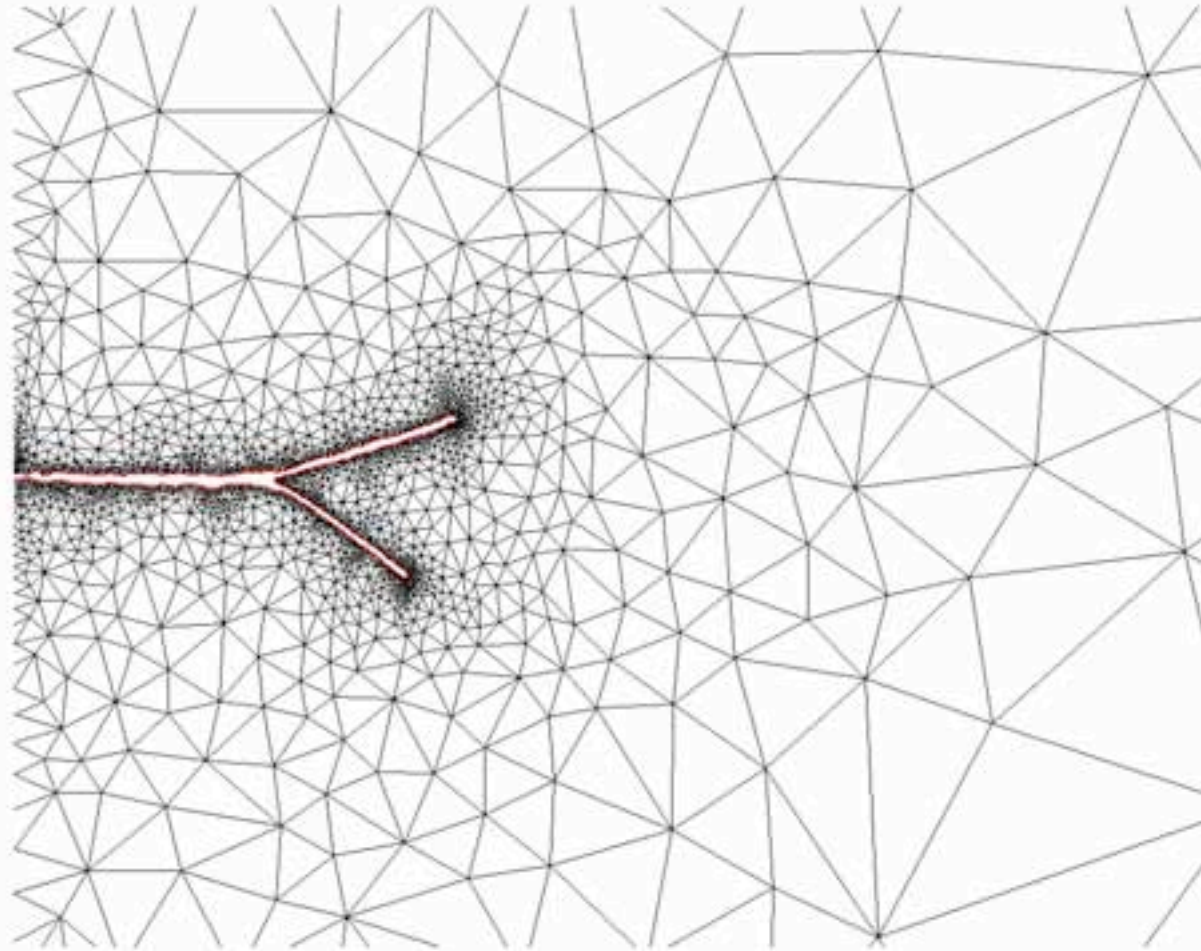
Branching



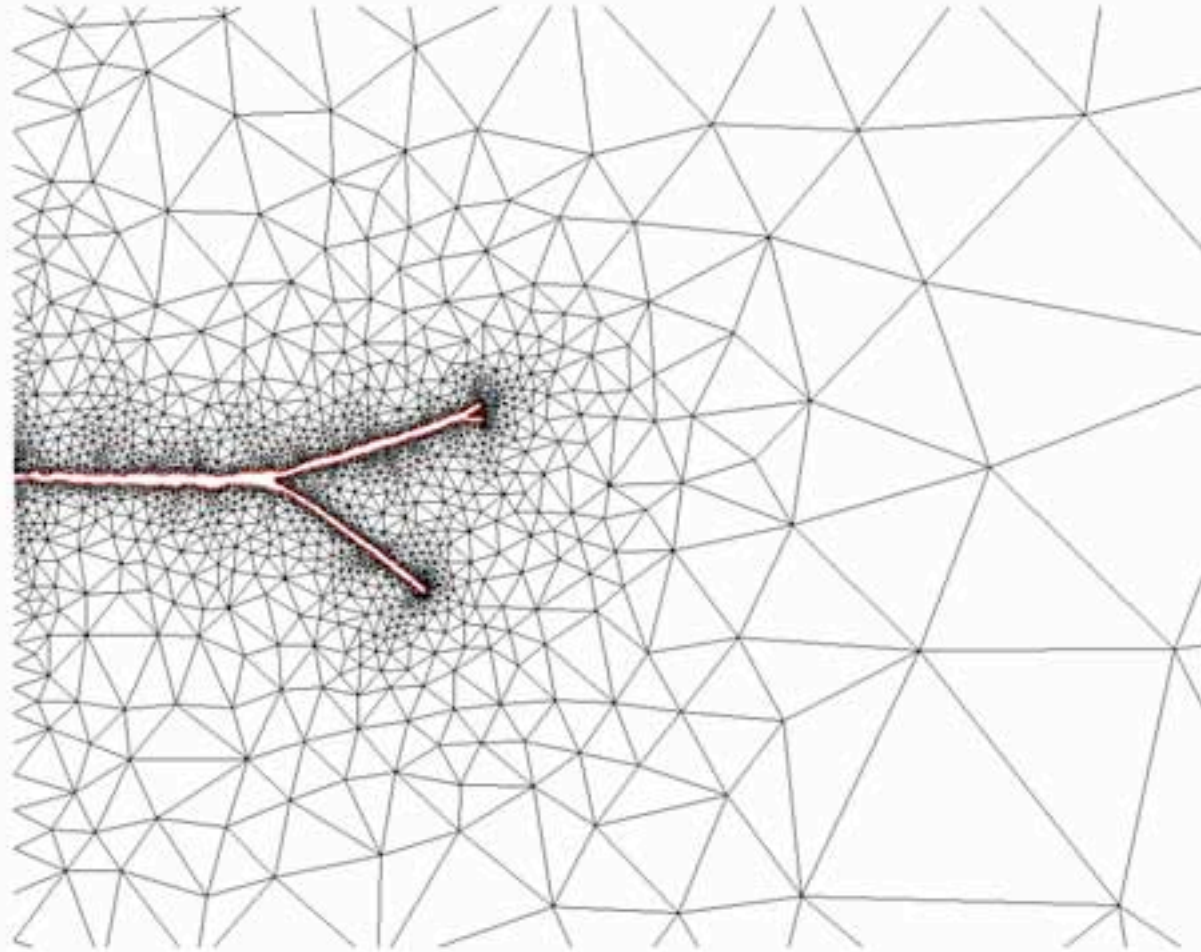
Branching



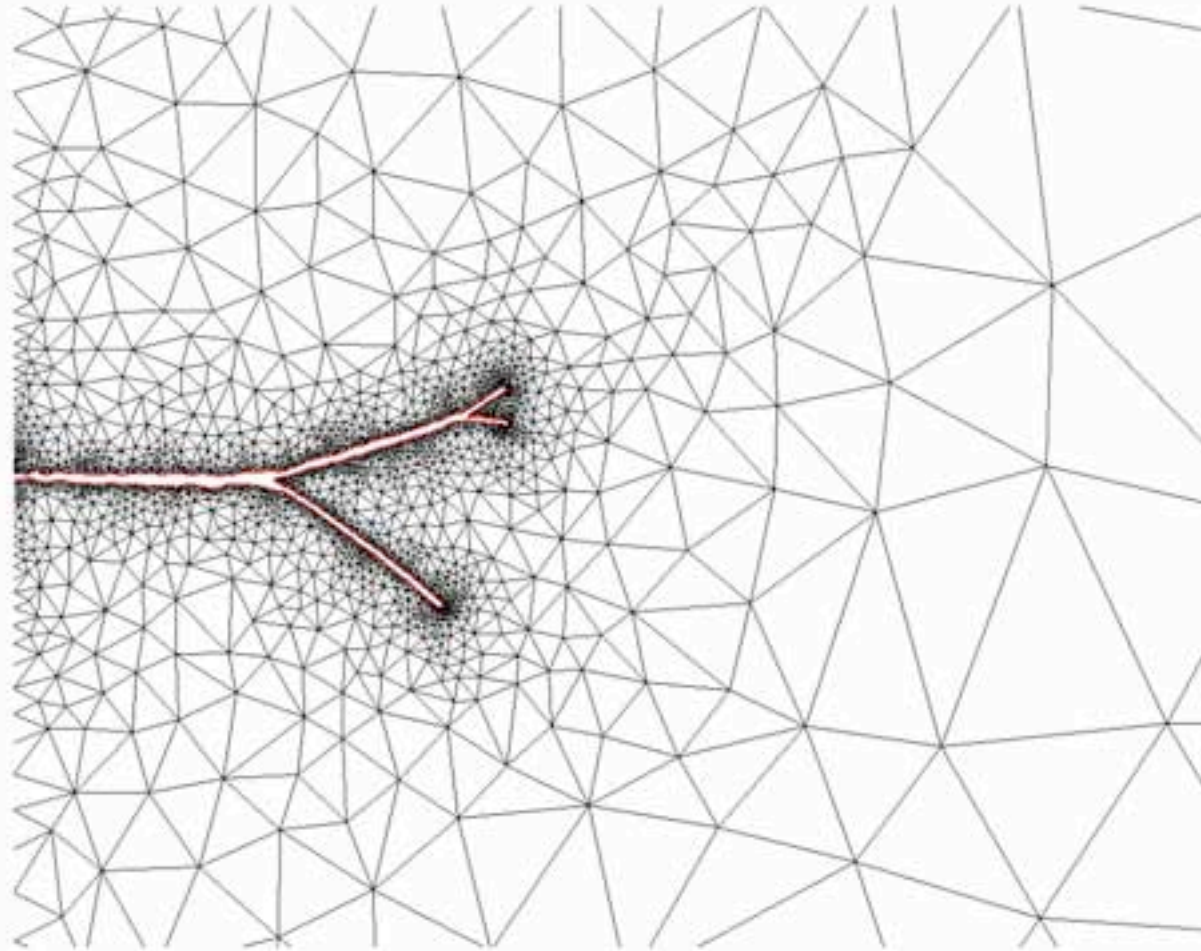
Branching



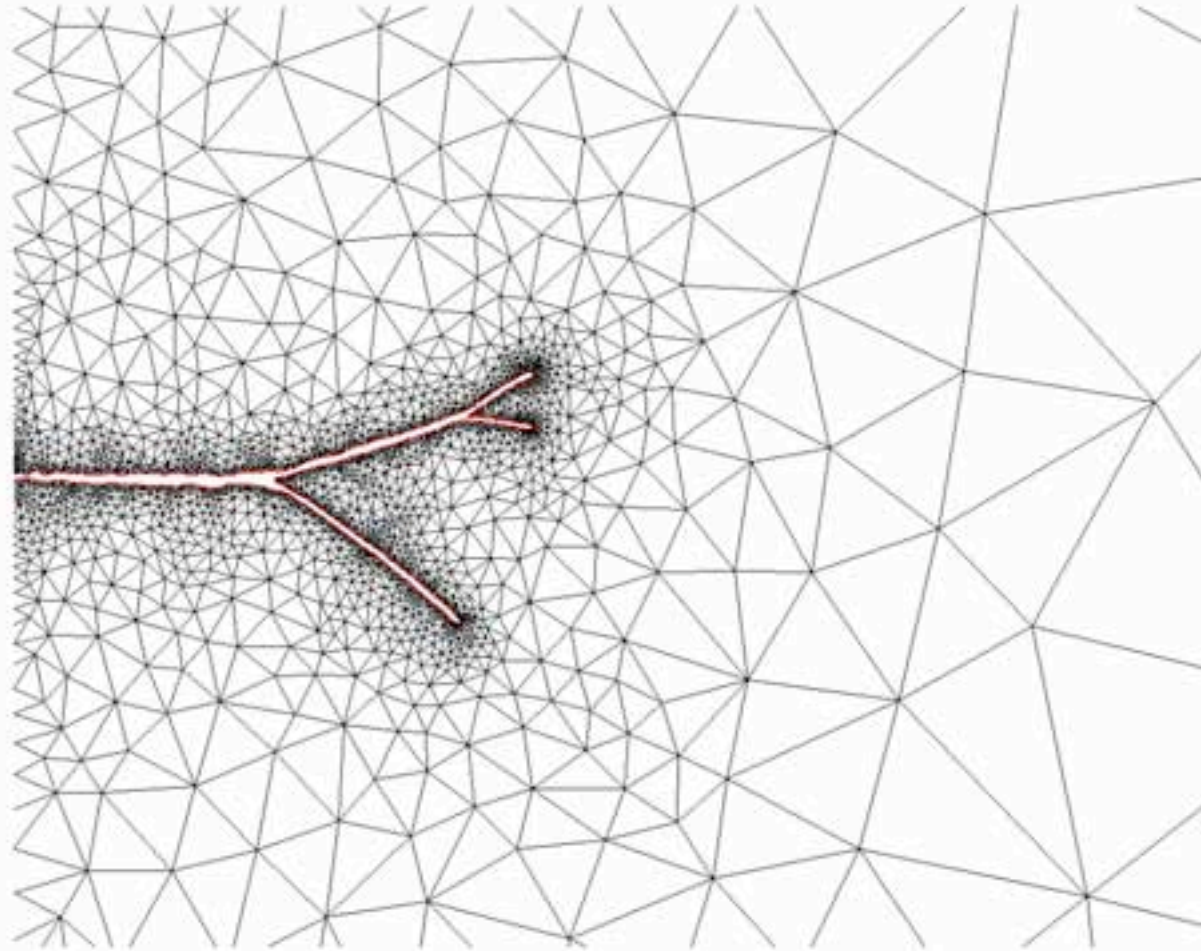
Branching



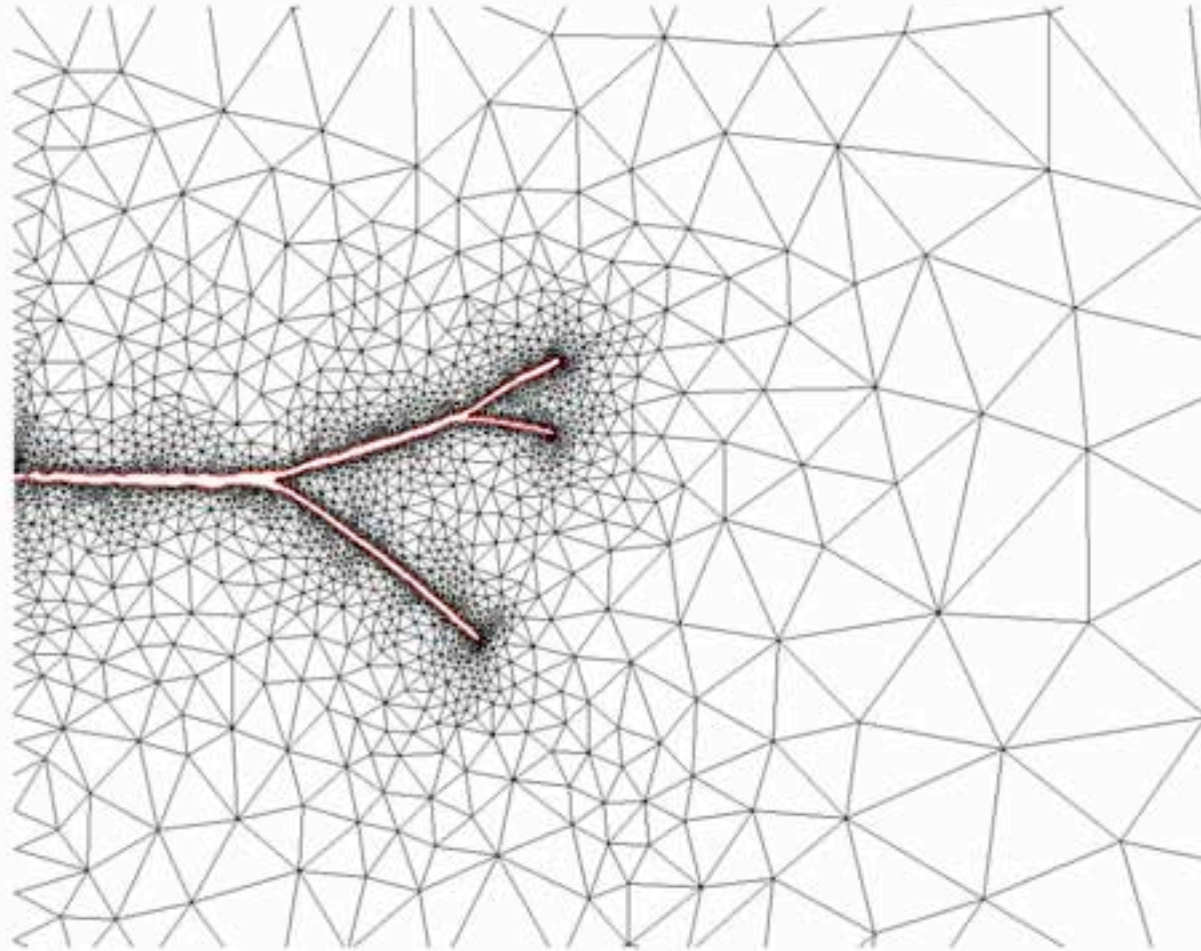
Branching



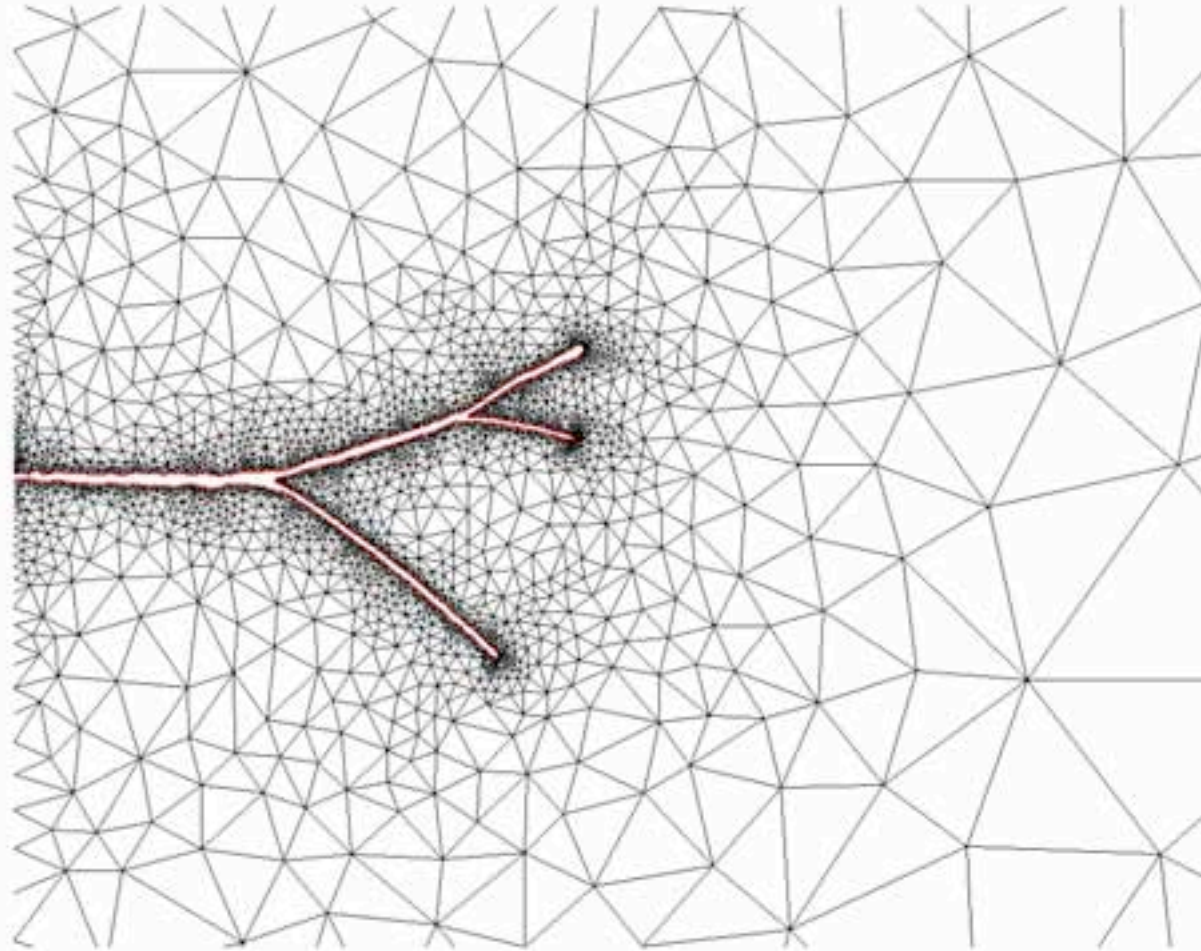
Branching



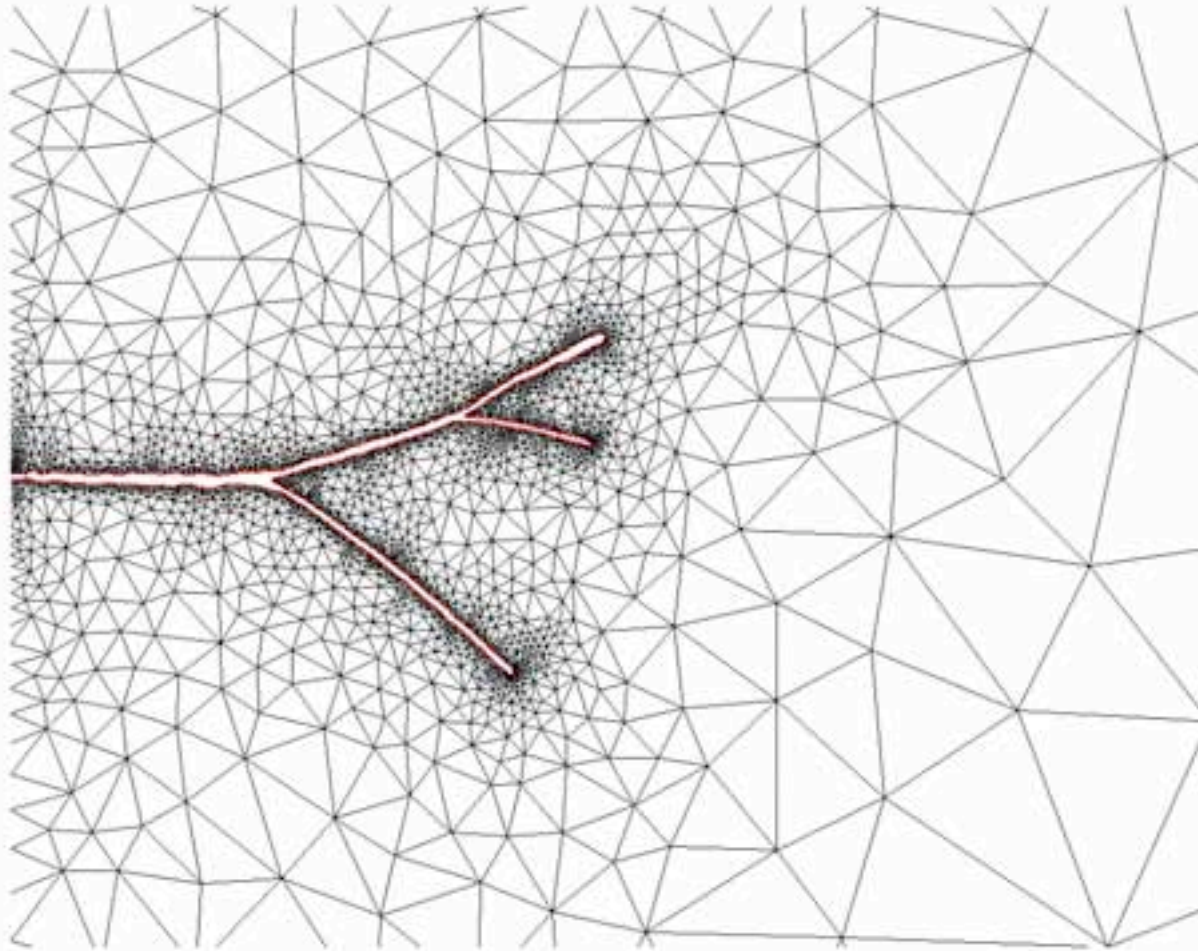
Branching



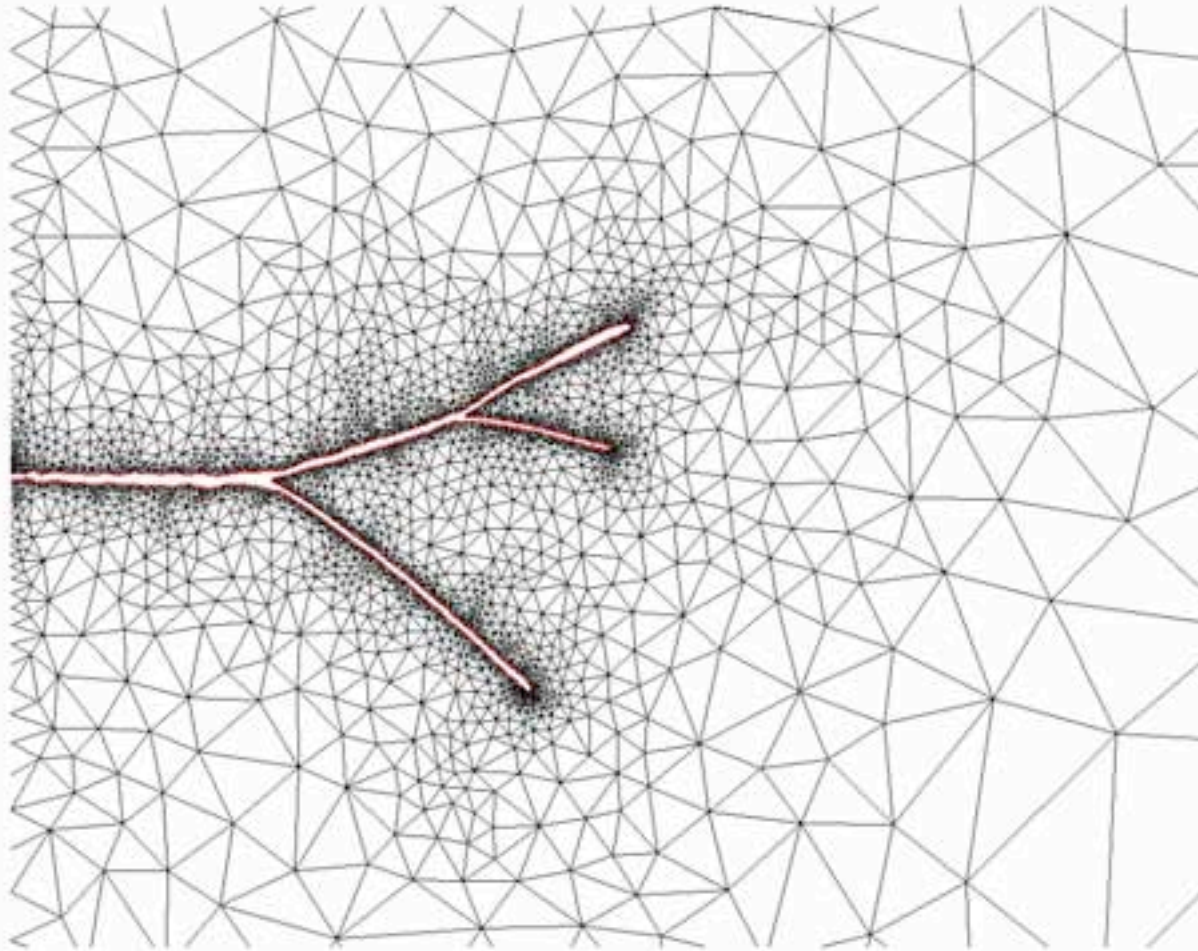
Branching



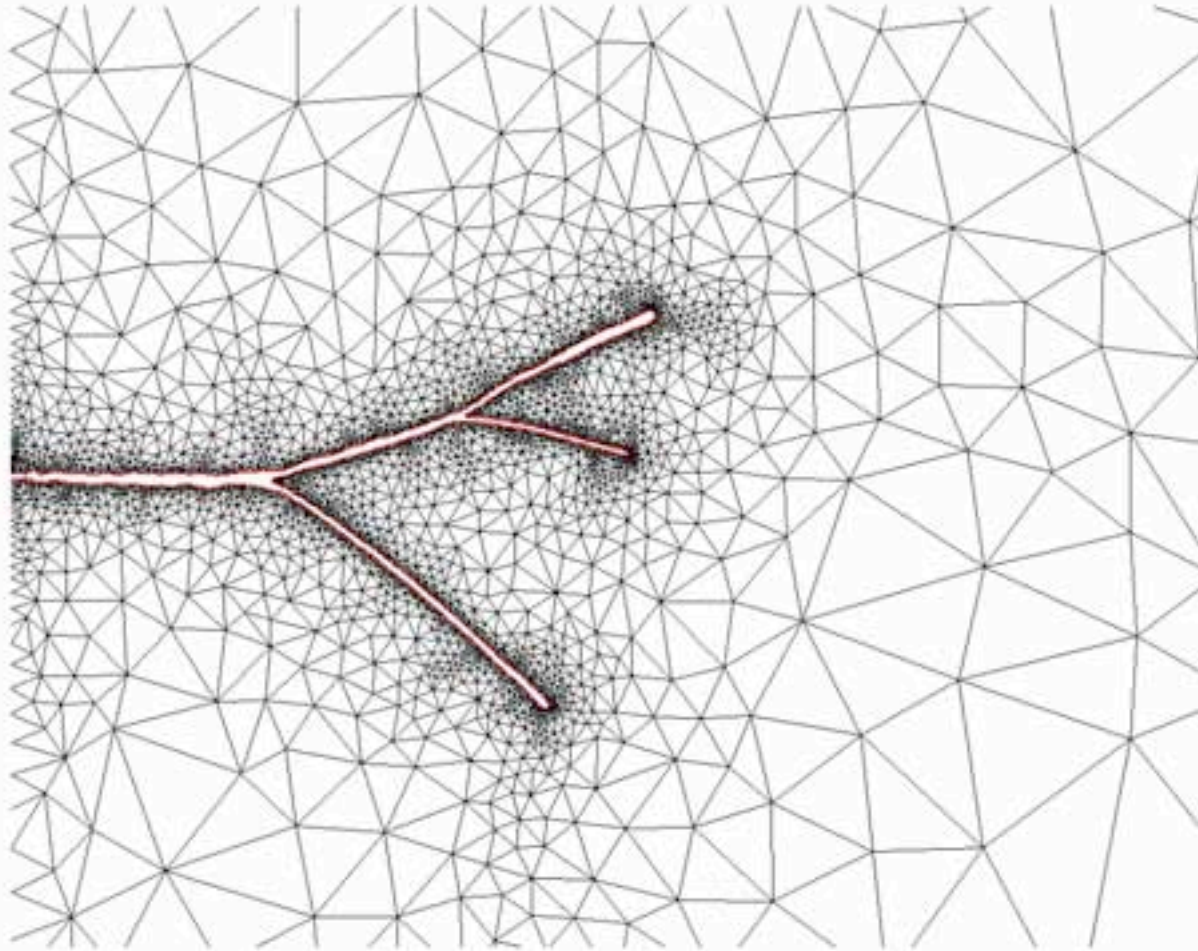
Branching



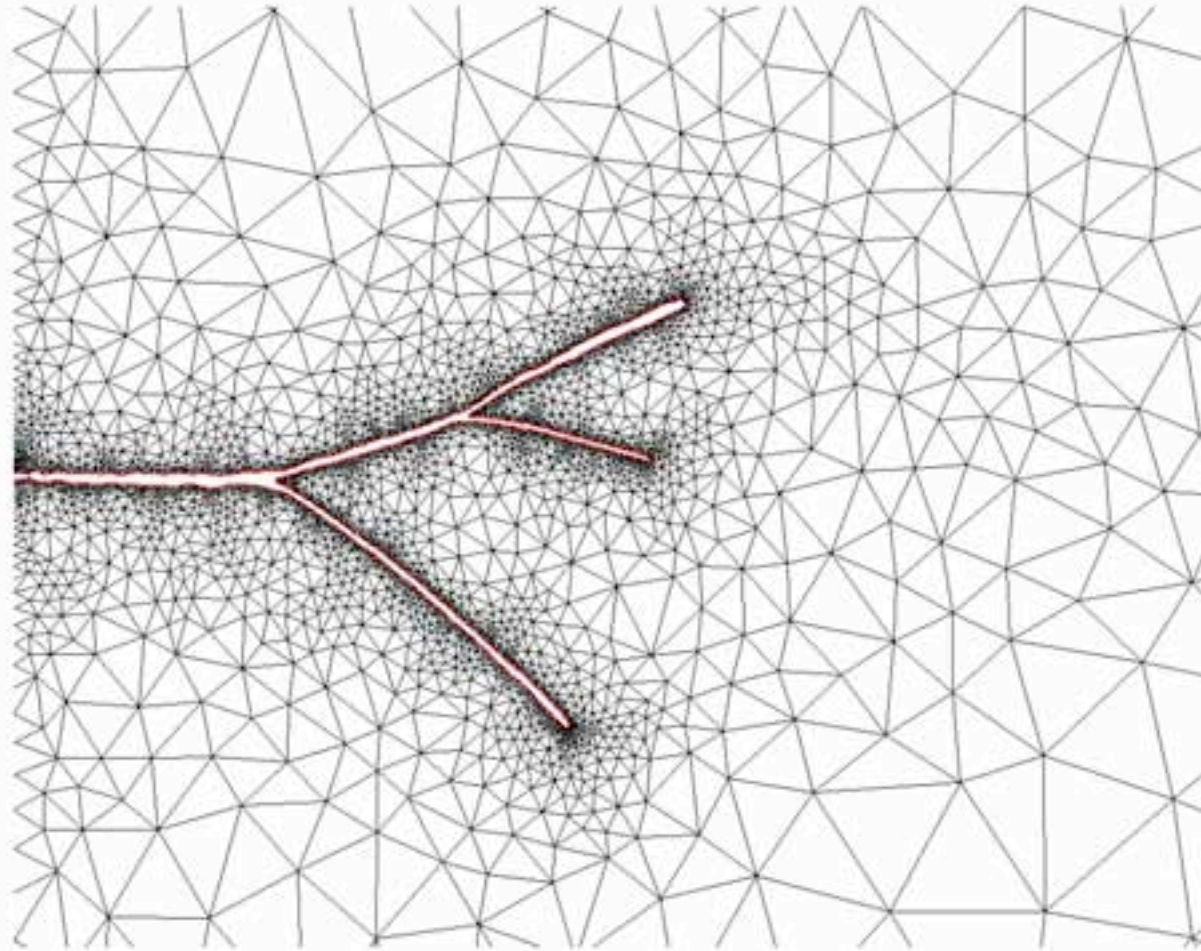
Branching



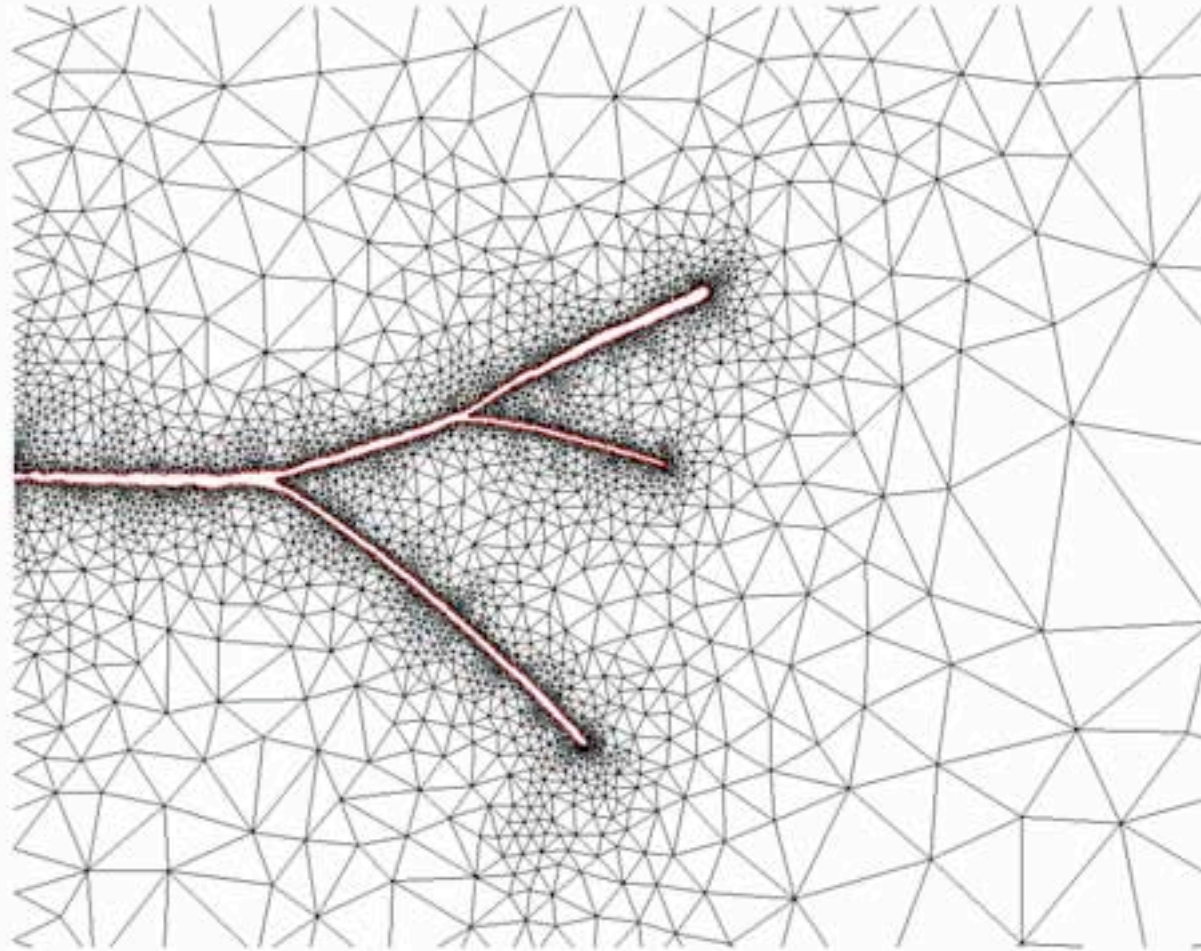
Branching



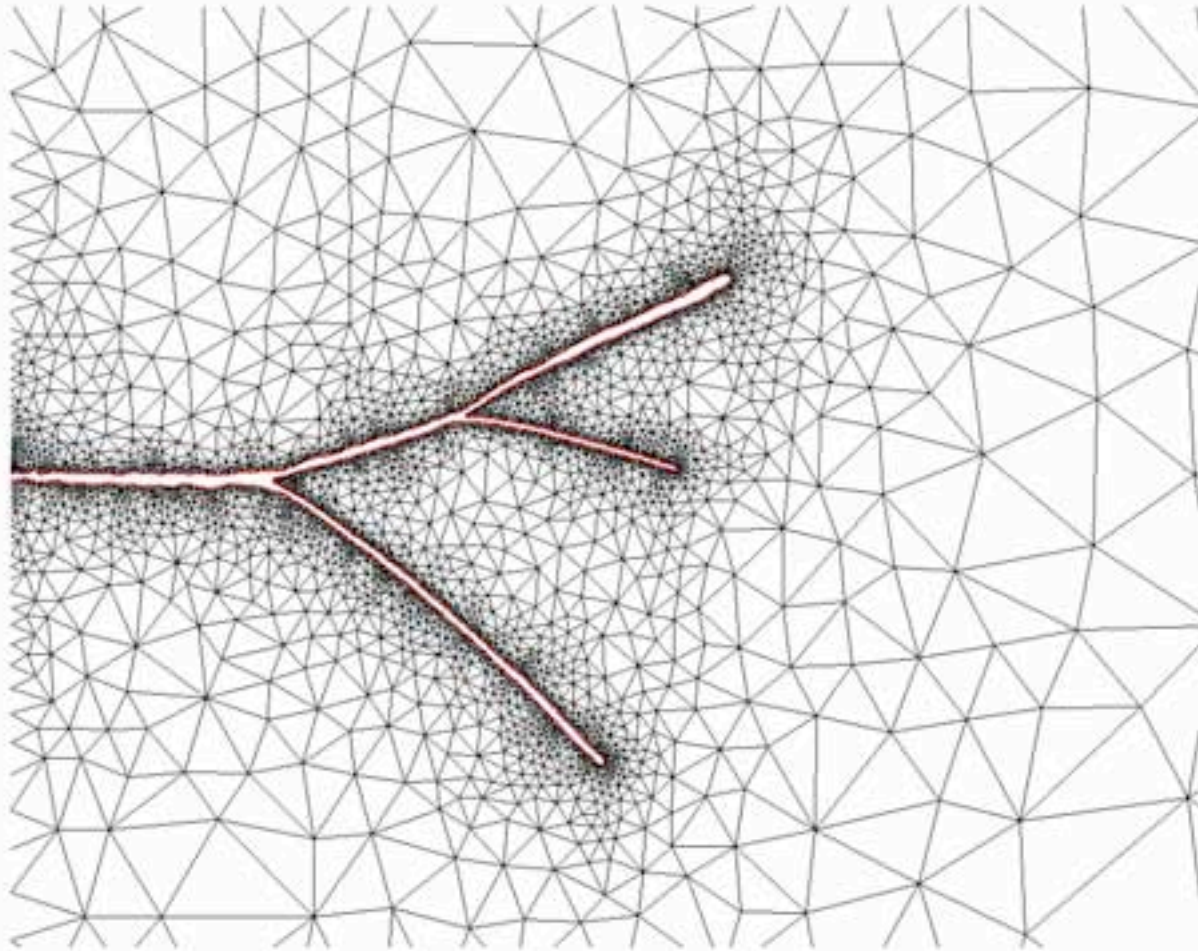
Branching



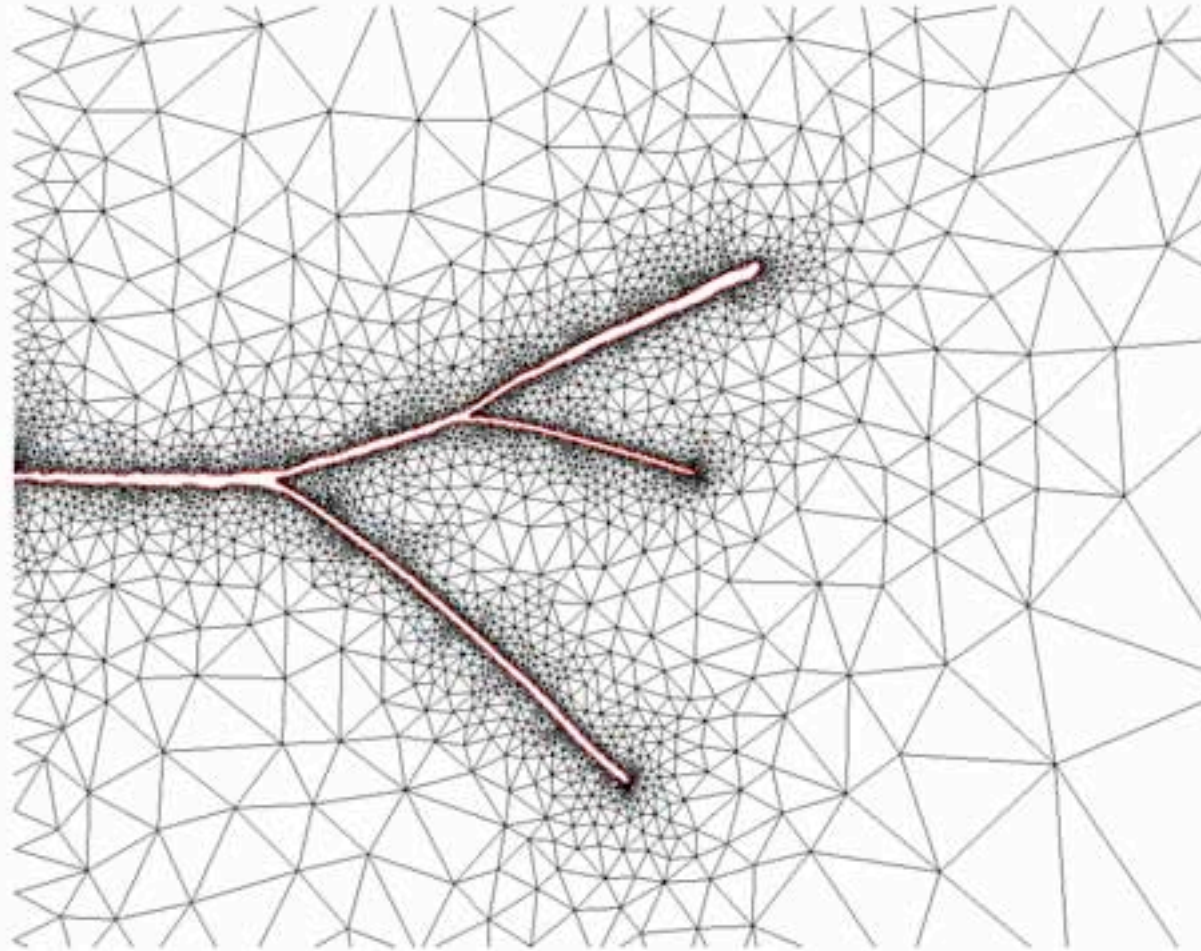
Branching



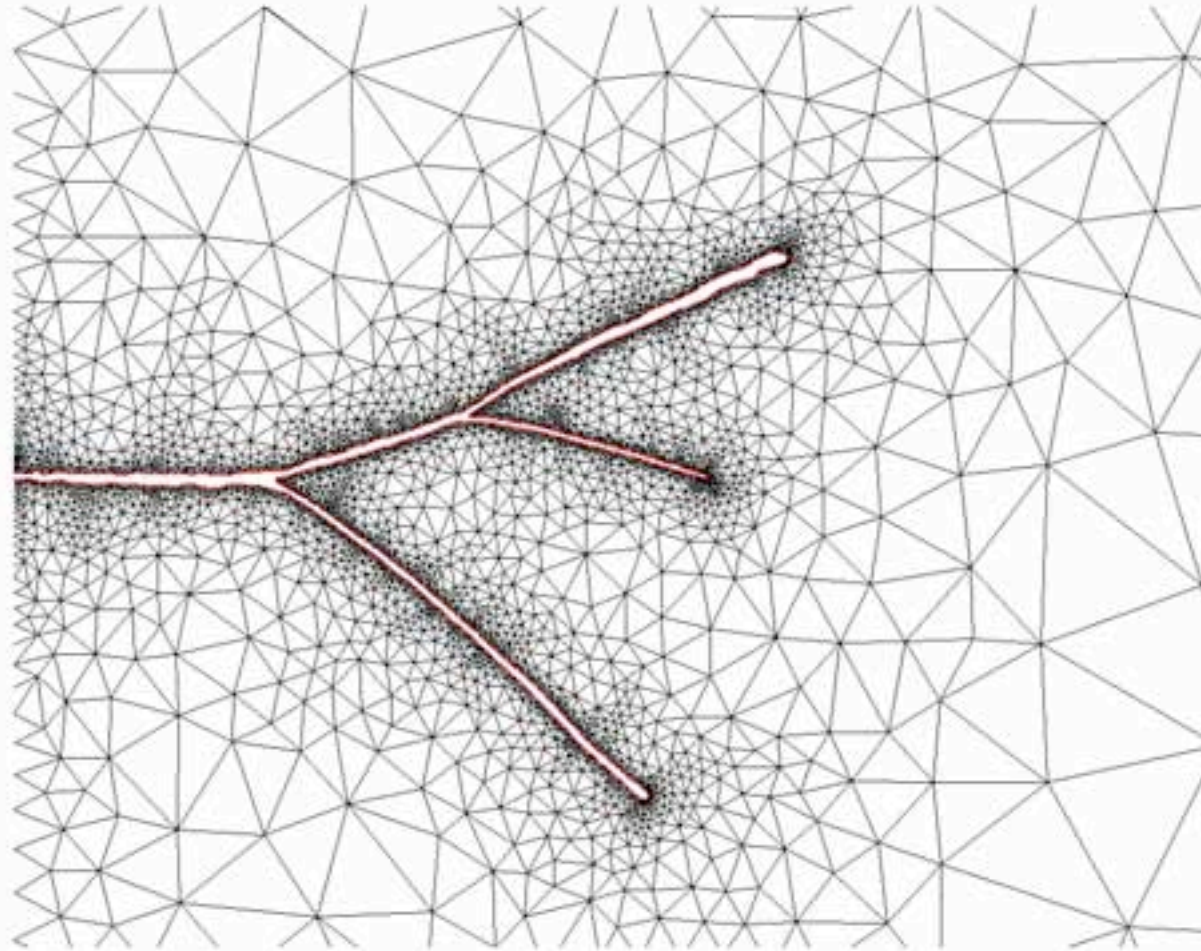
Branching



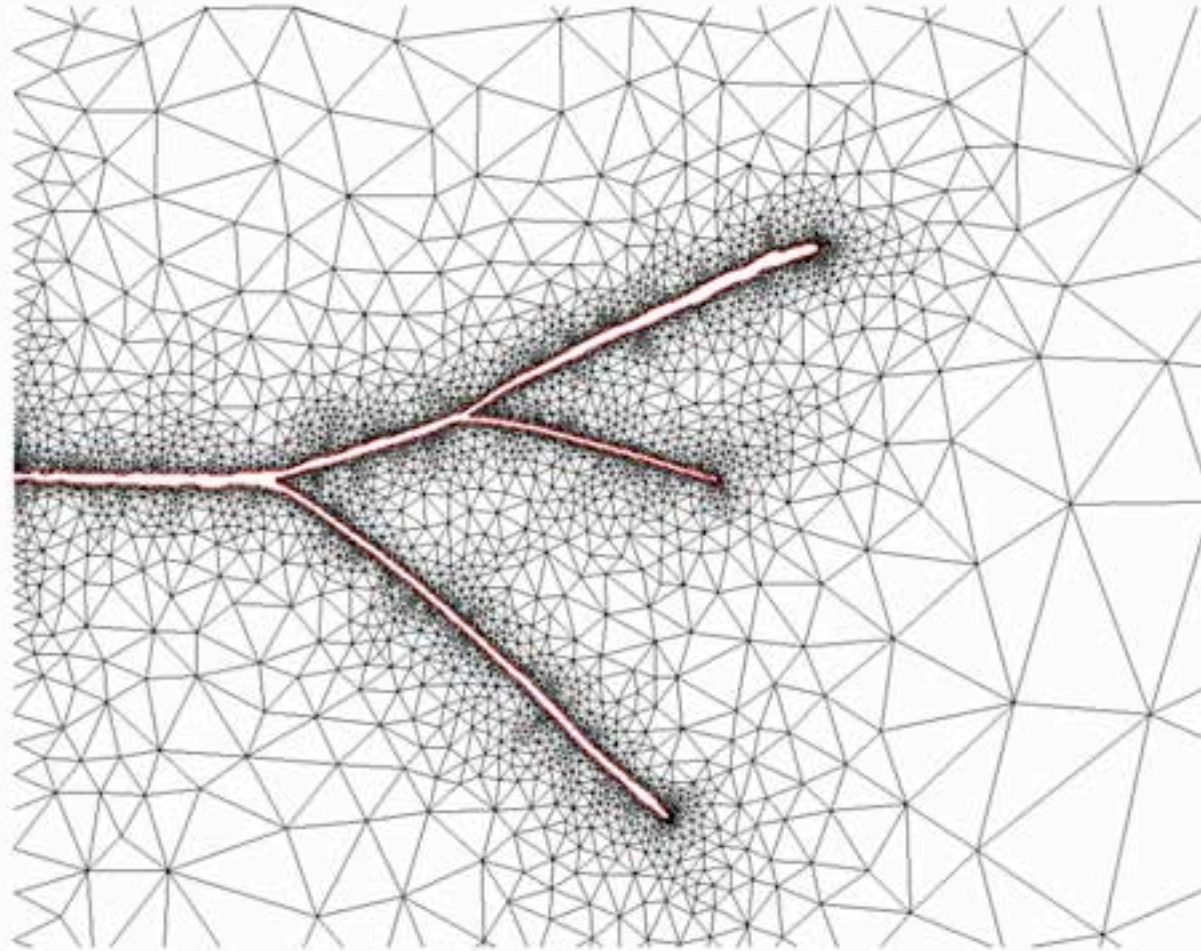
Branching



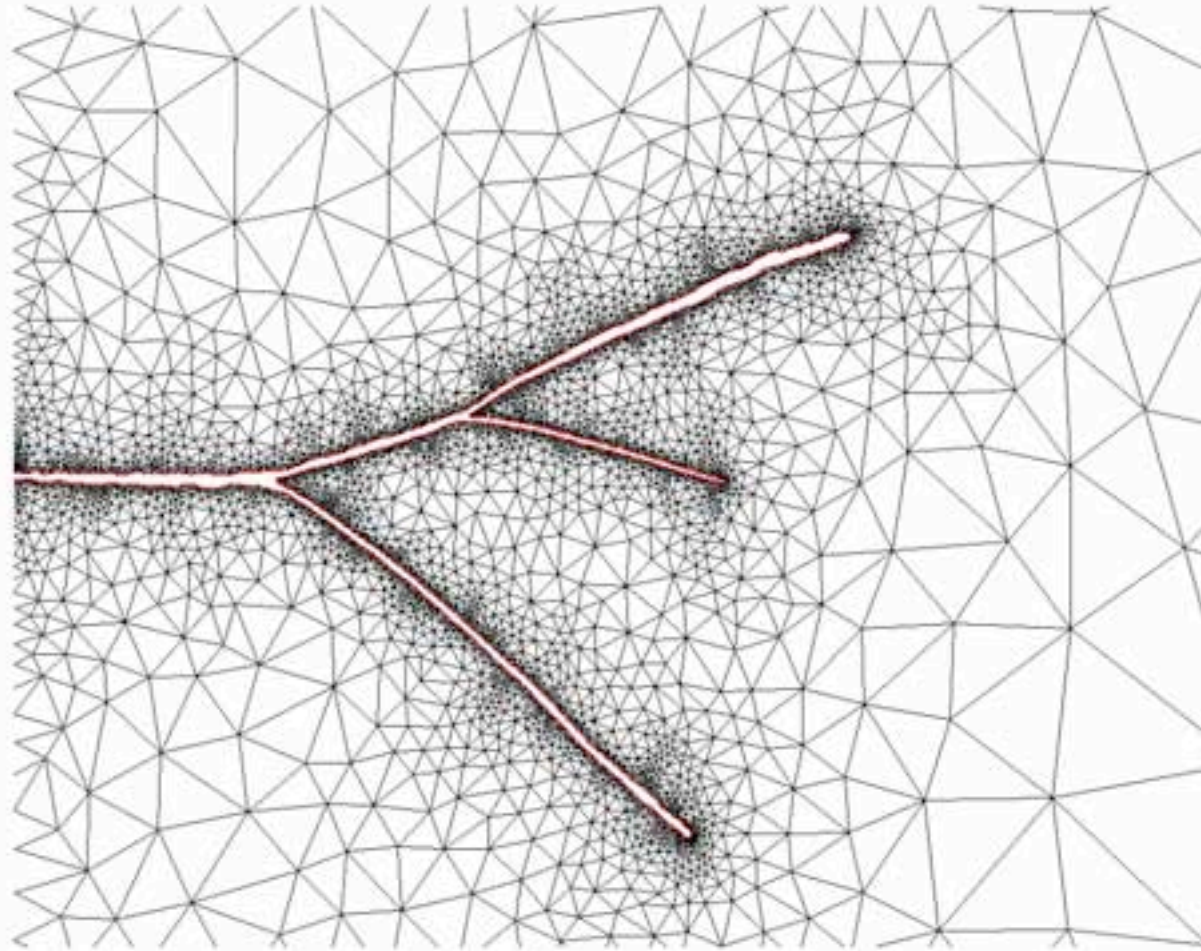
Branching



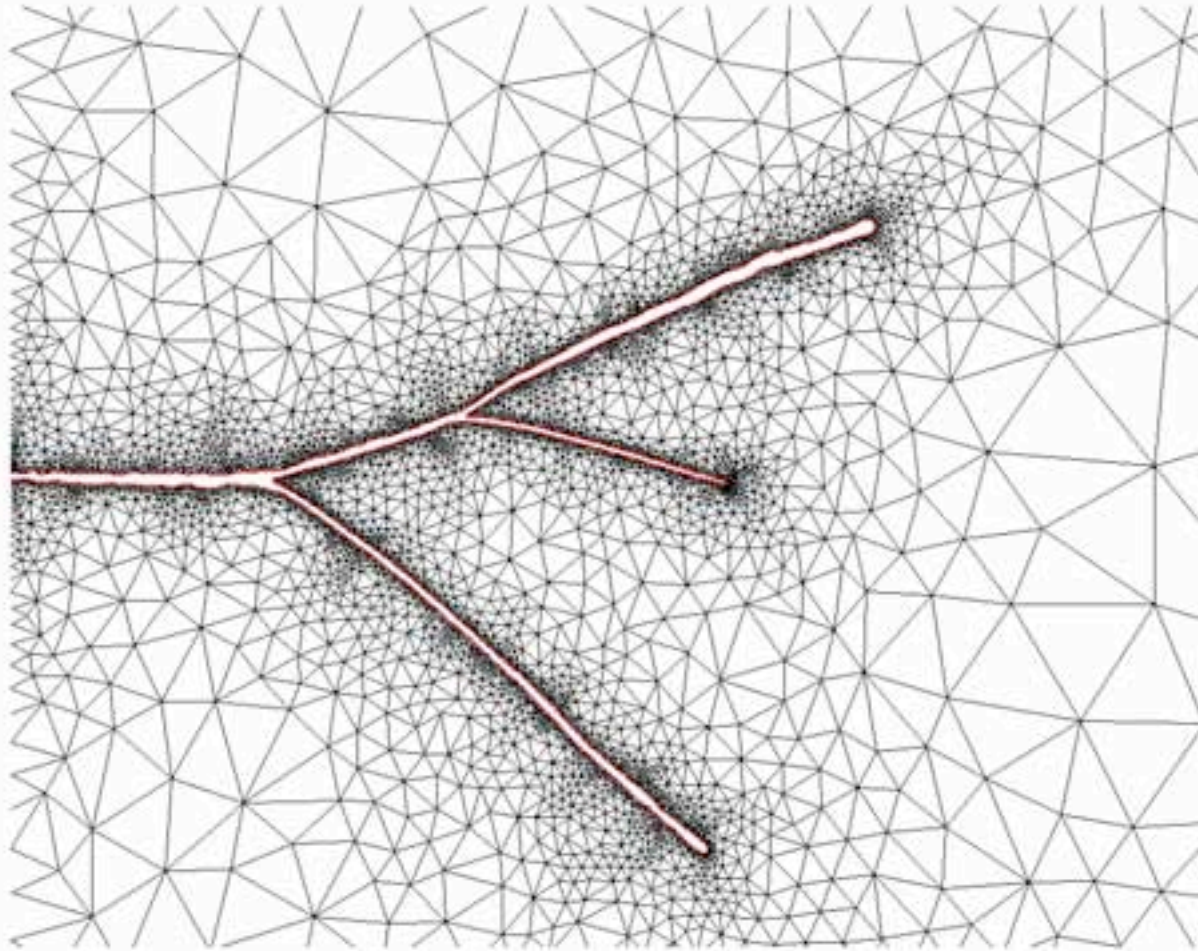
Branching



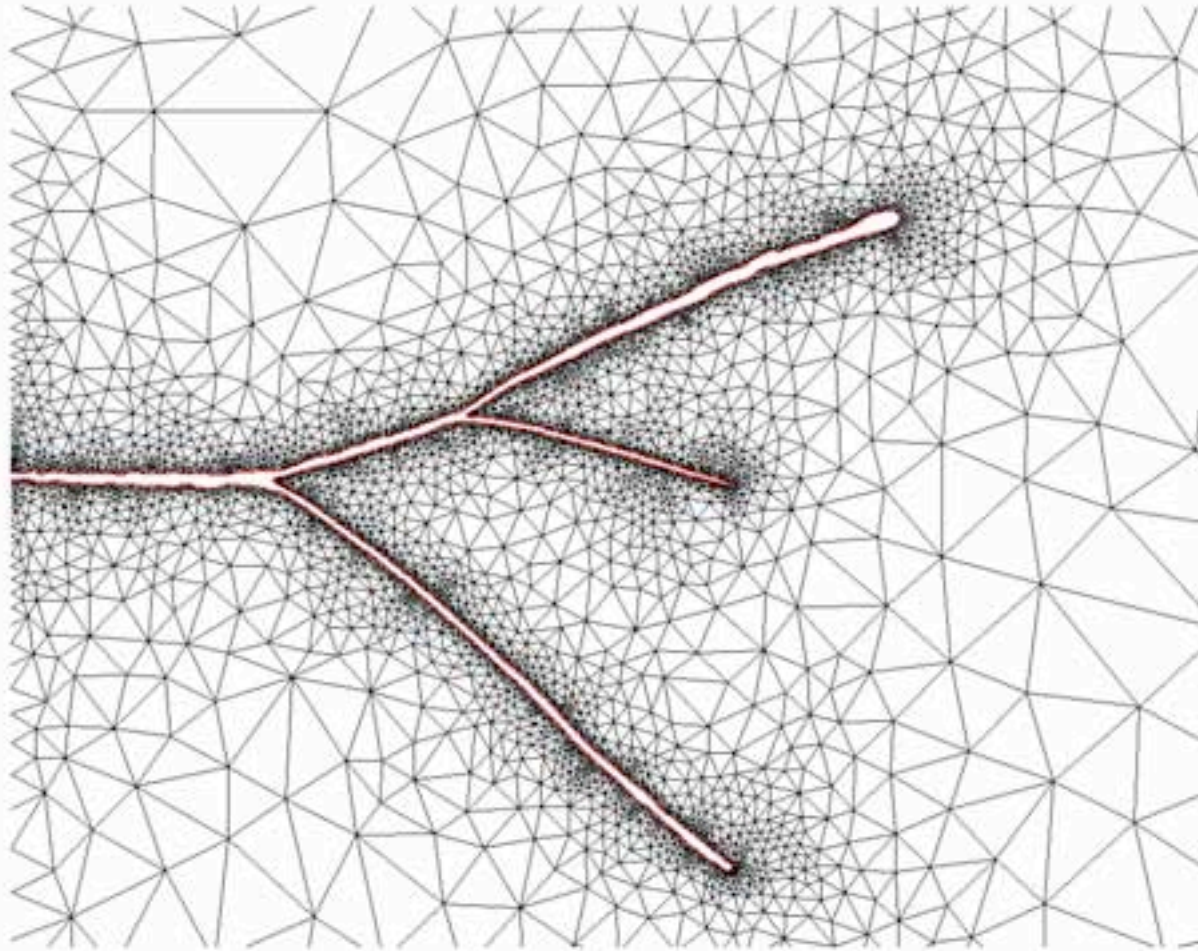
Branching



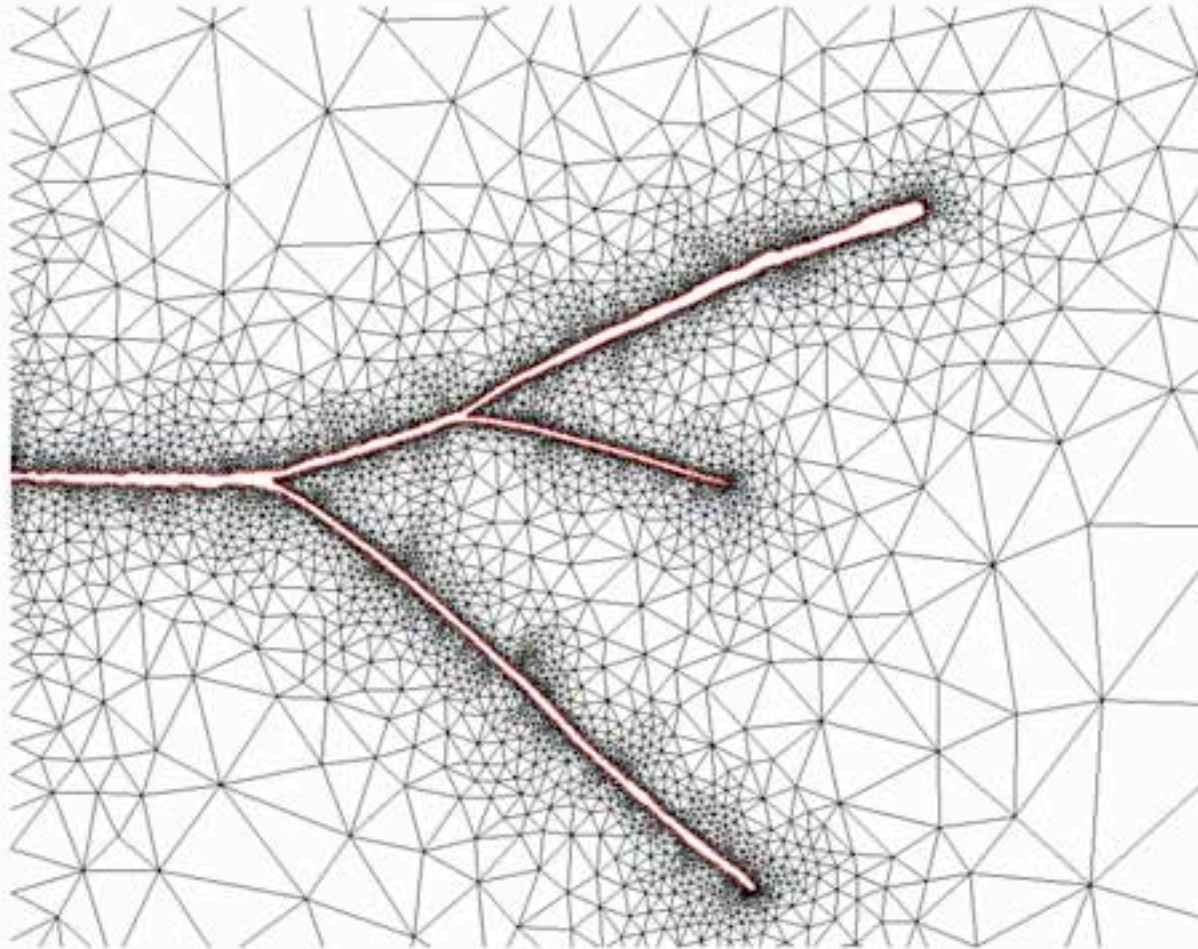
Branching



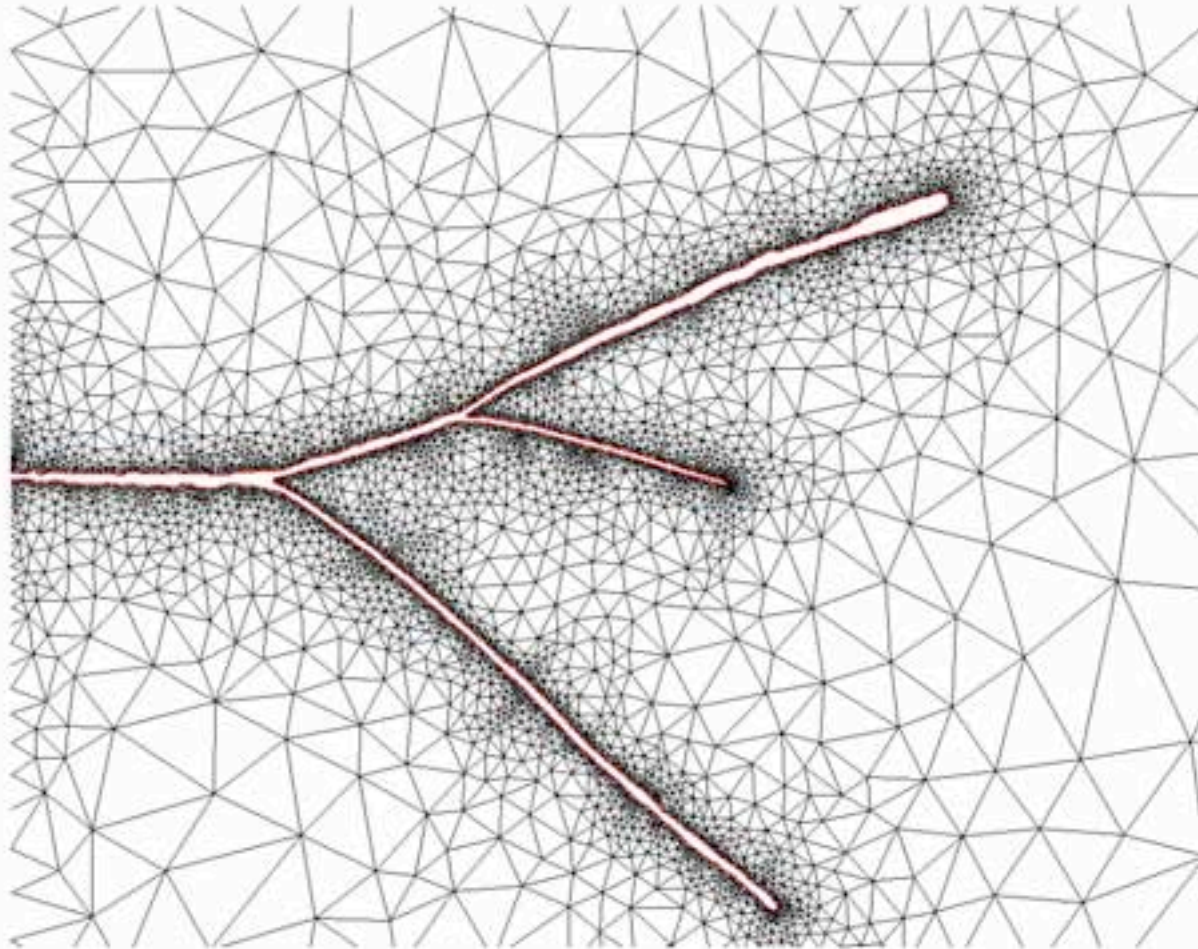
Branching



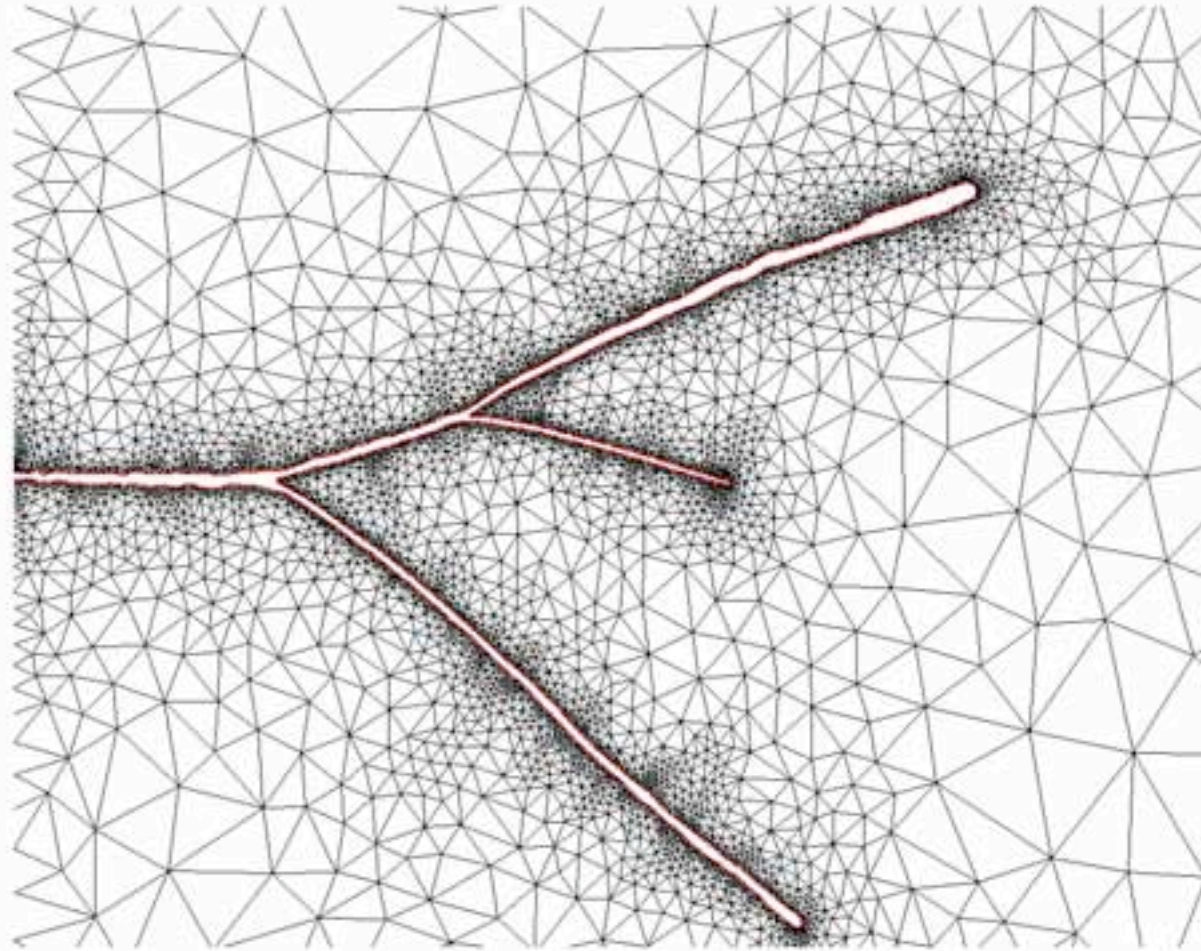
Branching



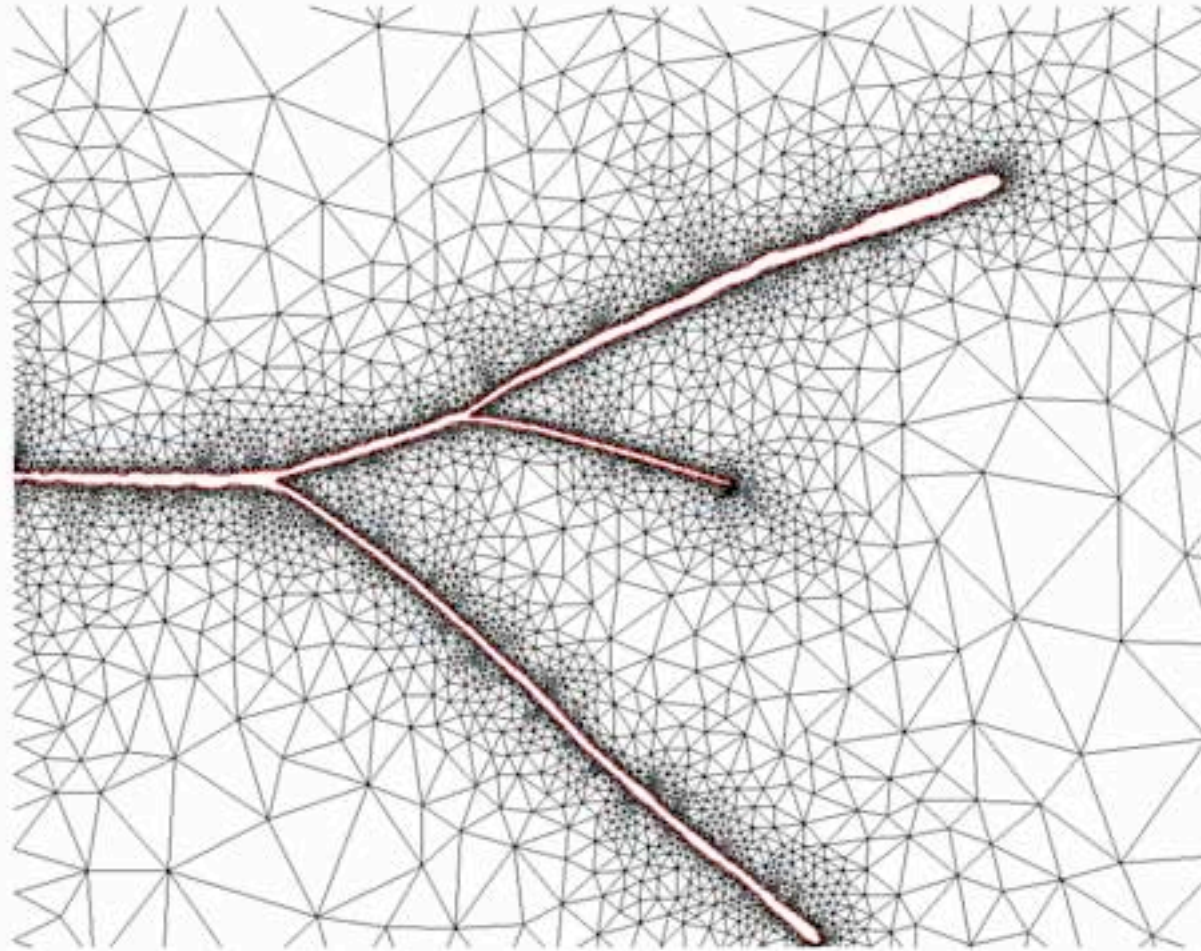
Branching



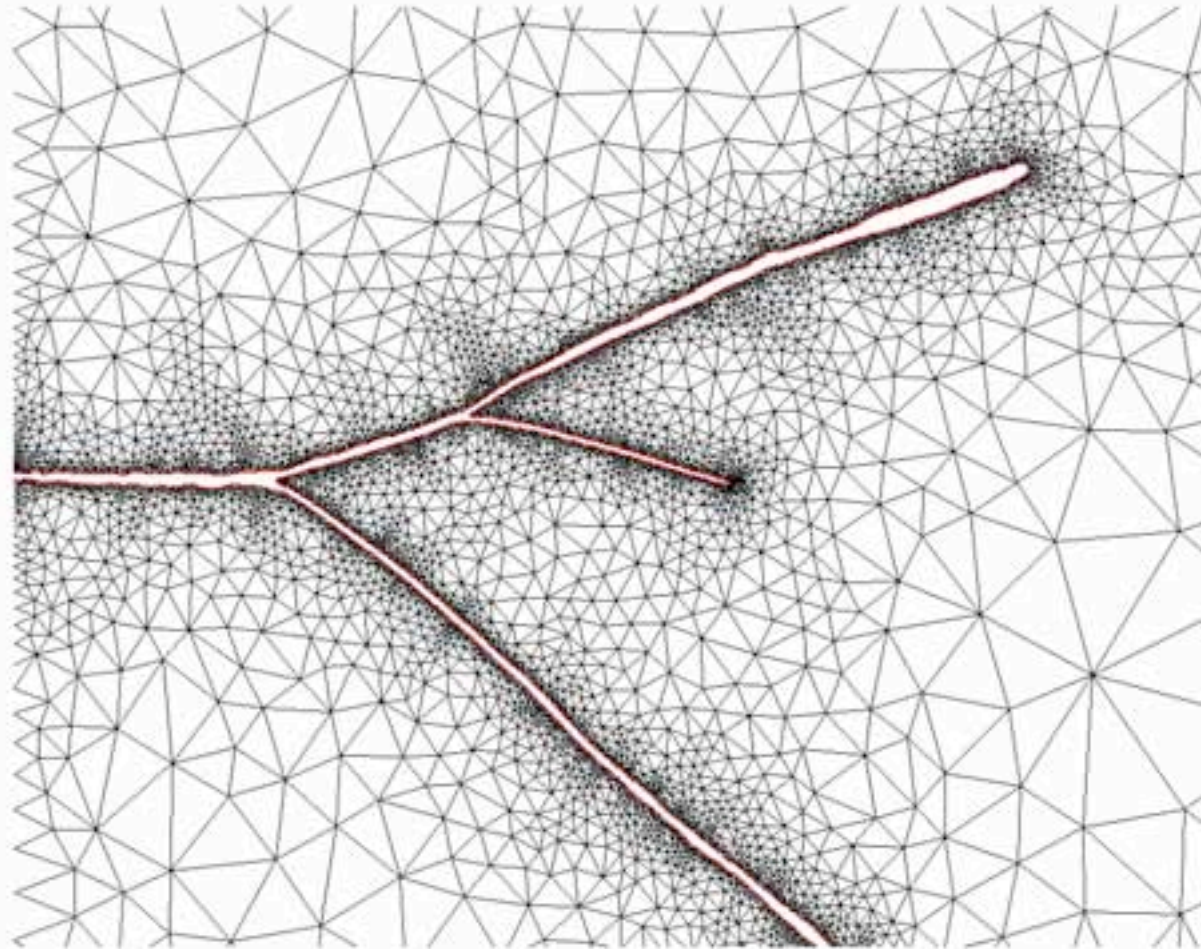
Branching



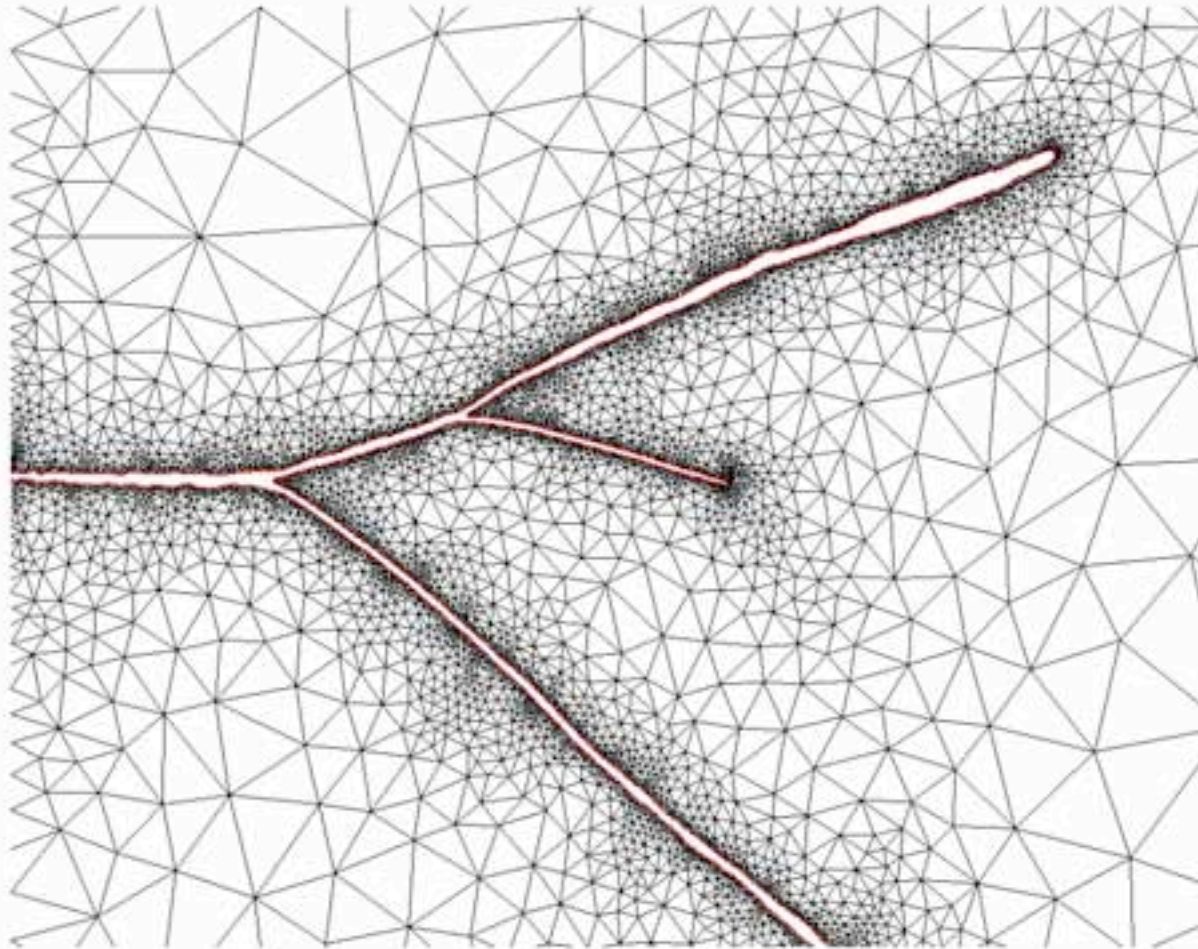
Branching



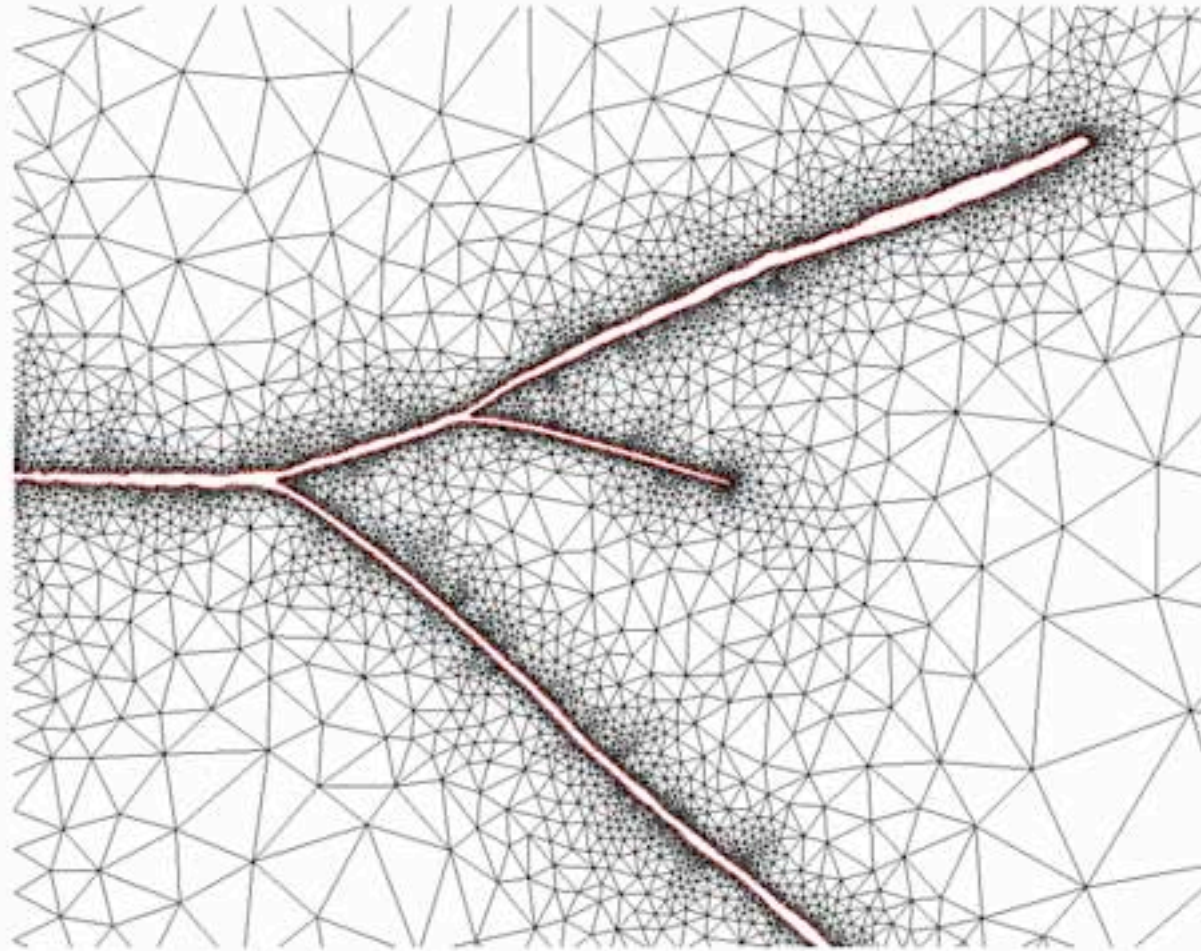
Branching



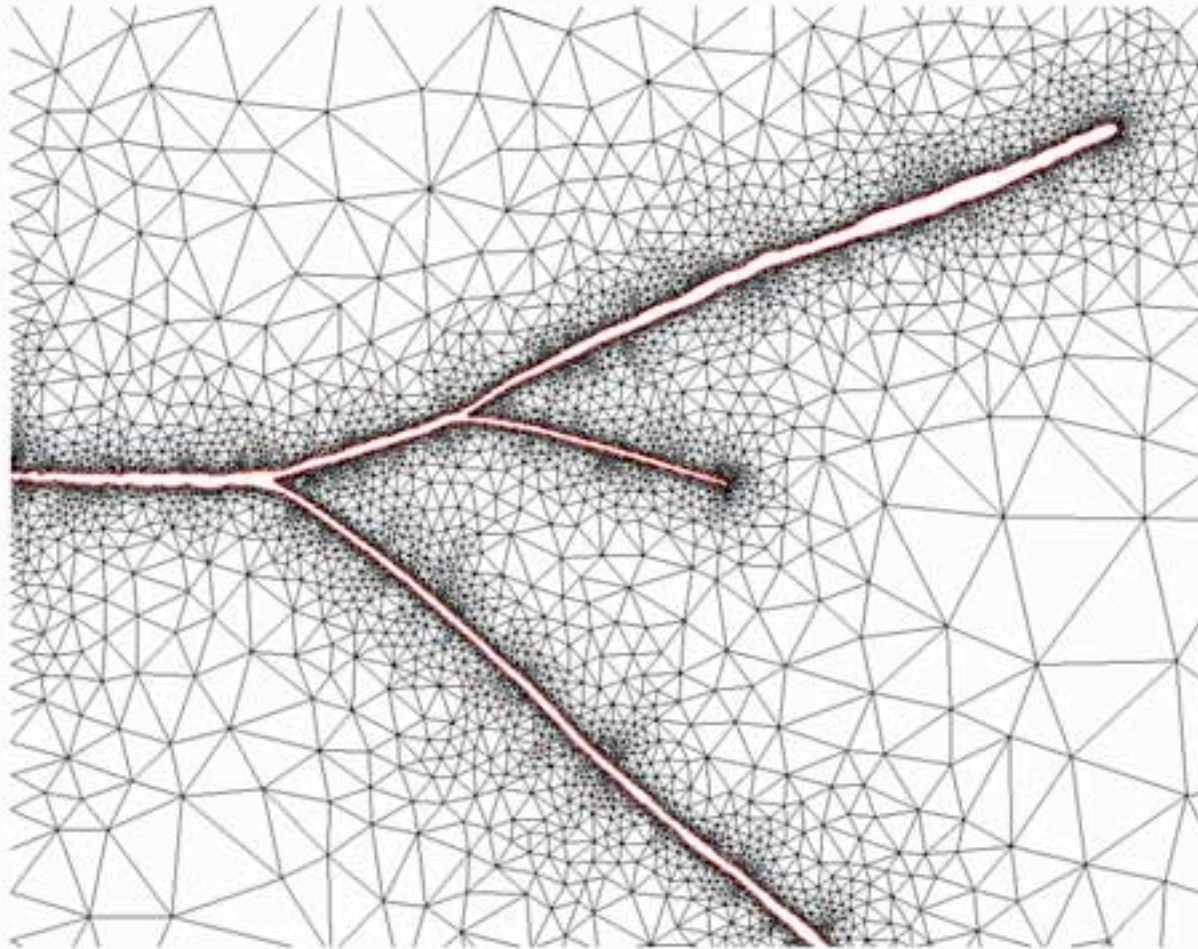
Branching



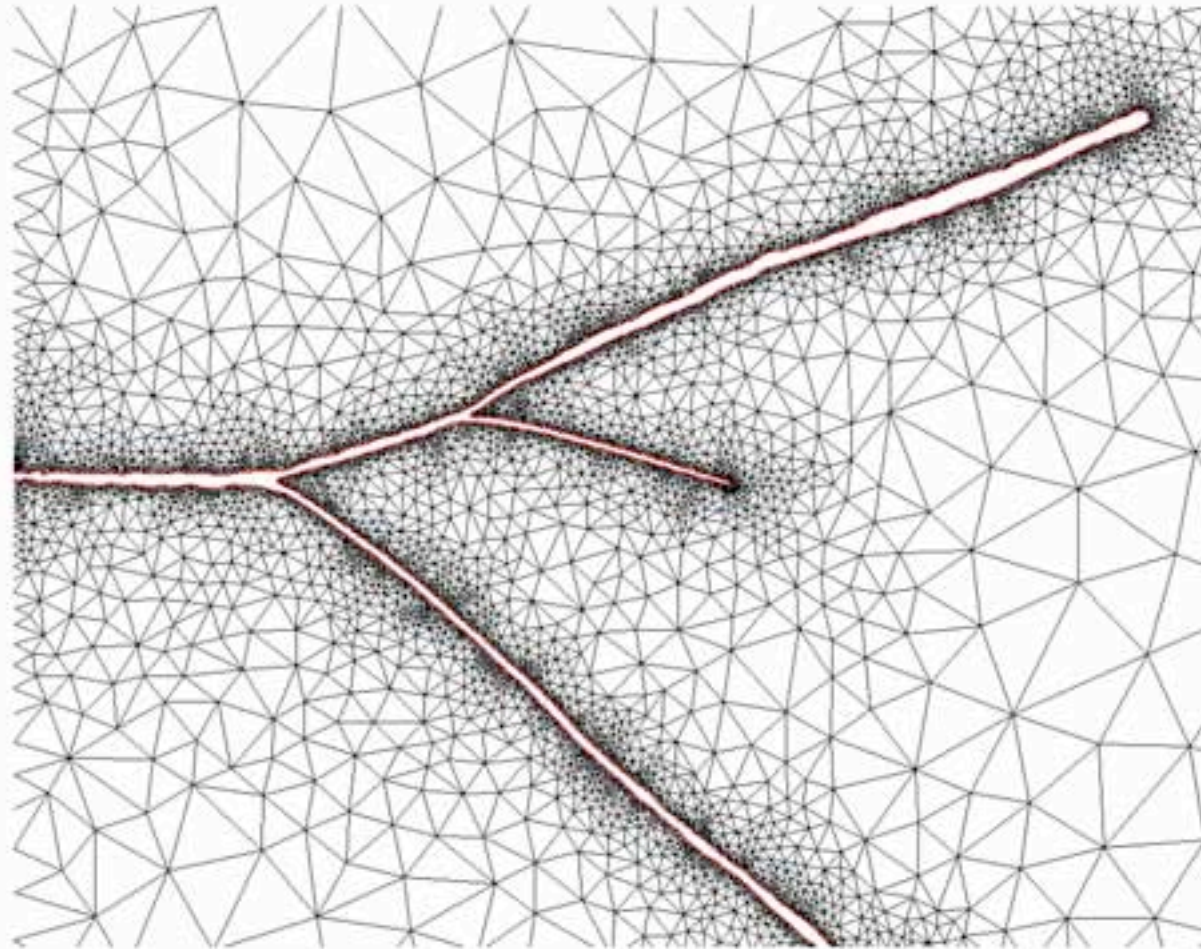
Branching



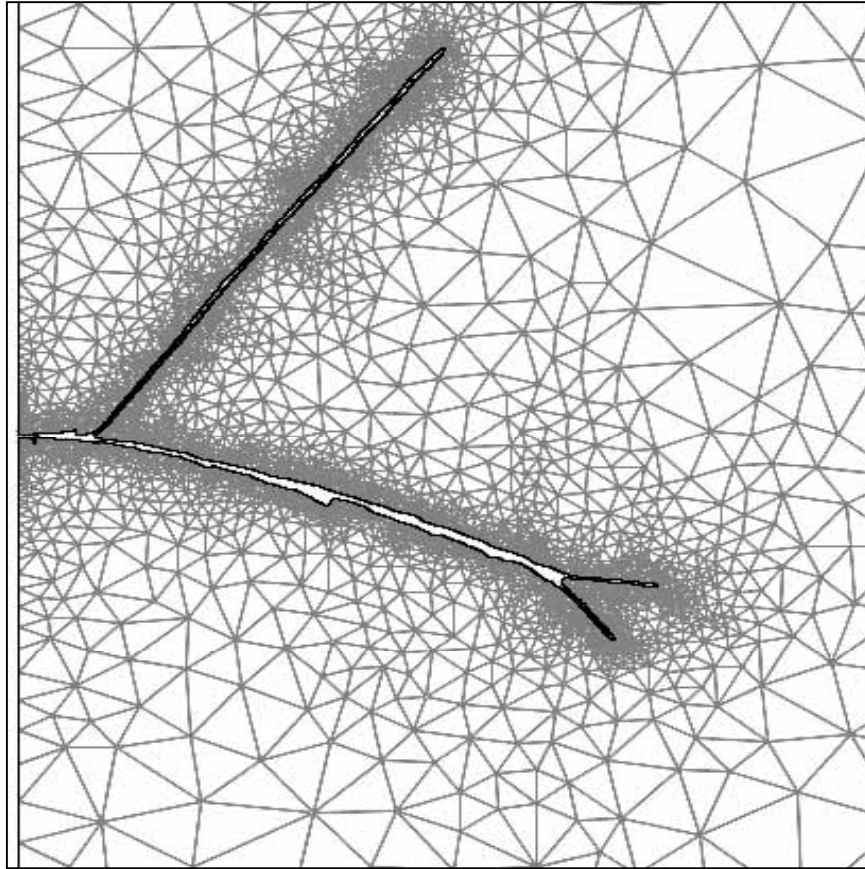
Branching



Branching



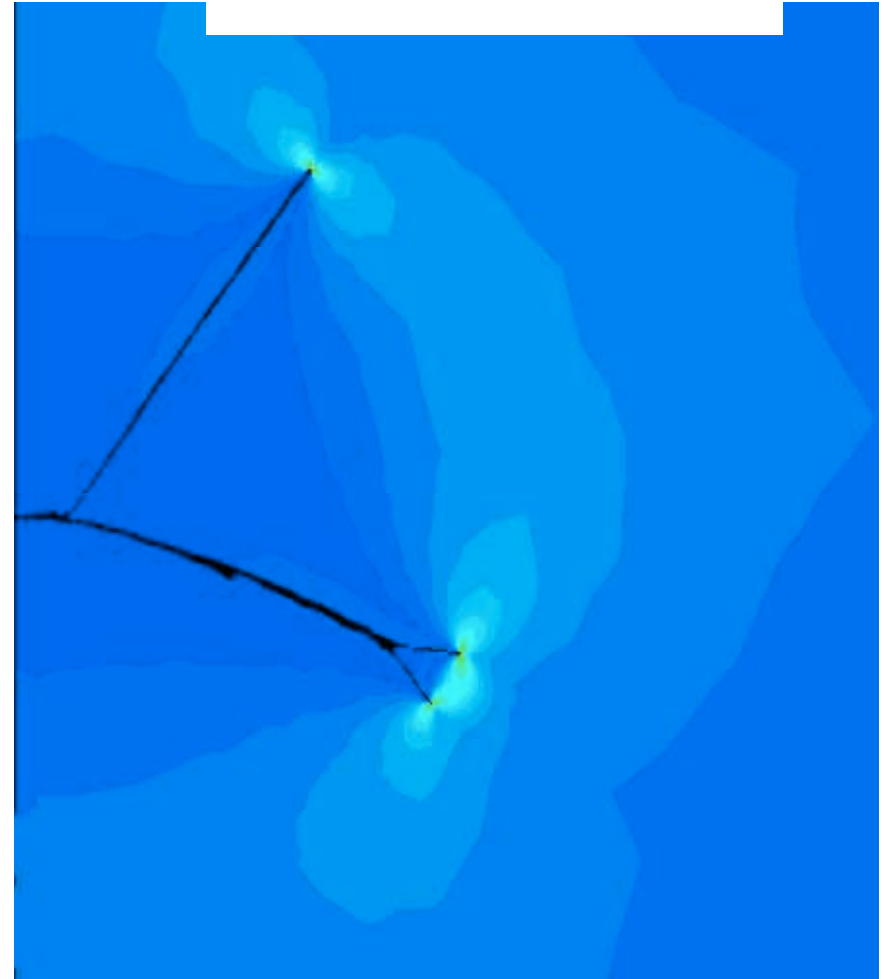
Crack-tip load



Before branching

$$K_I = K_I', \rho = \rho'$$

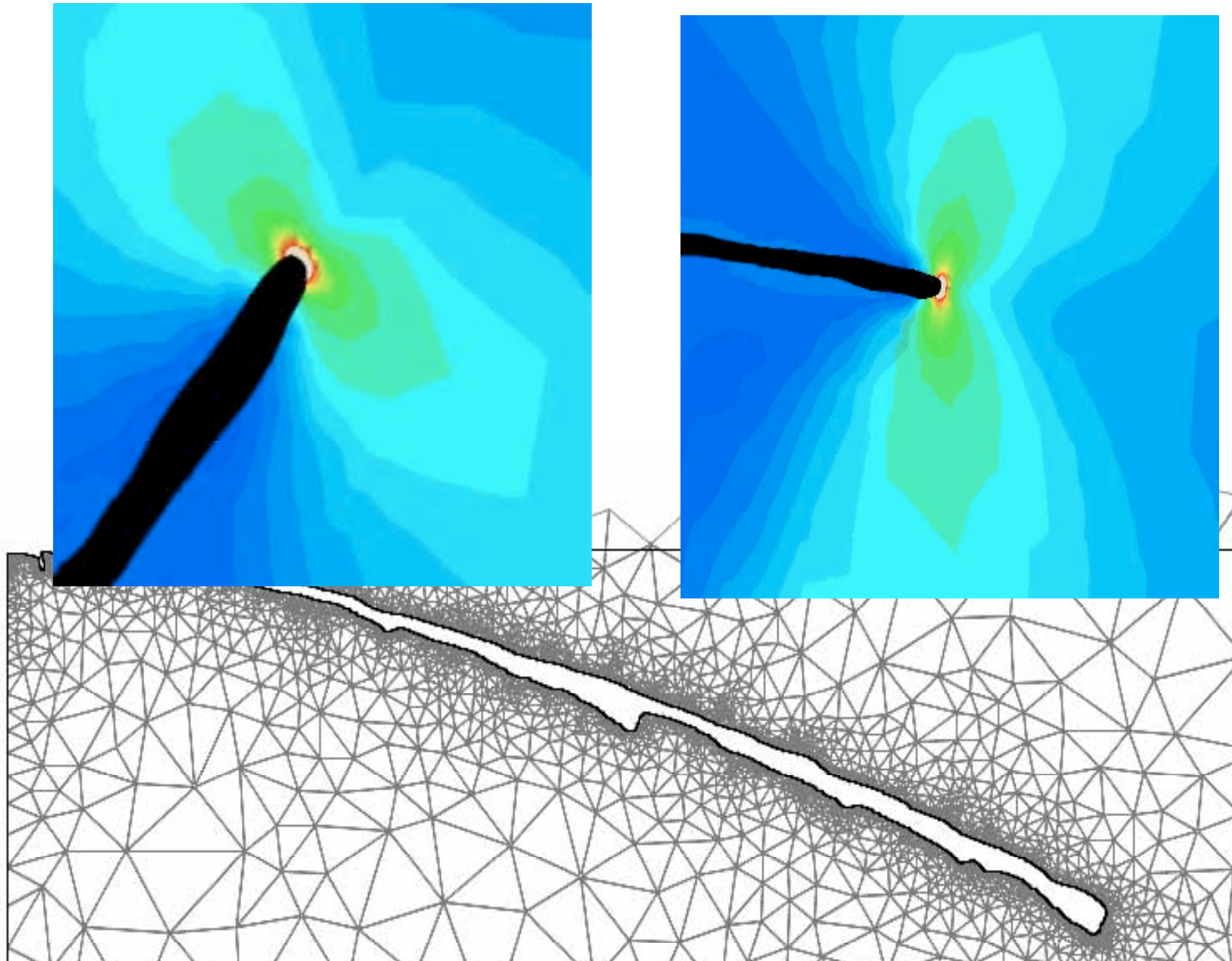
effective stress



After branching

$$K_I \approx 0.7K_I', \rho = \rho'/2$$

Crack-tip Load



Phase Field Modelling of Stress Corrosion

**Per Ståhle, Eskil Hansen
LU, Lund Sweden**

Contributions to the free energy (Ginzburg & Landau, 1950)

$$\mathcal{F} = \mathcal{F}_{el} + \mathcal{F}_{ch} + \mathcal{F}_{gr}$$

Volume totals:

Elastic energy $\mathcal{F}_{el} = \int \frac{G(\psi)}{2} (\nabla w)^2 dV$

Chemical energy $\mathcal{F}_{ch} = \int U(\psi) dV$

Gradient energy $\mathcal{F}_{gr} = \int \frac{g_b}{2} (\nabla \psi)^2 dV$

Antiplane deformation \Rightarrow Two free variables

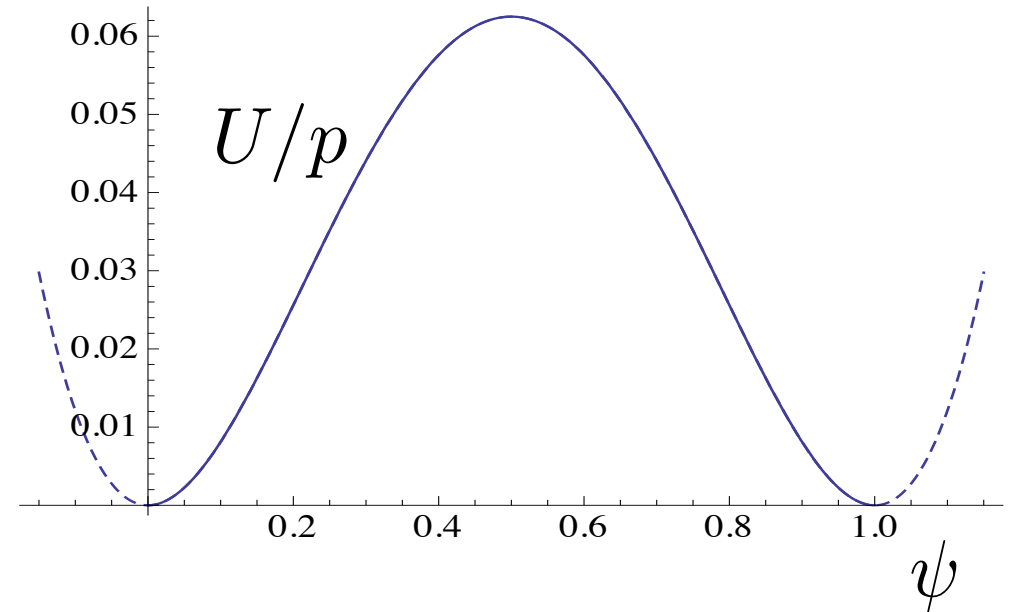
Displacements w and phase (density) ψ

$$\frac{\partial \psi}{\partial t} = -L_{\psi} \frac{\delta \mathcal{F}}{\delta \psi} , \quad \frac{\partial w}{\partial t} = -L_w \frac{\delta \mathcal{F}}{\delta w}$$

Ginzburg, Landau (50)

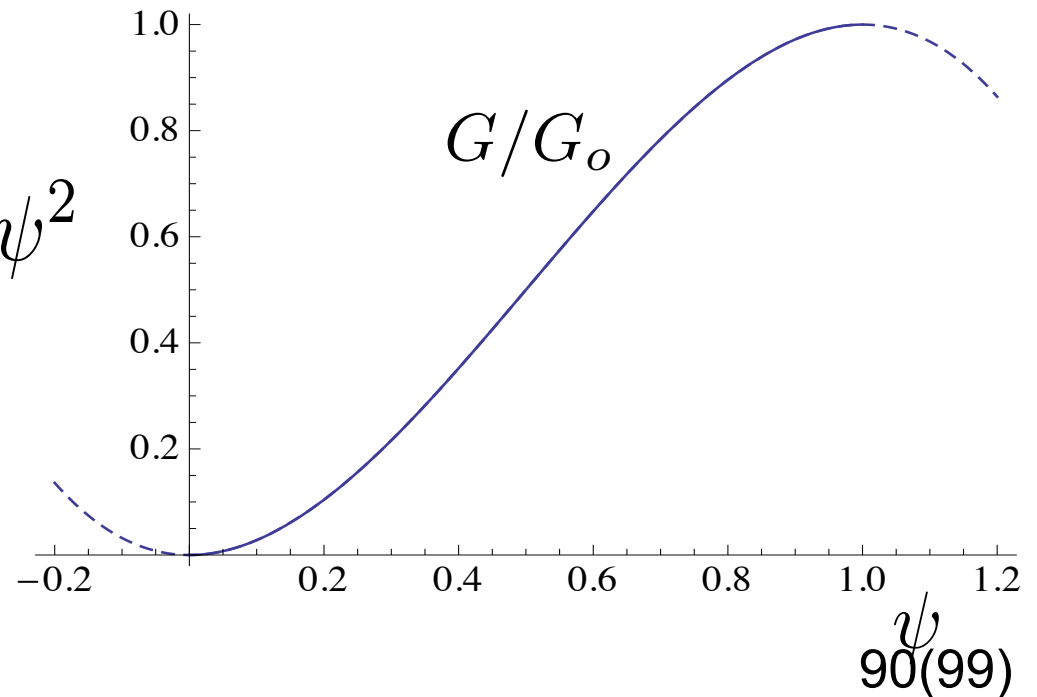
Double-well
chemical potential

$$U(\psi) = p \psi^2 (1 - \psi)^2$$



Shear modulus

$$G(\psi) = G_o(\psi)(-2\psi + 3)\psi^2$$



Evolution of the phase

$$\frac{\partial \psi}{\partial t} = -L_\psi \left[\frac{1}{2} G'(\psi) (\nabla w)^2 + p\psi(\psi^2 - 1) - g_b \Delta \psi \right]$$

Evolution of the displacements

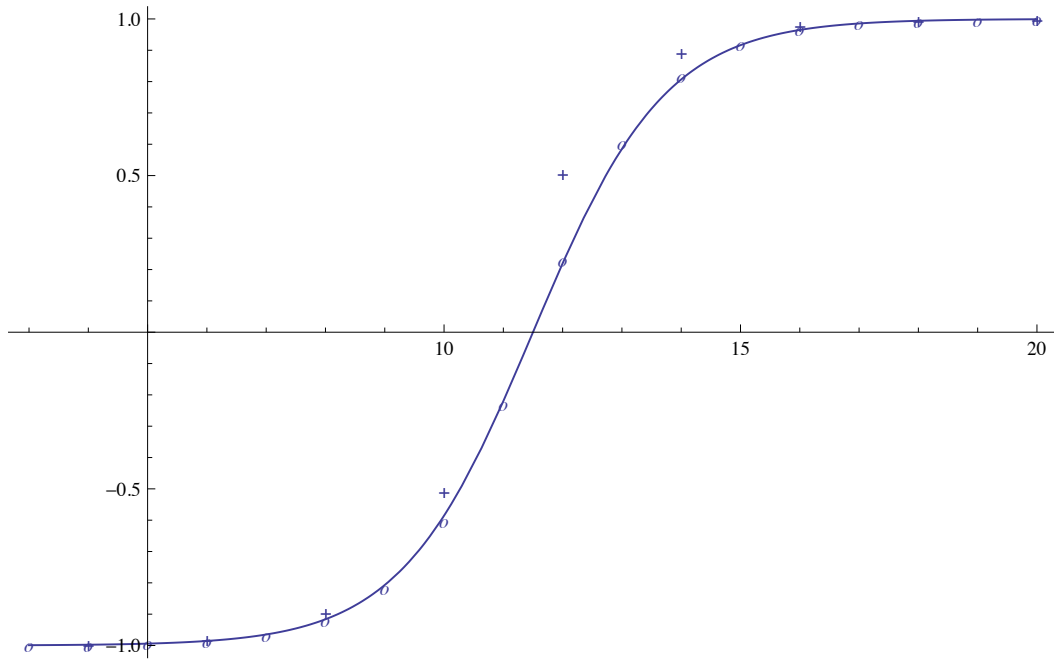
$$\frac{\partial w}{\partial t} = L_w \nabla \cdot [G(\psi) \nabla w]$$

At equilibrium: $\nabla \cdot [G(\psi) \nabla w] = 0$

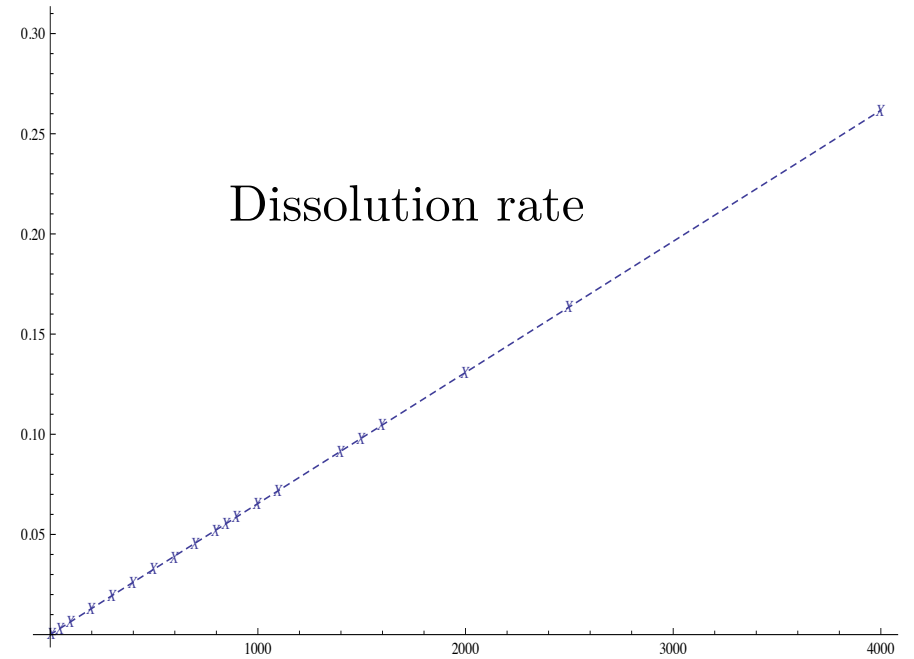
Steady state solution

$$\psi = -\tanh\left(\sqrt{\frac{p}{2g_b}}x_2 + \frac{3}{4}L_\psi G_o(\nabla w)^2 \sqrt{\frac{2g_b}{p}}t\right)$$

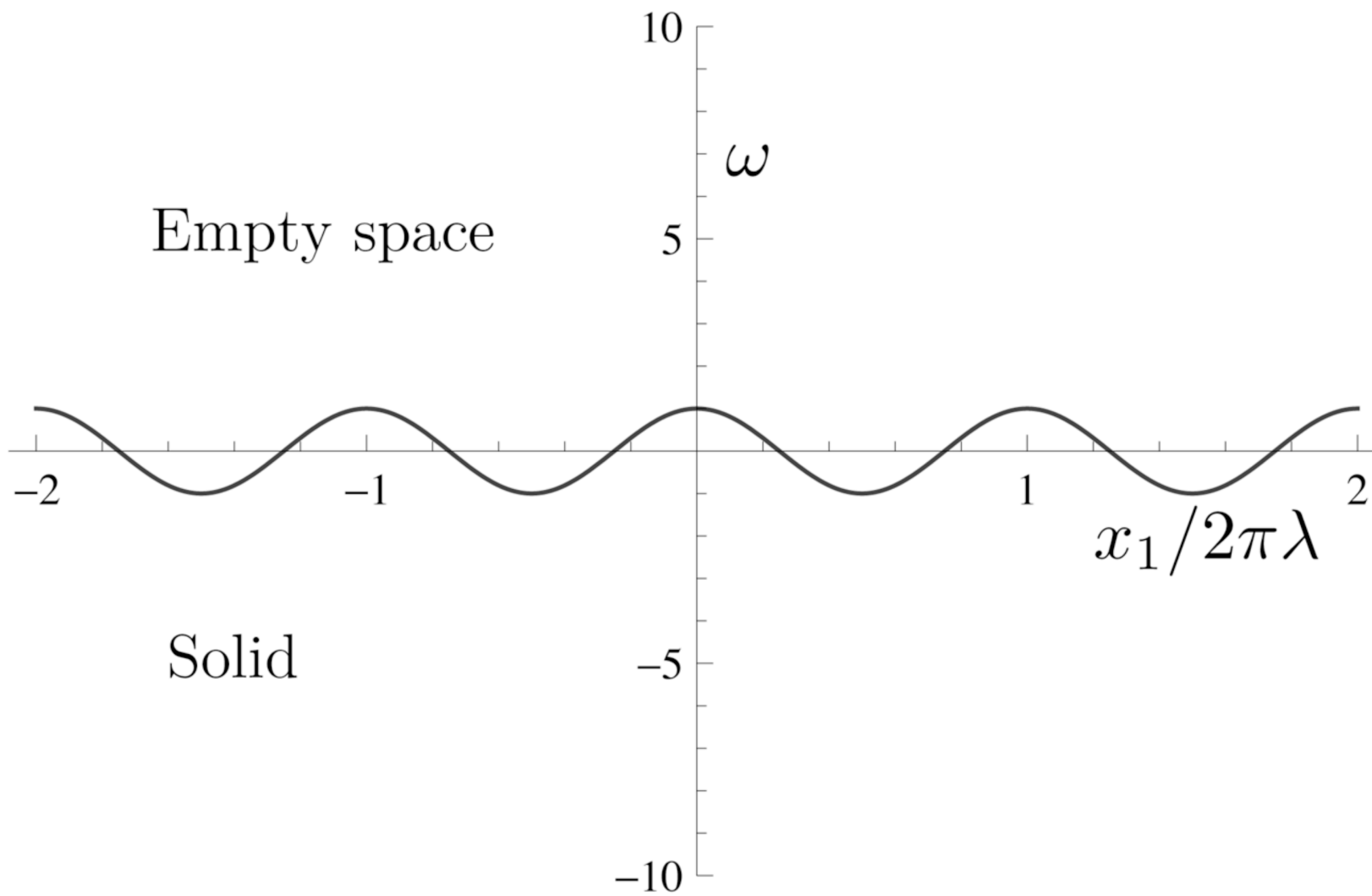
Transition Rate vs. Distance



Dissolution Rate vs. Tensile Stress

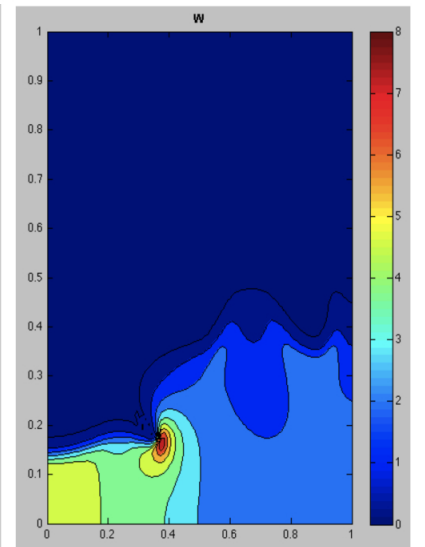
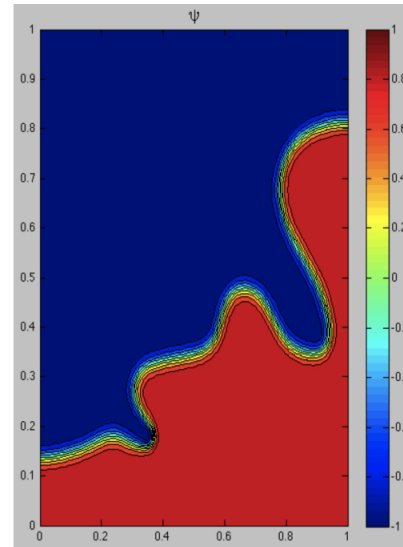
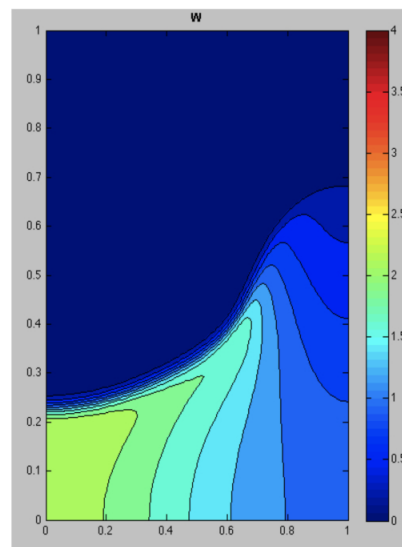
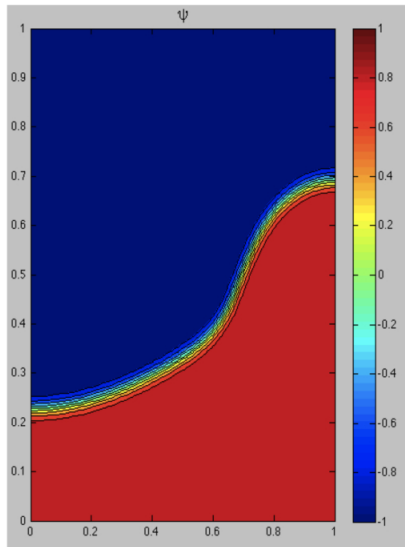
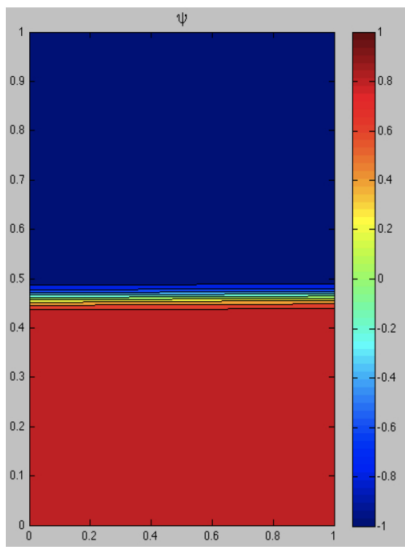
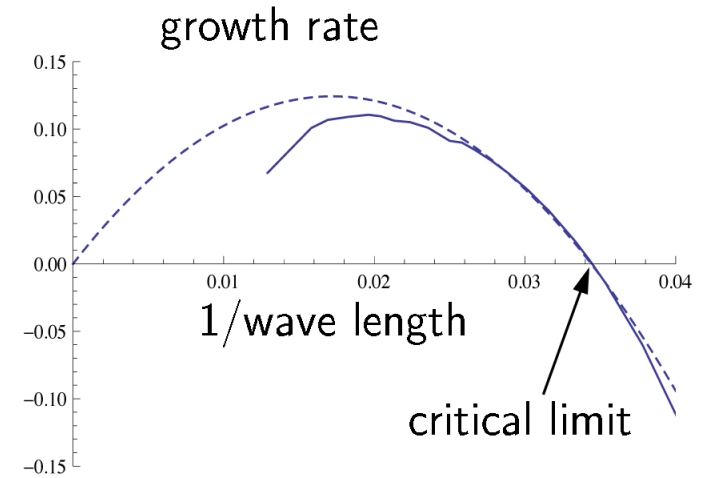


Tensile stress



$$\left(\frac{d}{dx_2} - 2\beta\right)(f' + f^2 - 1) = 0$$

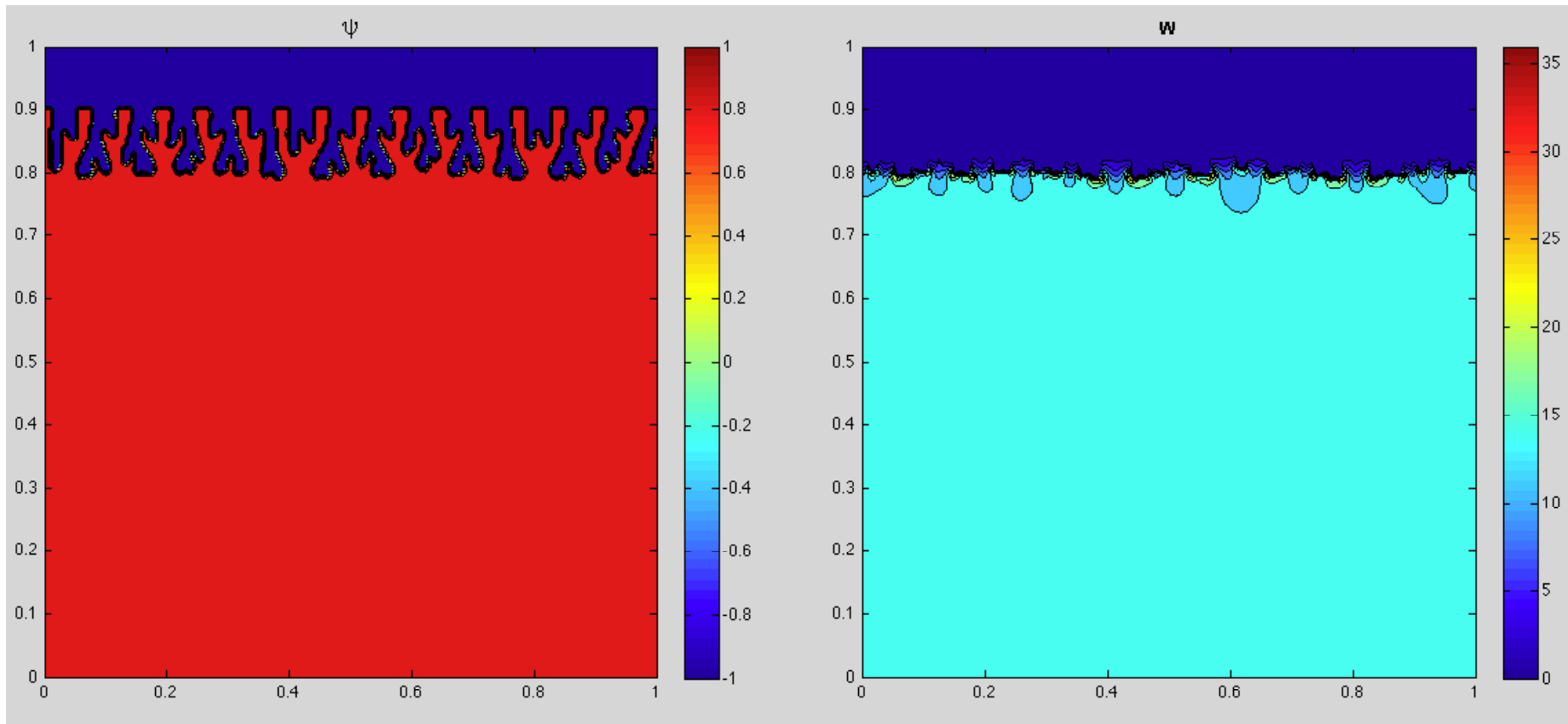
$$\psi = -\tanh\left(\sqrt{\frac{p}{2g_b}}x_2 + \frac{3}{4}L_\psi G_o(\nabla w)^2\sqrt{\frac{2g_b}{p}}t\right)$$



Red is remaining material

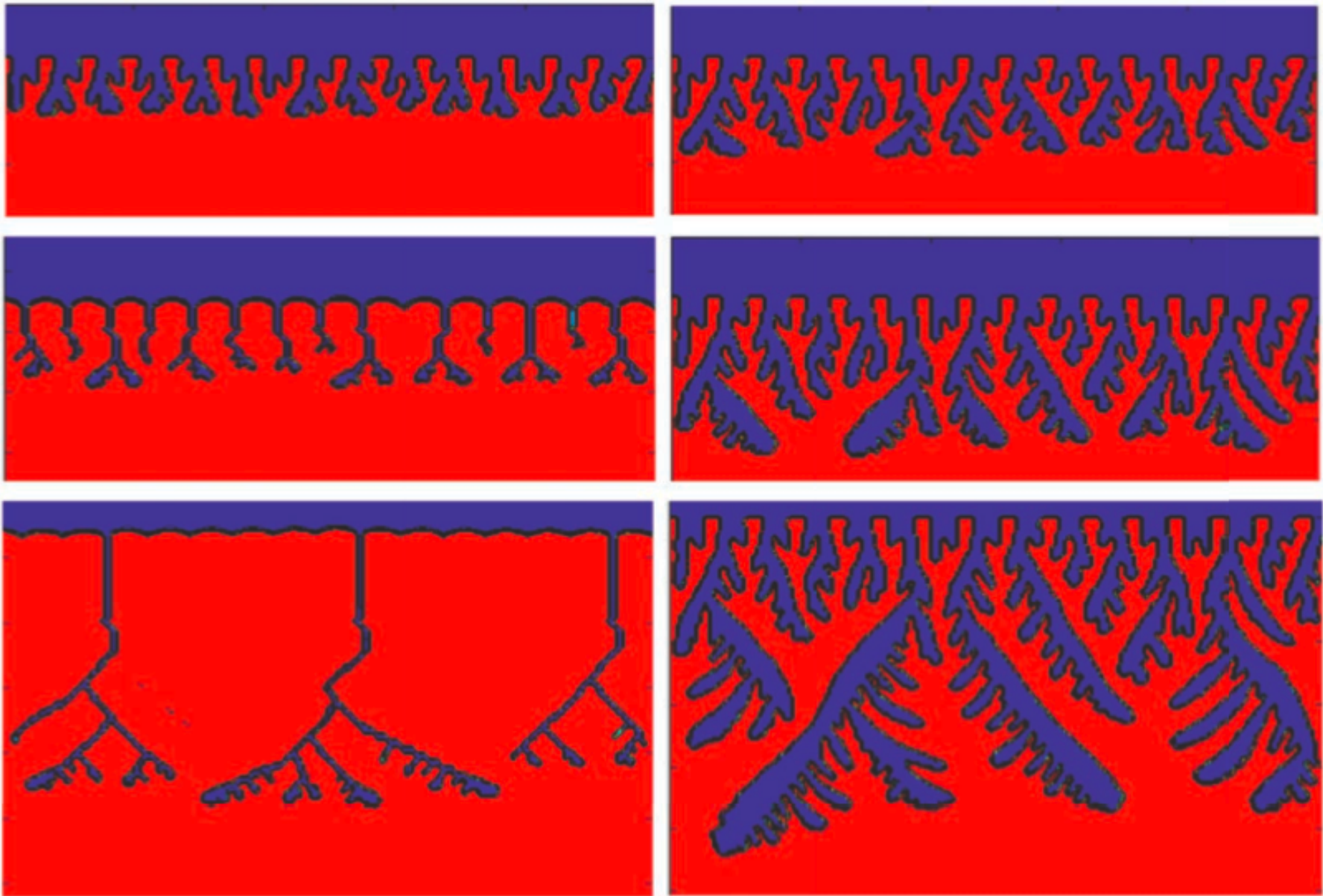
Effective Stress

Effective Stress



Red is remaining material

Effective stress



Without general corrosion

with general corrosion

Formation and growth of hydrides

Per Ståhle

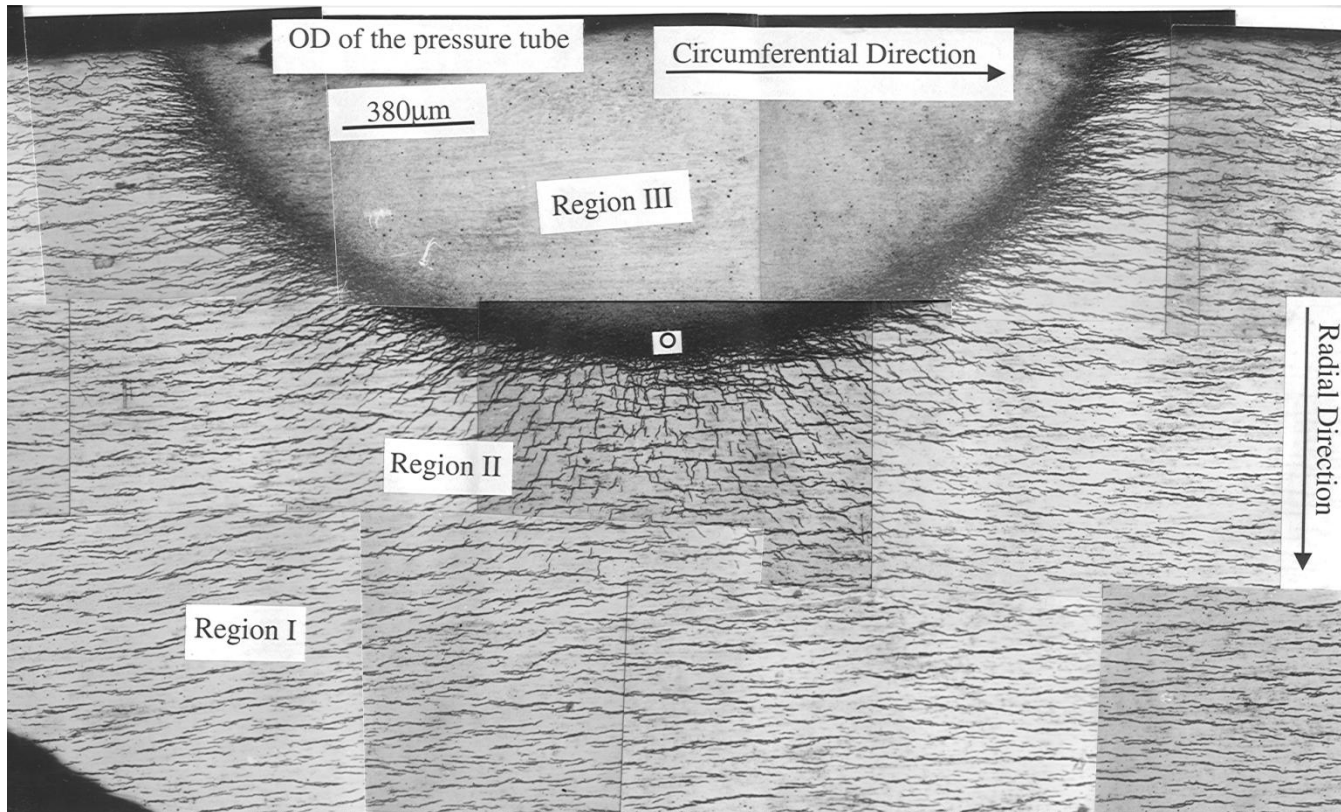
Solid Mechanics,
Lund University, Sweden

Collaborators:

Wurigul Reheman, Ram N Singh,
Martin Fisk, Srikumar Banerjee,
Ali Massih, Christina Bjerken



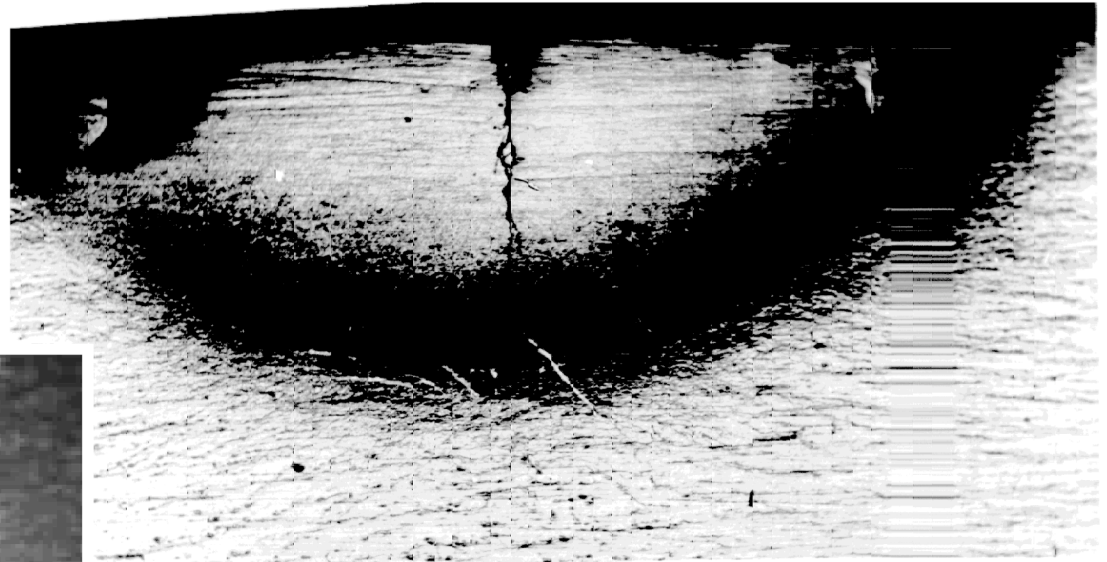
Hydride Blister section



Optical micrograph of hydride blister section, grown in Zr-2.5wt.% Nb pressure tube material. Three regions - Region I - matrix & circumferential hydrides, region II - matrix containing both radial and circumferential hydrides and region III - mainly of δ -hydride.

The basis of radial hydride formation is the stress field of blister in the matrix surrounding it.

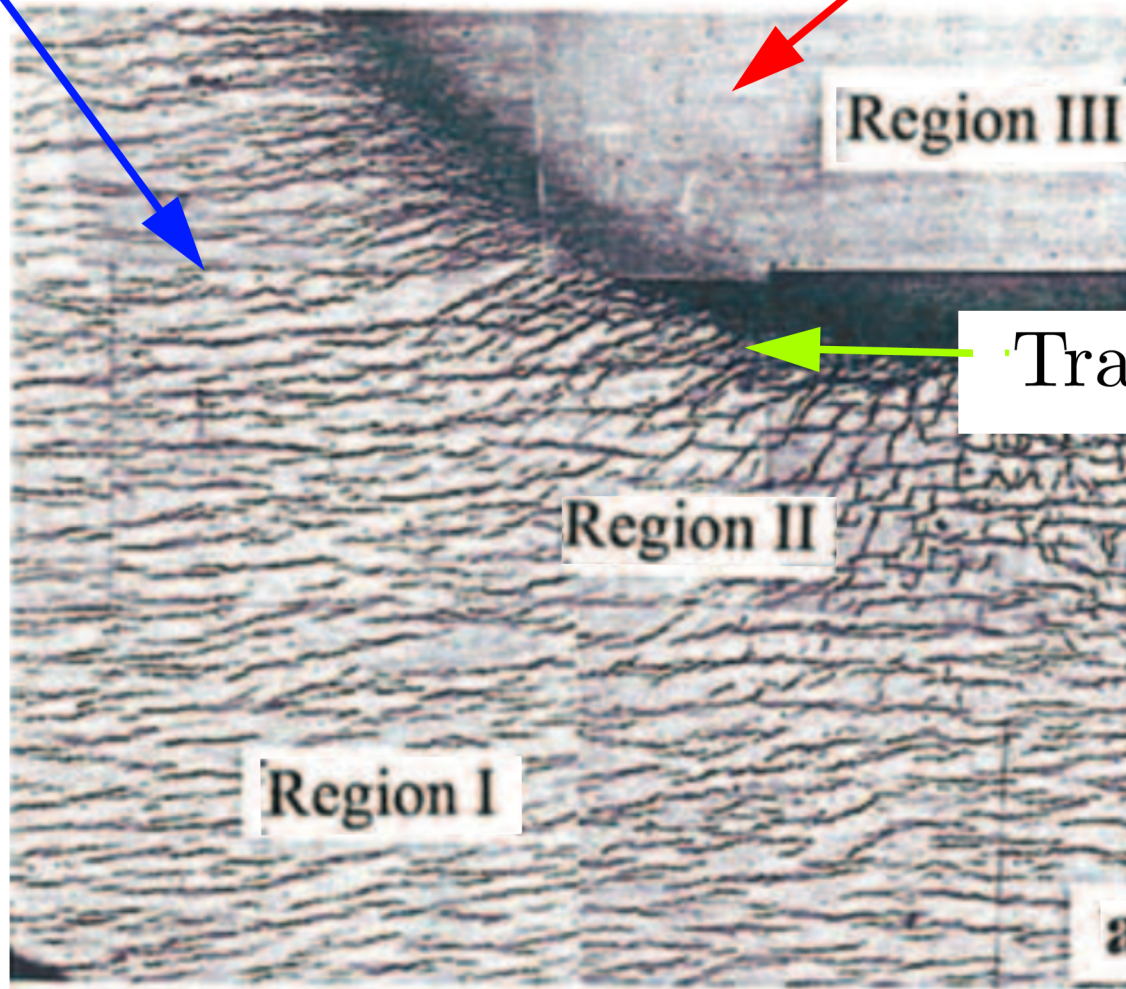
a hydride blister grown in Zr–2.5wt%Nb
pressure tube alloy (Singh *et al.*, 2001)



The Phase Field

$\psi = 0 \rightarrow \text{Zr}$

$\psi = 1 \rightarrow \text{Zr}_n\text{H}$



Transient region
 $0 < \psi < 1$

Contributions to the free energy

$$\mathcal{F} = \mathcal{F}_{el} + \mathcal{F}_{ch} + \mathcal{F}_{gr}$$

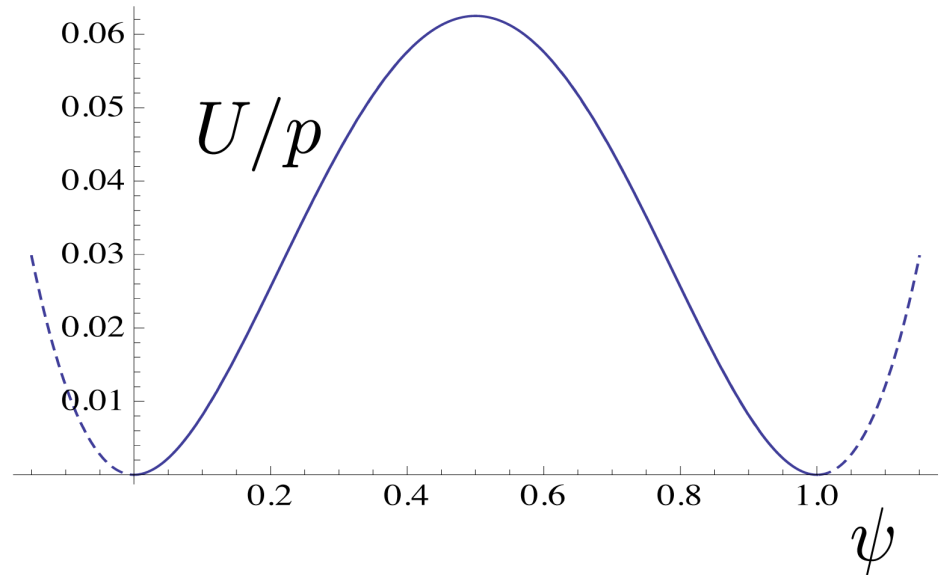
Elastic energy $\mathcal{F}_{el} = \int \sigma_{ij} d\epsilon_{ij}$

Chemical energy $\mathcal{F}_{ch} = U(\psi)$

Gradient energy $\mathcal{F}_{gr} = \frac{g_r}{2} (\psi_{,i})^2$

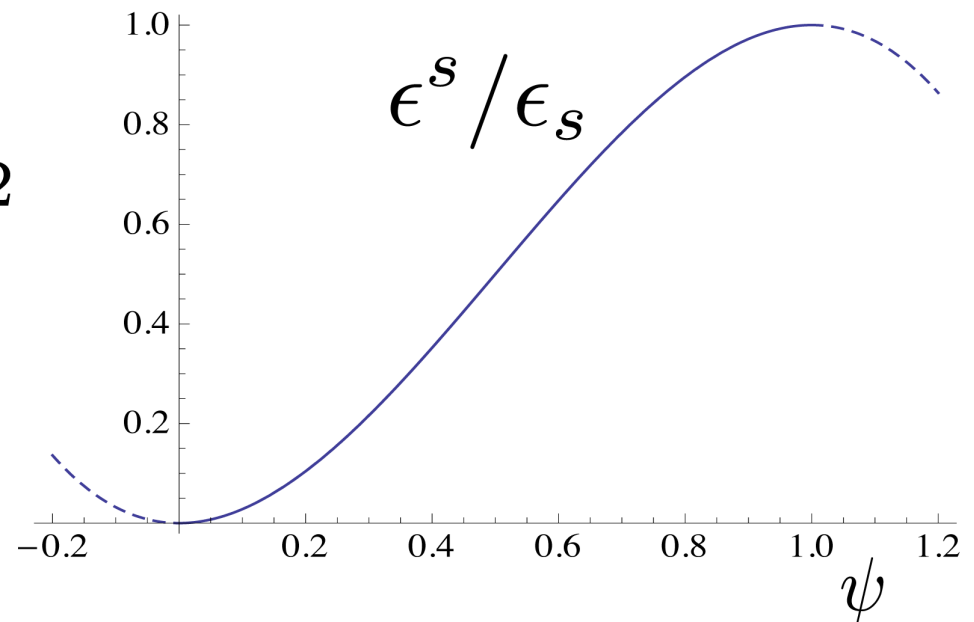
Double-well
chemical potential

$$U(\psi) = p\psi^2(1 - \psi)^2$$



Expansion

$$\epsilon^s(\psi) = \epsilon_s(3 - 2\psi)\psi^2$$



Plane cases.

Unknown: ψ, u_1, u_2

Phase:
$$\frac{\partial \psi}{\partial t} = -L_{\psi} \left(\frac{\partial \mathcal{F}}{\partial \psi} - \nabla \frac{\partial \mathcal{F}}{\partial (\nabla \psi)} \right)$$

Displ.:
$$\frac{\partial u_i}{\partial t} = -L_{u_i} \left(\frac{\partial \mathcal{F}}{\partial u_i} - \nabla \frac{\partial \mathcal{F}}{\partial (\nabla u_i)} \right)$$

Heat transfer with heat generation

$$\psi_{,ii} - \frac{\partial \psi}{\partial \tilde{t}} = \{3\epsilon_{ii}^{el} \tilde{\epsilon}_s + 2(1 - 2\psi)\} (1 - \psi)\psi$$

Mechanical equilibrium with thermal expansion

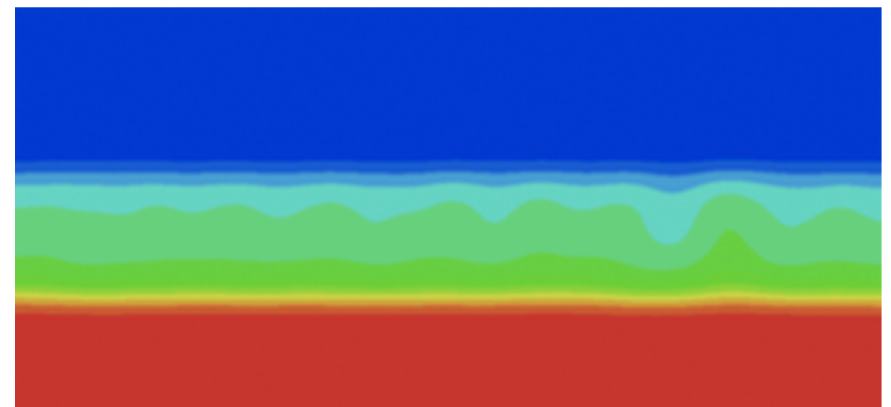
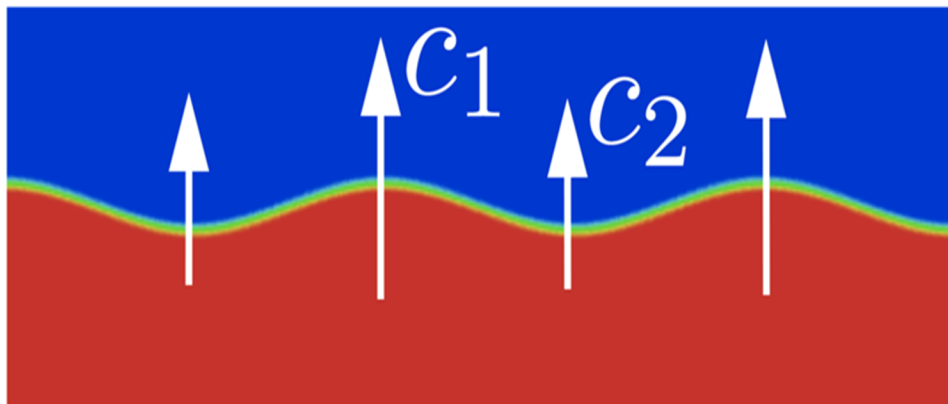
$$\tilde{u}_{i,jj} + \frac{1}{1 - 2\nu} \tilde{u}_{j,ij} - (\tilde{\epsilon}_s)_{,j} = 0$$

In analogy with a fully coupled thermal-stress

Surface energy $\gamma = \sqrt{2p g_b}$ [F/L]

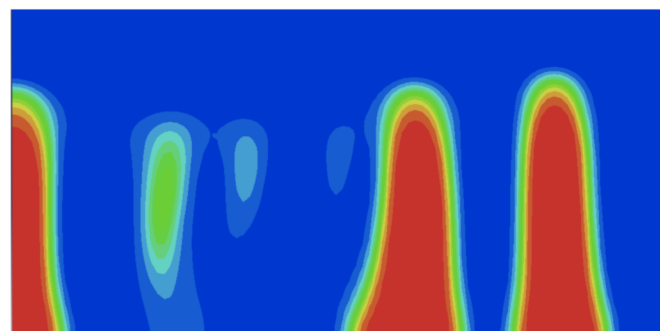
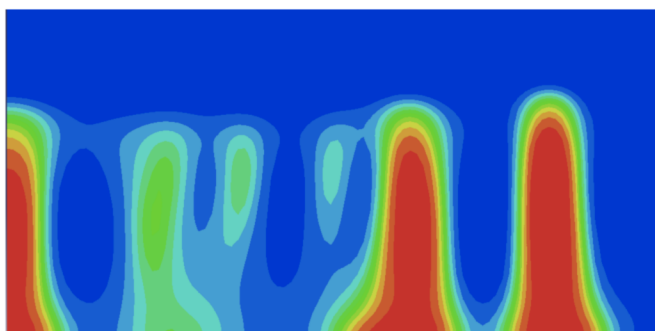
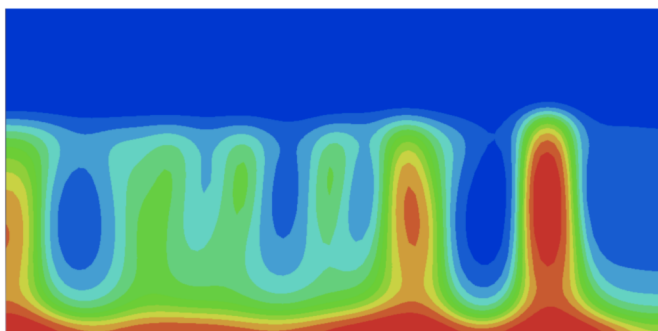
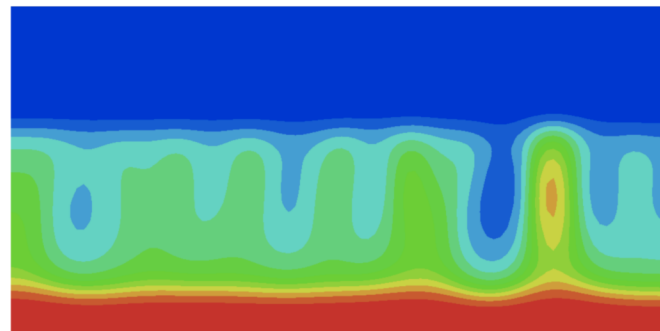
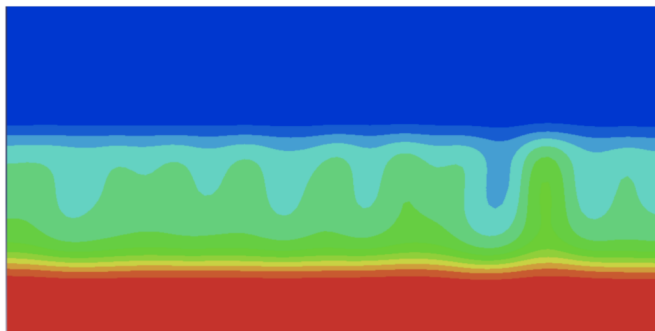
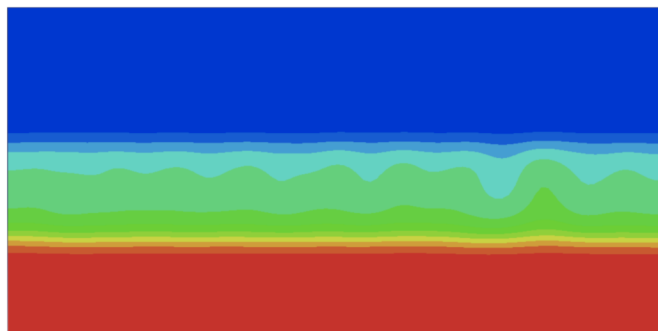
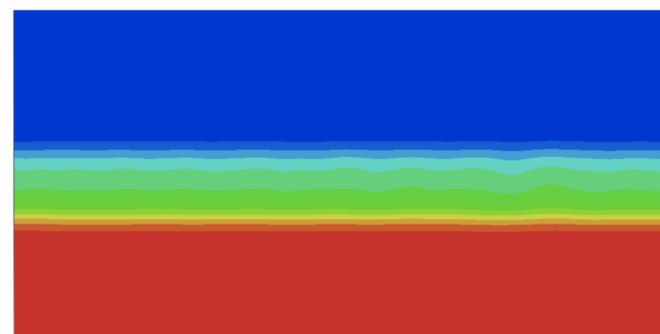
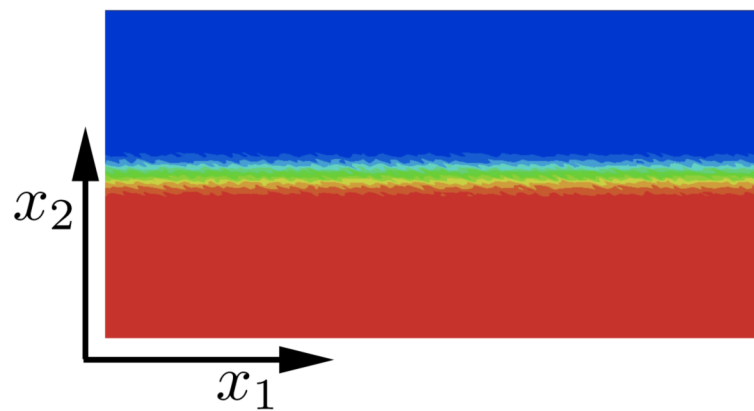
Strain energy density $W = \sigma_{ii} \epsilon_s$ [F/L²]

Length parameter γ/W [L]



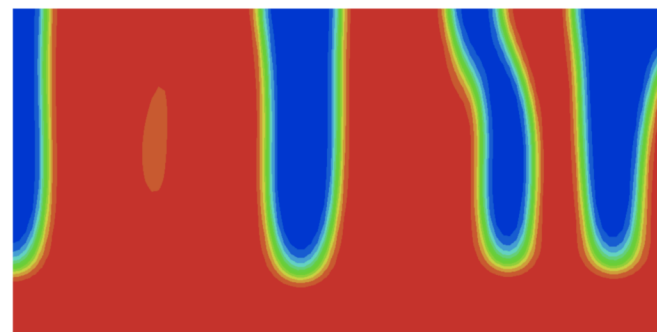
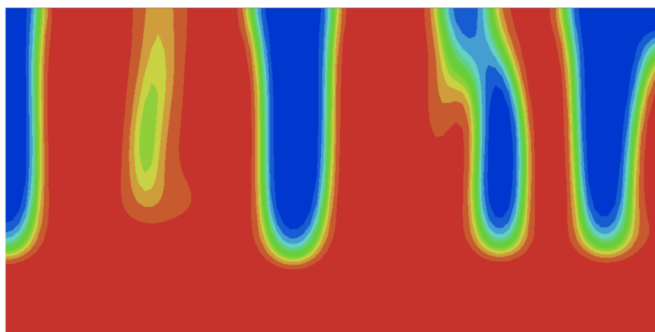
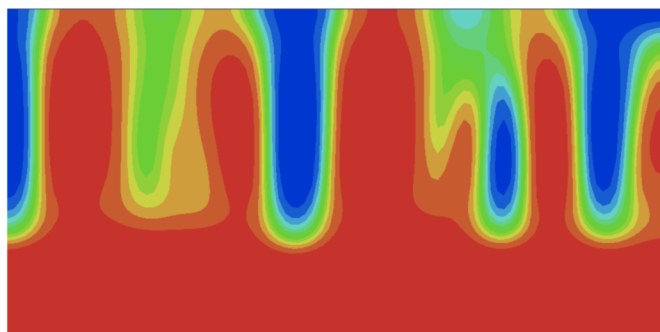
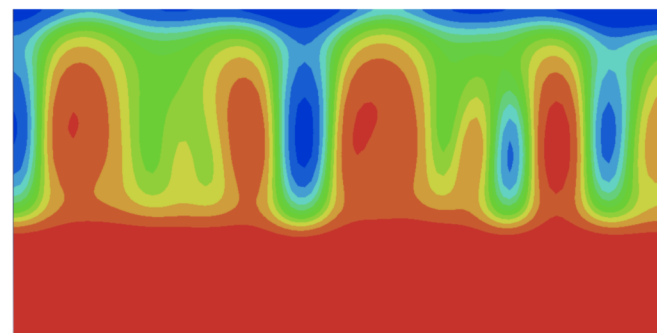
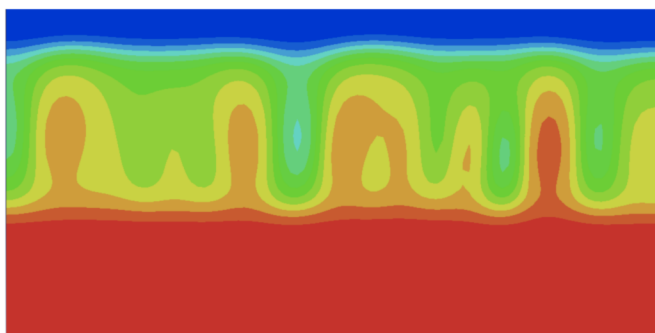
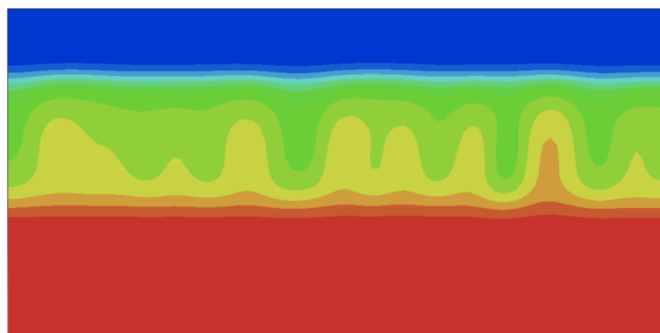
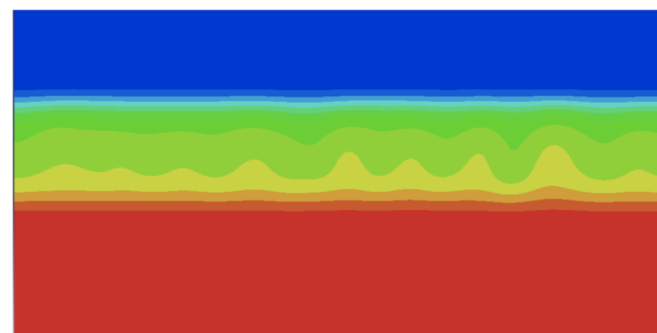
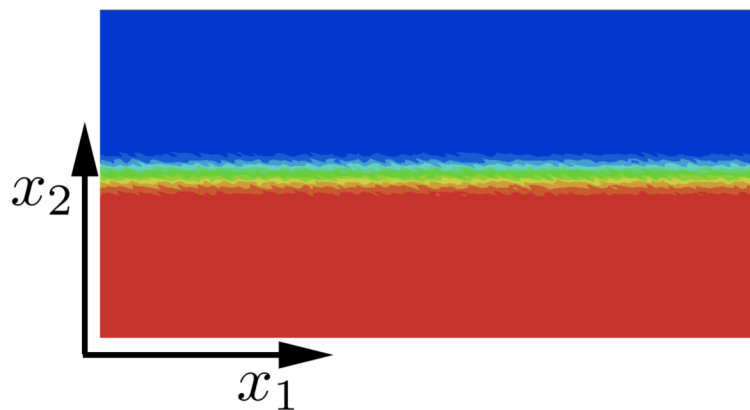
Noisy interface

$$\epsilon_{11} = 0.45\epsilon_s$$



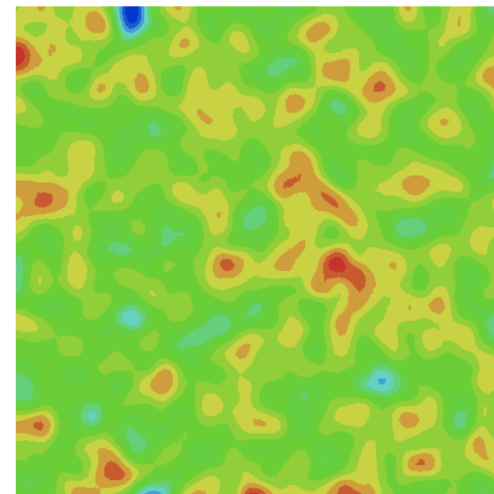
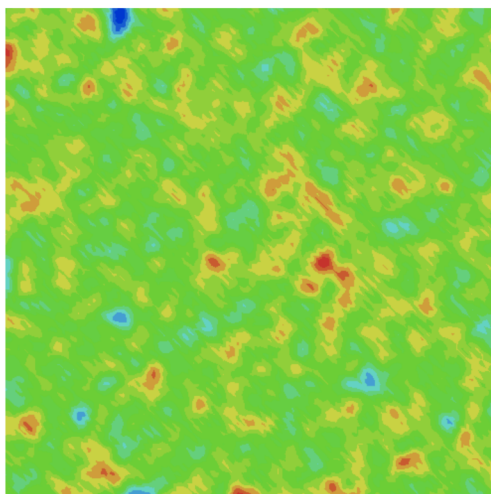
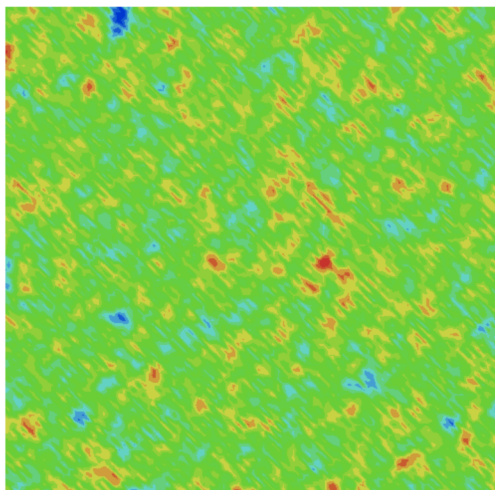
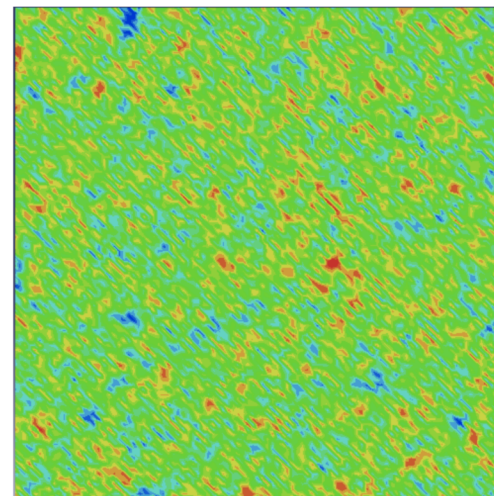
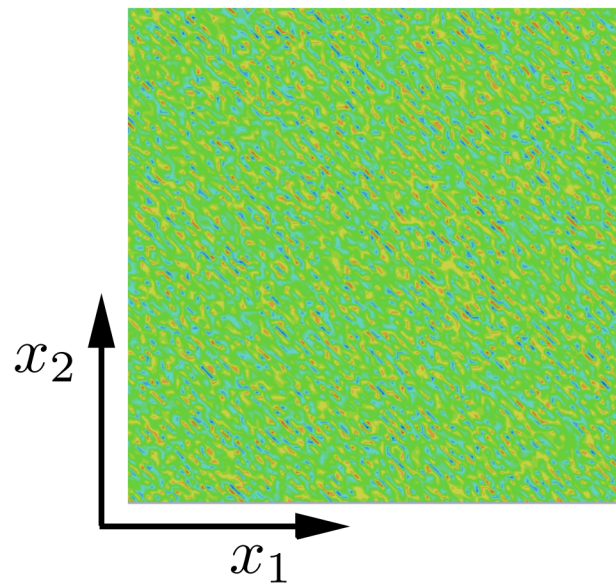
Noisy interface

$$\epsilon_{11} = 0.55\epsilon_s$$



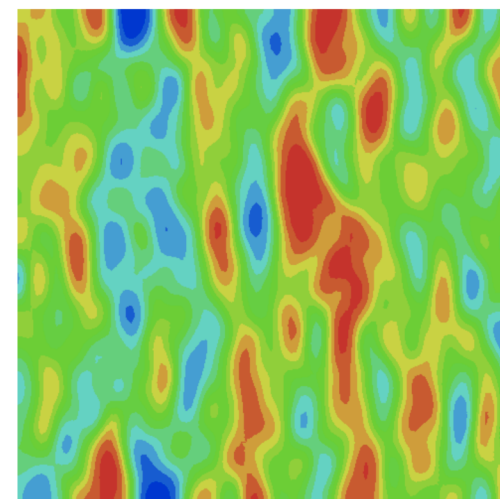
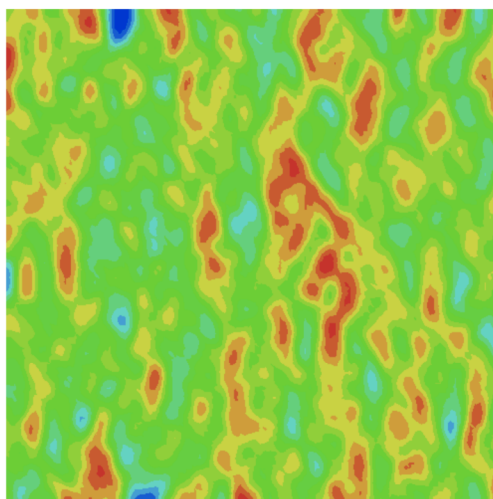
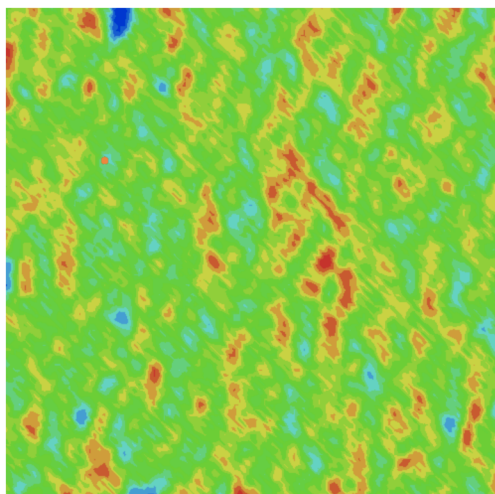
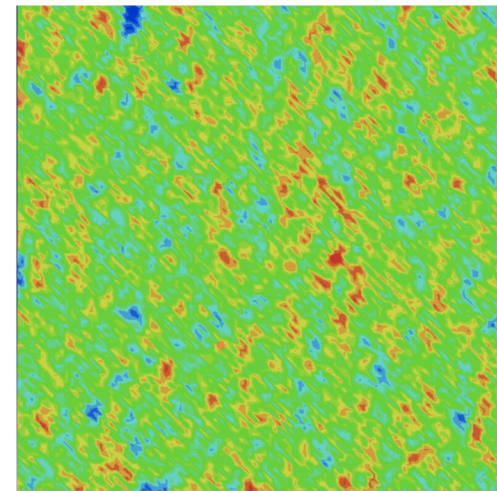
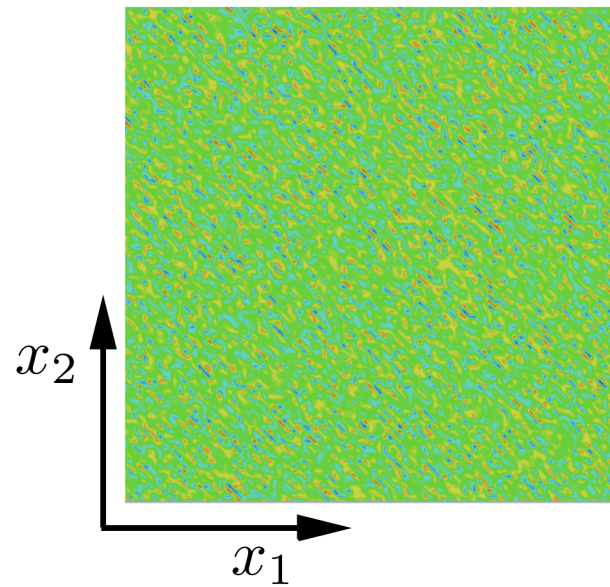
Noisy background

$$\epsilon_{11} = \epsilon_{22} = 0.5\epsilon_s$$



Noisy background

$$\epsilon_{11} = 0.5\epsilon_s$$



Evolution of the phase

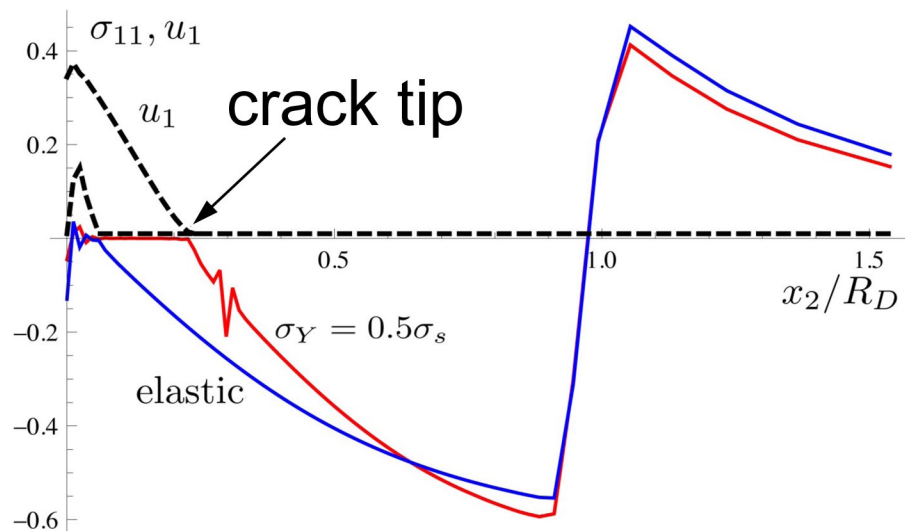
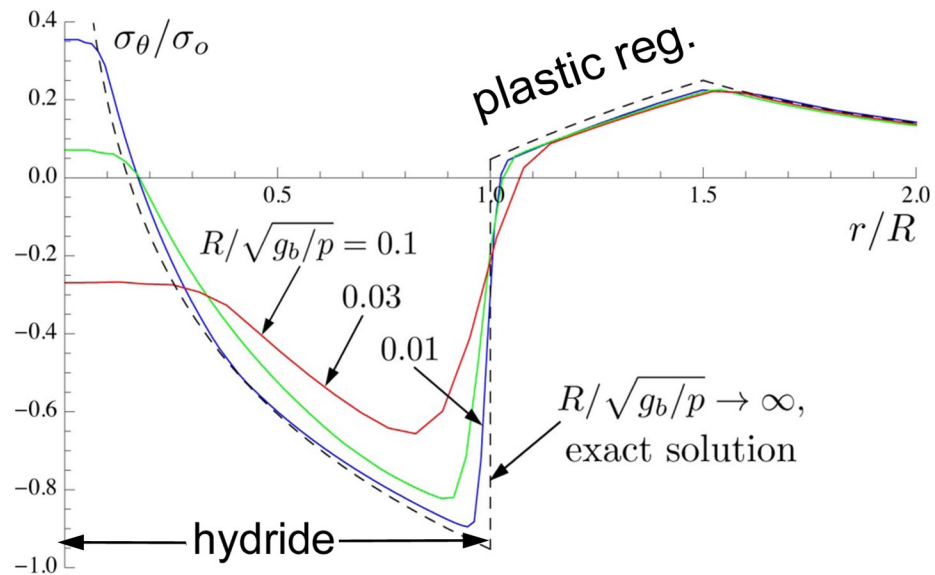
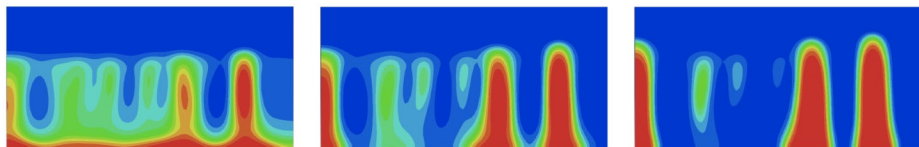
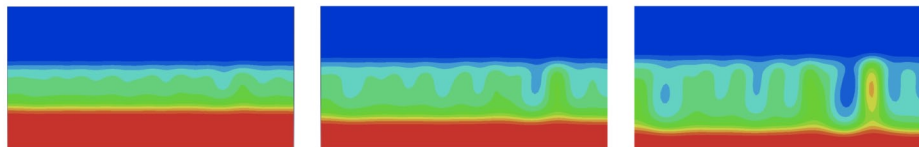
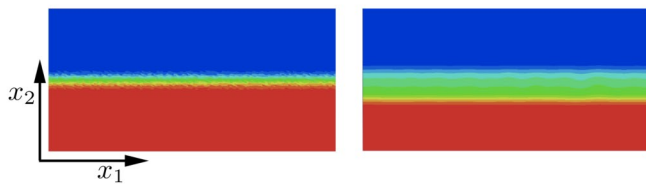
$$\frac{\partial \psi}{\partial t} = -L_\psi (\{3\sigma_{ii}\epsilon_s + 2p(1 - 2\psi)\} (1 - \psi)\psi - g_b \psi_{,ii})$$

Evolution of the displacements

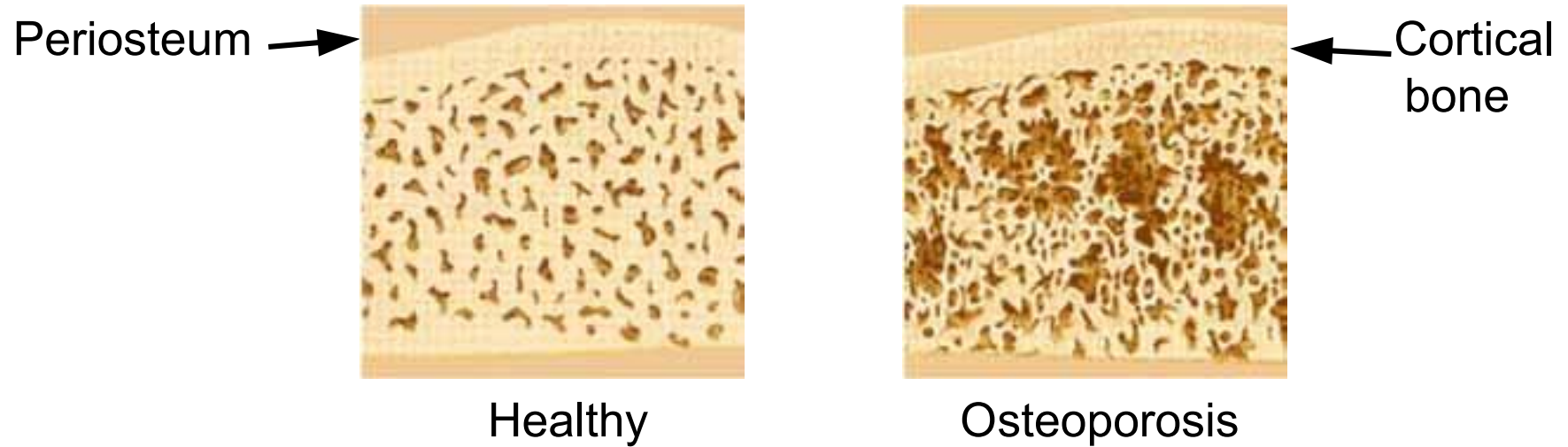
$$\frac{\partial u_i}{\partial t} = -L_u (\mu u_{i,jj} + (\mu + \lambda) u_{j,ij} - (2\mu + 3\lambda) \epsilon_{,i}^s)$$

Noisy interface

$$\epsilon_{11} = 0.45\epsilon_s$$



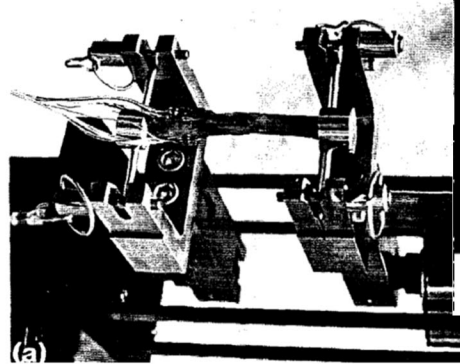
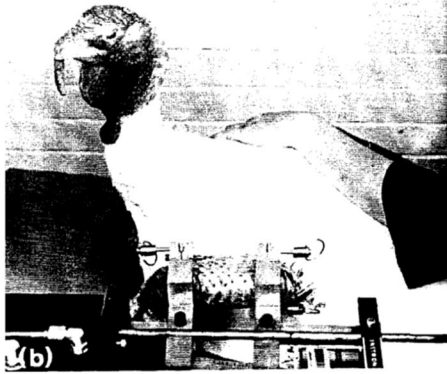
Osteoporosis



100.000 fractures related to osteoporosis each year in Sweden.

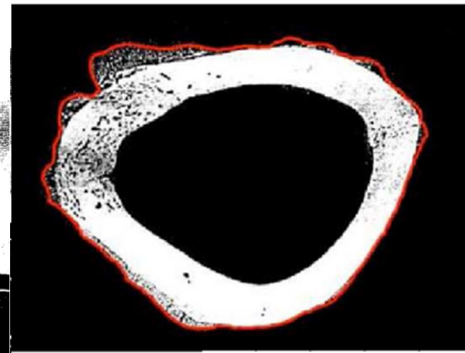
(Sweden has a population of 9 million people)

Observations of exercise stimulated bone growth

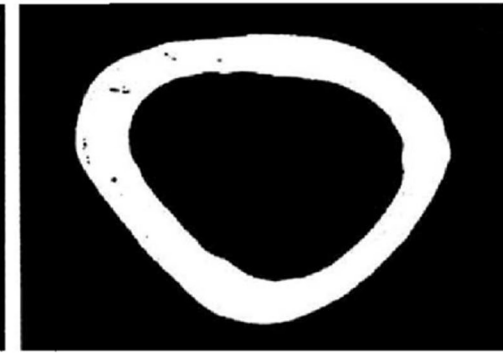


(Lanyon and Rubin, 84)

Experiments performed on the left wing, while the right wing was used as reference for each turkey.



Left wing, dynamic load



Right wing, no load

The dynamic load was applied at a frequency of 1 Hz during 100s per day during 8 weeks. Max force 525 N.

The flow \mathbf{J} , and the concentration c ,

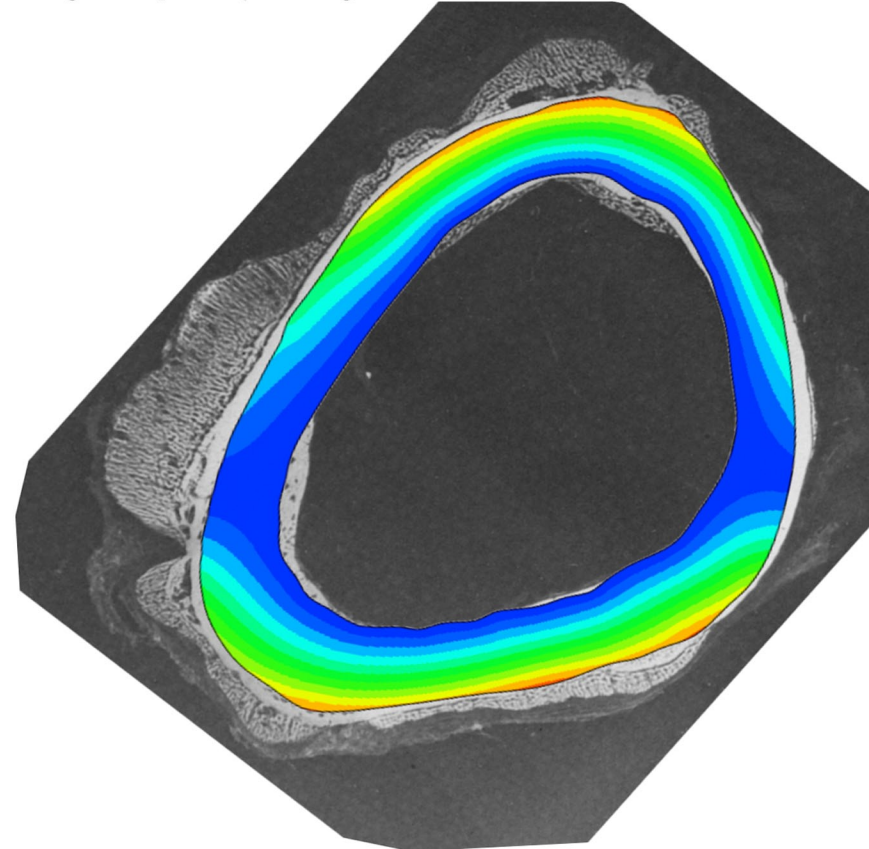
$$\mathbf{J} = -D\nabla c + B\nabla\sigma_h$$

$$\nabla\mathbf{J} = -\dot{c}$$

Hooke stress tensor

$$\sigma_{ij} = 2\mu\epsilon_{ij} + \lambda\delta_{ij} - \beta\delta_{ij}c$$

$$\Rightarrow -\nabla D\nabla c + \nabla B\nabla\sigma_h = -\dot{c}$$



Landau phase field model

phase field variable

$$-1 \leq \psi \leq 1$$

Young's modulus

$$E(\psi) = -\frac{1}{4}(\psi^3 - 3\psi - 2)E_b$$

Gibbs free energy

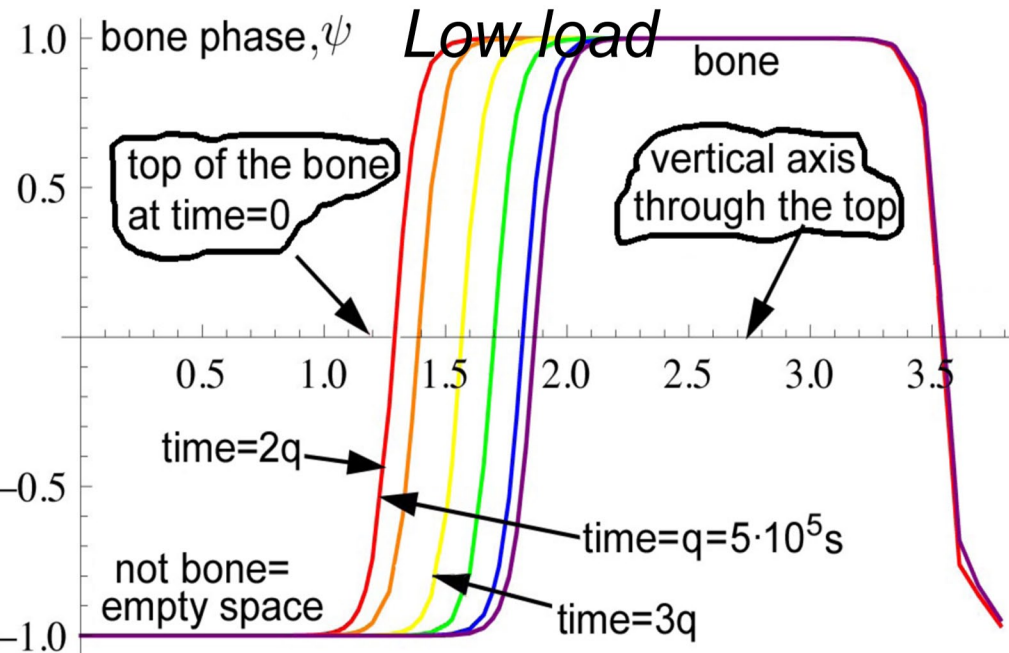
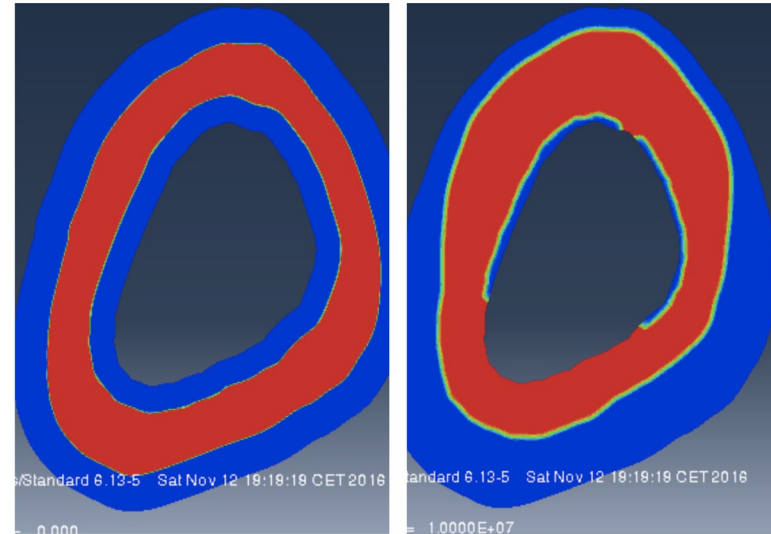
$$\mathcal{F} = \int_V (F_{ch} + F_{gr} + F_{el})dV$$

Governing PDE

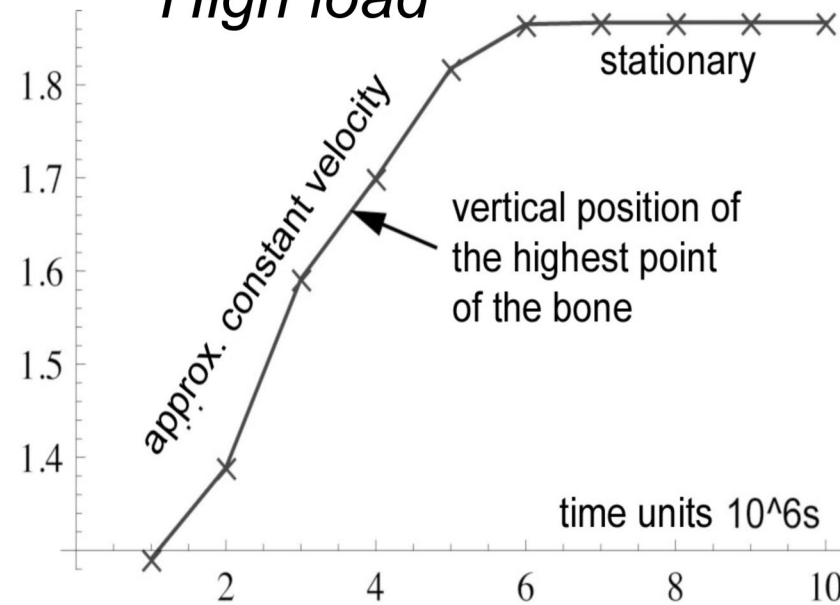
$$\frac{\partial \psi}{\partial t} = L_\psi \left(p(1 - \psi^2)\psi + g_b \psi_{,ii} + \frac{1}{8} \epsilon_{ij} \sigma_{ij} (1 - \psi^2) E_b / E_o \right)$$

before

after 4 months



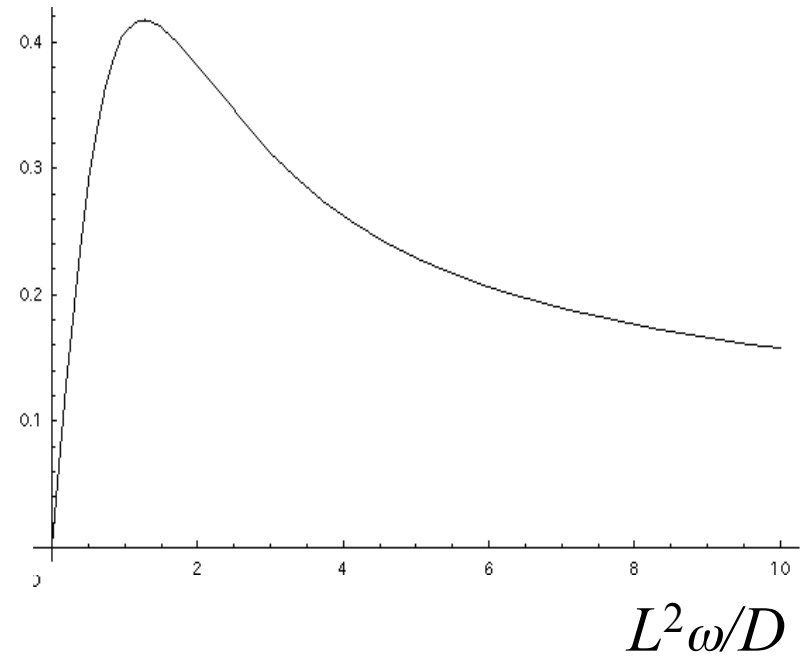
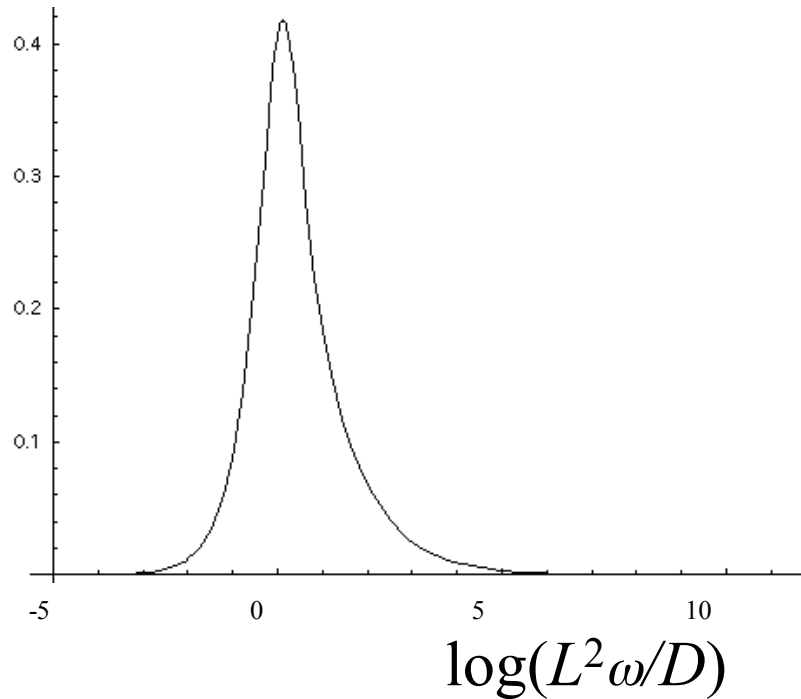
High load



Amplitude, A , as a function of load frequency ω

$$C = C(x, t) = A f(x) \sin(\omega t), \quad f(L) = 1$$

$ADW/(BML)$



Concentration per unit of area

